



Università degli Studi di Cagliari

**PHD DEGREE
IN NEUROSCIENCES**
Cycle XXXI

TITLE OF THE PHD THESIS

**Involvement of microRNAs and their targeted genes
in the pharmacogenomics of lithium response in
bipolar disorder: a genome wide study**

Scientific Disciplinary Sector

BIO/14 FARMACOLOGIA

PhD Student: Eleni Merkouri Papadima

Coordinator of the PhD Programme Antonio Argiolas

Supervisor Maria Del Zompo
 Alessio Squassina

Final exam. Academic Year 2017 – 2018

Thesis defence: February 2019 Session

Abstract

Bipolar disorder (BD) is a frequent mood disorder characterized by manic and depressive episodes. The disease affects approximately 1-2% of the population. Lithium is a mood stabilizer used as first line treatment of BD episodes and for maintenance. Despite 30% of patients show full remission of symptoms under chronic treatment, a high percentage of patients do not respond sufficiently. Moreover, lithium is a drug with a particularly narrow therapeutic window and wide range of mild to severe side effects. Lithium response has an apparently strong genetic background and lithium responders consist in a group with more homogenous manifestation of the disease. However, a vast body of research on the field was not enough to explain the existing variability, suggesting that factors other than DNA variants could be involved. Thus, more and more studies turn towards epigenetic research in order to explain the mechanisms of lithium response and identify predictive biomarkers. We attempted to investigate the total miRNAs expression profiles through a Next Generation Sequencing (NGS) approach.

Lymphoblastoid cells lines (LCLs) derived from 20 BD patients, 10 Full Responder (FR) and 10 Non-Responder (NR) to chronic lithium treatment according to the “Retrospective Criteria of Long - Term Treatment Response in Research Subjects with Bipolar Disorder”, Sardinians for four generations and part of the Consortium on Lithium Genetics (ConLiGen) sample. The LCLs from both groups were cultured either in presence or in the absence of 1mM LiCl. Total RNA was extracted enriched in miRNAs and sequenced with MiSeq instrument (Illumina) and the reads were mapped using miRBase database. A comparative analysis between FR vs NR groups was performed and the effect of lithium treatment in vitro on the miRNA expression was estimated in FR and NR. Available transcriptomic data from the same cohort were used for a correlation analysis between the top hits of the two datasets. Subsequently, target prediction with online miRNA target prediction software helped to narrow down the list of the inverse correlated couples (miRNA-mRNA) and select miRNAs and target mRNAs for validation with qRT – PCR.

Two out of four selected miRNAs, miR-320a and miR-155-3p, and three of the corresponding mRNA targets (two targets of miR-320a and one of miR-155-3p) were validated as significantly differentially expressed: miR-155-3p - *SP4*, miR-320a – *CAPNS1* and miR-320a – *RGS16*. Specifically, hsa-miR-320a was downregulated in FR in comparison with NR, while the levels of miRNA’s possible targets, *CAPNS1* and *RGS16*, were increased in FR and decreased in NR. The opposite was observed for hsa-miR-155-3p and *SP4* gene.

Table of Contents

1. Introduction.....	5
1.1 Bipolar Disorder.....	5
1.1.1 Definition.....	5
1.1.2 Diagnosis.....	5
1.1.3 Epidemiology.....	7
1.1.4 The Biology of Bipolar Disorder.....	7
1.1.5 The Genetics of Bipolar Disorder.....	13
1.1.6 Treatment.....	15
1.2 Lithium.....	16
1.2.1 Mechanism of action.....	16
1.2.2 Lithium Pharmacogenomics.....	20
1.3 Epigenetics.....	22
1.3.1 Definition.....	22
1.3.2 Epigenetics of mood stabilizers.....	22
1.4 microRNAs.....	23
1.4.1 Biogenesis.....	23
1.4.2 Functions.....	25
1.4.3 MicroRNAs as biomarkers.....	25
1.4.4 MicroRNAs in BD.....	26
1.4.5 MicroRNAs in lithium response.....	30
2. Aim of the study.....	34
3. Materials and methods.....	36
3.1 Sample.....	36
3.2 Cell cultures and treatment.....	39
3.3 Total RNA extraction.....	40
3.4 RNA Quantitation and Quality Control.....	41
3.5 Next Generation Sequencing (NGS) with MiSeq.....	43

3.5.1 Library Preparation and Sequencing	43
3.5.2 Data analysis	48
3.6 Microarrays.....	50
3.6.1 Microarrays Experiment	50
3.6.2 Statistical analysis of mRNAs data.....	50
3.7 miRComb correlation analysis and Gene target prediction	51
3.8 Validation with qRT-PCR.....	52
3.8.1 Introduction to qRT-PCR.....	52
3.8.2 miRNA quantification by qRT-PCR.....	53
3.8.3 mRNA quantification by qRT-PCR.....	55
4. Results	58
4.1 Next Generation Sequencing (NGS) of miRNAs.....	58
4.1.1 NGS dysregulated miRNAs in full-Responders (fR) vs non-Responders (nR) to lithium.....	58
4.1.2 Correlation analysis between mRNA and miRNA expression data and software prediction of miRNA-mRNA couples dysregulated in fR vs nR.....	60
4.1.3 NGS dysregulated miRNAs due to in vitro lithium treatment	65
4.1.4 Correlation analysis of genome wide expression data and miRNA expression data and software prediction of miRNA-mRNA couples regulated by lithium in vitro	66
4.2 Choice of targets for validation	67
4.3 Validation of selected miRNAs and targets with qRT-PCR	71
5. Discussion and Future Directions	76
References.....	87
Appendices	102
Appendix A: Sequencing of total miRNome using sequencing by synthesis (MiSeq®, Illumina, CA, US)..	102
Appendix B: Full Protocol for TruSeq Small RNA Library Preparation.....	112
Appendix C: Fragment Analyzer	125
Appendix D: Introduction to qRT-PCR	128

1. Introduction

1.1 Bipolar Disorder

1.1.1 Definition

Bipolar disorder (BD) or “manic depressive illness” as is commonly referred to, is an episodic, recurrent, often debilitating, lifelong mood disorder. In BD mania, hypomania, depression or mixed episodes followed or not by a period of remission (euthymia) alternate one another. BD is classified as a mood disorder because its main features are disturbances in thinking and behavior. The manic (or hypomanic) episodes are periods of elevated mood and are necessary in order for someone to be diagnosed as bipolar. Generally, it is characterized by an episodic course and is highly variable among patients. BD is highly heritable and difficult to manage with the available medications and psychiatric approaches.

Clinically, BD is characterized by the severity of episodes, the pattern of recurrence of the depressive and manic episodes, the speed of cycling, the presence or absence of recovery periods between episodes and the duration of these periods. The psychiatric features include psychosis, catatonia, comorbid psychiatric disorders or substance abuse and suicidal, homicide or violence ideations. BD has a particularly high influence in the social and occupational life of the individual and his family and a big socioeconomic impact on the community. A meta-analysis of 22 studies regarding USA, Taiwan and European countries estimated that the economic burden of BD related to health care ranged from 2,500 to 5,000 US\$ (via purchasing power parities) per person per year ³. Moreover, the morbidity rate of the patients due to suicide and comorbid conditions (cardiovascular and pulmonary disease, diabetes, substance abuse) is particularly high among BD patients ⁴. The percentages of suicide and suicide attempts are 25%–56%, while 6%–20% of bipolar patients actually succeed in committing suicide. In fact, the risk of suicide in BD is 27.5 times higher in comparison with general population ^{5,6}.

1.1.2 Diagnosis

BD and unipolar disorder belong to the recurrent affective disorders. To the bipolar spectrum belong disorders characterized by their episodic and bipolar (mania and depression) nature; these are Bipolar Disorder I (BDI), Bipolar Disorder II (BDII), BD - not otherwise specified and cyclothymia. Diagnostic criteria of BD are based on the Diagnostic and Statistical Manual of Mental disorders –

fourth edition (DSM – IV) ⁷ and classified in the international classification system, ICD-10 ⁸. According to these criteria, diagnosis depends on the clinical characteristics. The diagnosis of BDI requires the appearance of a manic or mixed (mania and depression) episode, not induced by substances or a pre-existing medical condition. On the contrary, in order to diagnose Bipolar Disorder II (BDII) it is prerequisite at least one hypomanic episode preceding or following one Major Depression Episode (MDE). Manic episodes are mainly featured by elevated mood or activation of the motor and cognitive processes in some patients. Expansive or irritable mood might accompany the elevated mood or can be present as independent symptoms. The main symptoms should last at least one week, to cause considerable social or occupational dysfunction, need for hospitalization or to be accompanied by psychotic features. Besides these main features, the presence of at least three of the following symptoms are necessary to diagnose a manic episode if the mood is expansive or elevated, or four if the mood is irritable: inflated self-esteem or grandiosity, decreased need for sleep, pressure of speech, flight of ideas, distractibility, hyperactivity and excessive involvement in pleasurable activities with a high potential of painful consequences. Hyperactivity is a frequent symptom and is described in DSM-IV as goal directed activity and psychomotor agitation.

In 90% of the cases, a single manic episode is followed by more manic, depressive or mixed episodes. Depression appears as the first symptom in most cases, while manifestation of mania as first episode is more likely in men than in women. A depressive episode is defined by the existence of depressed mood and loss of interest or pleasure in most activities for at least two weeks. In addition to the core features, at least four of the following symptoms should be present to confidently define the episode as depressive: changes in appetite, weight or sleep, psychomotor agitation or retardation, fatigue or loss of energy, feelings of worthlessness or guilt, difficulty thinking or concentrating, indecisiveness, recurrent thoughts of death (not just fear of dying), recurrent suicidal ideation with or without a specific plan or previous suicide attempt. Sleep and eating disturbances are among the most common co-existing symptoms. Finally, mixed episodes fit the criteria for both manic and depressive episodes. Hypomanic episodes that distinguish BDII from BDI can last less than one week but at least 4 days and they are not severe enough to provoke marked functional social and occupational impairment, hospitalization or psychosis. Besides the disruption of behavior, the clinical picture of BD involves alterations of the circadian rhythms, of the neurophysiology of sleep and changes in the neuroendocrine and biochemical regulatory systems within the brain. Up to date, those characteristics of BD are mainly used in research or as additional to the diagnosis but are not indispensable for diagnosis.

1.1.3 Epidemiology

The lifetime prevalence of BD was updated in 2011 based on the World Health Organization (WHO) World Mental Health Composite International Diagnostic Interview (WMH-CIDI, version 3.0) used to interview individuals from an 11 country pooled sample. The updated prevalence for BDI disorder was 0.6%, while for BDII was 0.4%. Similarly, the 12 month prevalence was 0.4% and 0.3%, respectively. The prevalence of the Bipolar Spectrum Disorders arrived up to 2.4%. High income countries had a higher lifetime and annual prevalence than low income countries, with the exception of Japan and Colombia. Symptom severity was greater for depressive than for manic episodes, with approximately 75% of the interviewed patients with depression and 50% of the respondents with mania reporting severe role impairment. BD patients spend 3 times more time in depressive than in manic state and about half the time in euthymic state⁹. The mean age (SE) of onset of BDI was 18.4 (0.7) years and the mean age (SE) for BDI - BDII was 20.0 (0.6) years. Approximately half of those with BDI had onset before the age of 25 and those with BDII slightly later. Comorbidity rates (SE) were particularly high between patients with BDI and BDII, 88.2% and 83.1%, respectively. The most common comorbid disorders were anxiety disorders, BDI 76.5% (2.7) and BDII 74.6% (3.0), panic attacks in particular had a frequency of 57.9% (3.2) for BDI and 63.8% (3.4) for BDII, followed by behavior disorders with 44.8% (2.3) and that of substance use disorders with 36.6% (1.6). Among the abused substances the most overused was alcohol, 48.3% (2.9) for BDI and 33.5% (3.1) for BDII.

Assessment of the severity of symptoms is not a prerequisite for the diagnosis. Symptom severity can be assessed with the self-report versions of the Young Mania Rating Scale (YMRS) for mania/hypomania and the Quick Inventory of Depressive Symptoms (QIDS) for MDE. The severity of BD symptoms depended strongly on the type of the episode, with MDE being in the majority more severe than manic episode based on YMRS and QIDS scales questionnaires conducted by specialized personnel and referring to the most severe episode they had experienced within the last 12 months preceding the interview¹⁰.

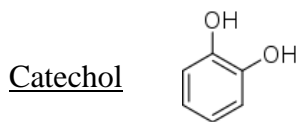
1.1.4 The Biology of Bipolar Disorder

The psychosocial studies have adopted their own theories on the mechanism of BD, such as the psychodynamic theory according to which depression is a demonstration of losses and mania is a way

to compensate for those losses. However, those theories do not explain what actually happens in a patient's body. Thus, this subsection will be dedicated to the biology behind BD.

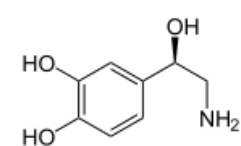
In general, BD is considered as a complex polygenic disease which manifests as a result of the combination of many low weight variants and environmental factors causing imbalances and dysregulation of certain systems, like the immune system or the mechanisms responsible for the maintenance of homeostasis. There have been many theories on the neurobiology of BD, the most prevalent of which are the following:

The catecholamine/monoamine theory



The catecholamines are monoamines, containing one catechol group (a 1,2- hydroxyl benzene) and a side-chain amine, produced biosynthetically by the amino acids, phenylalanine and tyrosine through tyramine. The family of catecholamines includes the most important sympathetic and parasympathetic system's neurotransmitters, namely epinephrine, norepinephrine, dopamine. These amines are distributed extensively in the limbic system, which is implicated in the regulation of sleep, appetite, arousal, sexual function, endocrine function, and emotional states such as fear and rage. According to the catecholamine theory, an increase in epinephrine or norepinephrine levels leads to mania and decrease of the same neurotransmitters leads to depression. A body of evidence from peripheral blood, cerebrospinal fluid (CSF), postmortem and most recently, brain imaging supports a role of alterations of the catecholamine neurotransmission in the etiopathogenesis of BD ^{11,12}. For example, it was noticed that the antihypertensive drug reserpine, which acts through depletion of catecholamines from nerve terminals, was causing depression ¹³.

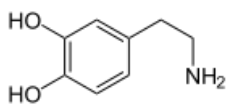
Norepinephrine



Peripheral plasma and urine levels of norepinephrine and its major metabolite, 3-methoxy-4-hydroxyphenylglycol (MHPG), all consistently demonstrated that in bipolar depression their levels are lower than in unipolar depression and higher during the manic episode than during depression. The increase of norepinephrine and MHPG in manic state is also confirmed by measurements of their levels in CSF. To strengthen the hypothesis,

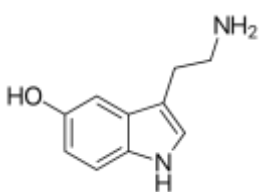
postmortem studies have shown an increased norepinephrine transport rate in the cortical and thalamic areas of BD patients ¹². Increased levels of norepinephrine have also been found in of schizophrenia subjects. Nevertheless, Single Nucleotide Polymorphism (SNPs) found in norepinephrine transporter are linked to attention deficit hyperactivity disorder (ADHD), psychiatric disorders, postural tachycardia and orthostatic intolerance and as we know cardiac and circulation problems are often encountered as BD comorbidities ¹⁴. Hypermethylation of CpG islands in the norepinephrine transporter gene promoter region seems to lead into decreased expression of norepinephrine transporter and consequently a phenotype of impaired neuronal reuptake of norepinephrine that has been implicated in both orthostatic tachycardia syndrome and a mental disorder, namely panic disorder ¹⁵.

Dopamine



The strongest direct finding from clinical studies implicating dopamine in depression is reduced homovanillic acid (HVA) levels, the major metabolite of dopamine, in the CSF. Indeed, this is one of the most consistent biochemical findings in depression. The pharmacological studies also support the involvement of the dopaminergic system in mental disorders treatment. Dopaminergic agonists are effective antidepressants and in some cases they contain efficiently manic symptoms in bipolar patients ^{12,16,17}.

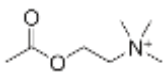
Serotonin



Data supporting the involvement of serotonin and its main metabolite (5-hydroxyindoleacetic acid (5-HIAA)) are derived from CSF studies, receptor and reuptake site binding studies and pharmacological studies, all conferring to the involvement of serotonin in BD. However, the results were not all indicating the same direction of change and often there were no differences between depressed and manic patients ¹⁶. Studies have also reported decreased radio-ligand binding to the serotonin transporter both in platelets and in the midbrain of depressed patients. Additionally, positron emission tomography (PET) study reported decreases in 5-hydroxytryptamine (5-HT) 1A (5-HT1A) receptor binding potential in raphe and hippocampus - amygdala of the brain in depressed patients, particularly in bipolar depressives and in unipolar patients with bipolar relatives ¹¹.

All the above listed neurotransmitters have one more thing in common that supports their involvement in BD. As it is common knowledge most of the antidepressants used for the treatment of the Major depressive disorder (MDD) symptoms are increasing catecholamines/monoamines levels at the synaptic cleft. These are the well-known Serotonin reuptake inhibitors (SSRIs), serotonin – norepinephrine reuptake inhibitors (SNRIs), norepinephrine – dopamine reuptake inhibitors (NDRIs), norepinephrine reuptake inhibitors (NRIs) and tricyclic antidepressants (TCAs), which also act by blocking serotonin and norepinephrine transporters.

Acetylcholine – cholinergic system



Acetylcholine regulates the cholinergic system which showed higher levels of activity in mania than in depression. During MDE, the noradrenergic system prevailed the cholinergic. Additionally, a study on the central cholinesterase inhibitor physostigmine showed that it had effects on mania symptomatology and that it induced depression in bipolar patients in remission. Finally, mood stabilizers, lithium and valproate, potentiated pilocarpine action on the cholinergic system ¹².

The neurotrophic factor theory

Neurotrophic factor theory was developed to explain why in the developing peripheral nervous system many neurons die shortly after their axons reach their target fields. The principal idea is that the survival of developing neurons depends on the supply of one or more neurotrophic factors that are synthesized in their target fields ¹⁸. Brain-derived neurotrophic factor (BDNF) is a member of the neurotrophin family of neurotrophic factors. It is important for synaptic plasticity and dendritic growth and essential for the long-term memory ¹⁹. Furthermore, BDNF has been associated with neurodegenerative diseases, anxiety and memory disorders and it has been implicated in a variety of neural processes in both animals and humans. A number of genetic studies have found an association between the Val66Val BDNF allele and BD, although there have been some negative findings as well (see Post, 2007 for review of studies ²⁰). Interest in the area has also been stimulated by a study that showed that plasma BDNF levels were significantly decreased in drug-free/naive subjects with BD in a manic episode compared to healthy controls ²¹. Later studies showed low levels of BDNF transcript and protein in BD and MDD first episode patients and even lower at the BD sample. The results of this study suggest the BDNF serum levels as a predictor of the development of BD after first diagnosis of MDD ²². A meta-analysis of 52 studies showed that levels of the BDNF are reduced to the same extent in manic and depressive episodes, while not significantly altered in euthymia ²³. However, in euthymia it increases in latter stages of the disease, acting as stage indicator ²⁴. Moreover,

the severity of the manic episode is negatively correlated with plasma BDNF levels ²⁵. Both lithium and valproate restore BDNF levels ²⁶.

Other neurotrophic factors associated with BD are Neurotrophin 3 (NT-3) and Neurotrophin 4 (NT-4), which were found elevated in serum during the episodes of BD patients ²⁷⁻²⁹. Nerve Growth Factor (NGF) is also likely to be involved in BD and although it interacts with TrKa, the second messengers of the PI-3K/Akt-glycogen synthase kinase-3 (GSK3) pathway and activates it, studies that investigated its relation to BD were conflicting and inconclusive ³⁰. Trophic factors, such as Glial cell line-derived neurotrophic factor (GDNF), insulin-like growth factor (IGF-1) and vascular endothelial growth factor (VEGF), present distinct patterns in the different stages of BD ³⁰. There is also genetic evidence supporting the involvement of IGF-1 in lithium response ³¹.

The hormonal dysregulation theory

Other factors that may exacerbate mania include hormonal imbalances and disruption of the hypothalamic-pituitary-adrenal (HPA) axis, involved in homeostasis and the stress response, causing symptoms of BD.

The HPA-axis and the inflammation theory

The HPA axis is dysfunctioning in BD patients. Specifically, they have hyperactive HPA axis, which leads to increase in the blood cortisol and resistance to the dexamethasone/corticotrophin releasing hormone test and dexamethasone suppression test. Similar findings have been found in high risk individuals, namely, first degree relatives of BD patients ^{32,33}.

Increased levels of cortisol in BD patients ^{34,35} activate the HPA axis, which in turns activates the sympatho-adrenal medullary axis. As a result, the peripheral levels of epinephrine and norepinephrine are augmented and as a response to that the expression of cytokines is increased through nuclear factor kappa (NF-kB) disinhibition ³⁶ or other non-canonical pathways, such as activator-protein 1 (AP-1), Janus kinase signal transducer and activator of transcription (JAKSTAT) factor ³⁷, and mitogen-activated protein kinase (MAPK) ³⁸. The cells of the innate immune system (for example, monocytes, macrophages, and T-lymphocytes) secrete proinflammatory cytokines, chemokines, and cell adhesion molecules that diffuse to the brain and trigger microglia, causing neuroinflammation and further activating the HPA axis. These events consist in a cycle that creates a permanent micro-inflammation state. This is evident from the increase in the levels of proinflammatory cytokines and C-reactive protein in the peripheral blood during manic or depressive episodes, whereas also in euthymic patients a low inflammation state was noticed ³⁹. The proinflammatory cytokines include

the interleukin (IL) 1 β (IL-1 β), IL-6, and tumor necrosis factor-alpha (TNF- α)⁴⁰. Mood stabilizers used to treat BD have been shown to normalize the levels of proinflammatory cytokines like IL-1 β and IL-6 but not TNF- α ⁴¹. Other studies confirmed lithium involvement in restoration of inflammation associated factors in BD^{42,43}. This indicates that inflammatory dysregulation could be important for the pathophysiology of BD. Finally, Padmos et al., (2008)⁴⁴ and Powell et al., (2014)⁴⁵ evaluated the expression of inflammatory cytokines peripherally as biomarkers and then later proposed Chemokine (C-C motif) ligand 24 (CCL24), which was consistently transcribed higher amongst MDD patients relative to controls and BD patients, for the differential diagnosis of BD.

The circadian rhythms theory

The circadian rhythms are linked to an internal “clock” that is responsible for the homeostasis in our bodies in various levels, such as body rhythms, adaptation to dark-light cycle, sleep regulation, hormonal secretion and body temperature. Data collected from the clinical evaluation of bipolar patients suggest a strong contribution of dysregulation of circadian rhythms to the disease. Levels of melatonin, cortisol and circadian rhythm length is affected in BD. Moreover, even during euthymia there are signs of circadian clock dysregulation: body temperature variations and sleep problems are some of them. Circadian abnormalities have been associated with relapses⁴⁶. Disturbances of sleep/wake cycle often can be a sign for a manic or a depressive episode⁴⁶ and either kind of episode exacerbates when seasons change⁴⁷. One of the most striking examples of circadian rhythms involvement in BD is a mouse model with an inactive CLOCK protein which presents with characteristic symptomatology of mania and hyperactive dopaminergic neurons⁴⁸. Genetic findings that show a number of SNPs onto circadian genes associated with BD also support the circadian rhythm contribution in BD symptoms and pathology⁴⁹. The heritability of the circadian rhythm abnormalities is also supported by the abnormalities of the circadian clock observed in relatives of the patients. Finally, mood stabilizers used to treat BD and especially lithium have a favorable effect on the regulation of the “clock” in BD and other recurrent disorders like Cluster Headache and unipolar depression, suggesting that regulation of the daily rhythms might actually assist to the stabilization of the mood in BD⁴⁹⁻⁵¹.

The oxidative stress theory

Oxidative stress is commonly associated with neurodegenerative diseases and with the central nervous system. Oxidative stress is caused by an imbalance of the antioxidants and pro-oxidants in the cell. This imbalance leads to the overproduction of radical oxygen species (ROS), like superoxide (O₂⁻), hydrogen peroxide (H₂O₂) and hydroxyl (OH \cdot) radicals. ROS have a free electron radical and

thus, they are destructive for the cell since they can easily initiate a series of internal reactions by reacting with lipids of the organelles, the membranes, or even with the DNA and finally lead to cell death. The nervous system is sensitive to oxidative stress, and that is probably due to the fact that ROS are oxygen byproducts of the mitochondrial respiration which is higher in the nervous tissue than to any other tissue. The oxidative stress has been held responsible for many neurodegenerative diseases like Parkinson's, Alzheimer disease (AD), Amyotrophic Lateral Sclerosis (ALS), etc. Most of the data supporting this theory come from studies estimating the levels of lipid peroxidation and DNA oxidation products and antioxidant enzymes in the periphery of BD patients ⁵².

1.1.5 The Genetics of Bipolar Disorder

The pathogenesis of BD is still not well understood and the diagnosis is solely based on the clinical features and not the clinical findings. The clinical findings only give supporting evidence for the differential diagnosis. To this end the development of the area of genetics and genomics has given us important insights into the etiopathogenesis of the disorder.

Heritability

BD is highly inheritable as has been proved by twin and family studies ^{53,54}. The child of at least one affected parent has 10 times higher risk developing BD than general population; first degree relatives have a relative lifetime risk 8 times higher compared to general population. However, not all the monozygotic twins of a BD affected subjects present the phenotype, resulting in an estimated heritability rate of 40 -70% ⁵⁵. This observation leads to the assumption that environmental factors are involved in the manifestation of BD. Besides the increased risk for BD, family members of BD patients are also in greater risk for other psychiatric conditions such as recurrent unipolar depression, schizophrenia and autism spectrum disorders, thus suggesting a partially common genetic background ⁵⁶.

Mechanism of inheritance and experimental approaches for the discovery of susceptibility markers

BD has a complicated inheritance pattern. Large pedigree studies attempting to establish linkage between rare variants of large effect size and the disease mostly failed to their task with some rare exceptions in some familial cases. Hence, it seemed that BD does not follow any Mendelian pattern of inheritance. Naturally, association studies seemed to provide the solution. Initially, association

studies investigated candidate genes and subsequently, as the technology advanced, they were focused on Genome Wide Association Studies (GWAS) which made it possible to test simultaneously for a large number of common variants and Whole Genome Sequencing (WGS) studies which besides common variants contribute to the discovery of rare and de-novo variants. GWAS pointed towards several loci of interest. In addition, GWAS and WGS helped us locating structural differences, which proved to be copy number variants (CNVs). CNVs were rarer and had a higher prediction weight than the variants identified by the GWAS, thus, contributing significantly to the risk for BD.

However, GWAS often failed to reach significance thresholds and made obvious that larger and larger samples were needed. Even when some variants reached significance they had a small effect size and as a result, the risk of an individual carrying the pathogenic allele to manifest the disorder increased slightly compared with a non-carrier⁵⁵. The answer came from meta-analysis which combined the results of existing scientific studies. Meta-analysis performed by Ferreira et al., (2008)⁵⁷ detected novel SNPs in genes already associated with BD, namely, genes *ANK3* (rs10994336, $P = 9.1 \times 10^{-9}$) and *CACNA1C* (rs1006737, $P = 7.0 \times 10^{-8}$). Importantly, many of the findings were replicated by other studies. For example, SNP rs10994336 mentioned above, was initially detected by Baum et al., (2008)⁵⁸ as an independent risk factors for BD. Another *ANK3* SNP, rs9804190 was initially associated with BD by Ferreira et al., (2008)⁵⁷ and subsequently replicated by Schulze et al., (2009)⁵⁹. In 2014, rs9804190 was again among the top SNPs detected from Muhleisen et al., (2014)⁶⁰ GWAS. Another high impact meta-analysis of GWAS studies was that of Xiao et al., (2017)⁶¹. This study included MDD and BD and compared them with control samples to investigate the common genetic background of these two major mood disorders. SNPs rs10791889 at 11q13.2, rs2167457 at the same locus (11q13.2), rs717454 at 2q11.2 and rs10103191 at 8q21.3 reached genome wide significance at the pooled sample; the combined samples arrived to more than 30000 patients and 90000 controls. The identification of common SNPs associated with mood disorders, supports the theory of common variants and highlights the need for larger sample sizes⁶¹. Several SNPs resulted statistically significant in a genome wide level, examples of genes nearby these SNPs are *ODZ4*, *CACNA1C*, *NCAN*, *SYNE1* *ANK3*, *ZNF804A*, *MAPK3*, *SESTD1*, *ERBB2* and more⁶²⁻⁶⁸. Despite specific genes, also the region 3p21.1 was associated with BD⁶⁹. Other approaches focused on signals from multiple variants that cluster on genes that belong to a biological pathway. Such pathway analysis indicated the calcium channel subunits *CACNA1C*, *CACNA1D* and *CACNB3*⁷⁰. Interestingly, Muhleisen et al., (2014) combined new and old GWAS datasets⁶⁰ and detected an association with SNPs close to a miRNA gene and specifically between *MIR2113* and *POU3F2*.

Other recent approaches are focused on combined GWAS and Genome Wide Gene Expression (GWGE) data. For example, in a study conducted by Muhleisen et al., (2018) ⁷¹, GWAS data were combined with expression data and used for gene set enrichment analyses. The analyses led to two most prevalent pathways Growth factor receptor-bound protein 2 (GRB2) events in Erb-B2 Receptor Tyrosine Kinase 2 (ERBB2) signaling and neural cell adhesion molecule (NCAM) signaling for neurite out-growth.

Linkage and GWAS studies advocate the accumulation of common variants with very small effect sizes as more likely to be responsible for the complicated genetic background of BD. Experience showed as, that even with these tools in our disposition the study of the genetics of BD remains challenging. So far, the most prevalent theory is the common SNPs and rare CNVs in combination with environmental factors as the model of BD inheritance ⁵⁵.

1.1.6 Treatment

BD is a recurrent disease that manifests with a cyclic alternation between mania, mixed episodes, depression or euthymia. The first-line treatment for all the stages are mood stabilizers, namely, lithium and valproate and alternatively, the anticonvulsants lamotrigine and carbamazepine. Mood stabilizers have at least two out of three of the following properties: antimanic, antidepressant and prophylactic effects, without increasing the risk for opposite episodes. Mood stabilizers are first line treatment for acute episodes of mania, mixed episodes and depression, often in combination with other medications, like antipsychotics and antidepressants, but are also administered during euthymia as maintenance treatment. Most commonly used antipsychotics that are considered to have also mood stabilizing properties are aripiprazole, olanzapine, quetiapine and risperidone. For less severe cases, monotherapy with lithium, valproate or an antipsychotic can be sufficient. Short-term addition of a benzodiazepine to the treatment regimen may also be helpful. For mixed episodes sometimes valproate is preferred over lithium salts. Maintenance treatment should be introduced gradually and almost always contains a mood stabilizer. After mania episodes, possible antipsychotics administered during the acute phase, like olanzapine and risperidone, are preferably not discontinued immediately during maintenance phase in order to reduce the risk of relapse during this difficult for the patient transitional phase; whereas, antidepressants have a prophylactic effect only in some individuals ⁷².

1.2 Lithium

Lithium is the cornerstone in the maintenance treatment of BD since it was introduced by Cade in 1950s⁷³. Interestingly, about 70 % of BD patients show a complete or a partial response to therapy with lithium salts⁷⁴. Lithium is also first line in suicide prevention, since is the only drug with a proved efficacy against suicide^{6,75}. Despite the fact that 30% of patients show full remission of symptoms, a high percentage of patients do not respond sufficiently and need to be switched to other mood stabilizers⁷⁶. Moreover, lithium is characterized by a narrow therapeutic window and a wide range of mild to severe side effects⁷⁷. The most frequent side effects of lithium are disturbances at the stomach, fine tremor, polydipsia, polyuria^{78,79}, weight gain⁷⁹, hypothyroidism and renal dysfunction. The above listed side effects and especially thyroid and renal dysfunction are the reason why lithium levels and tolerance are frequently monitored. According to the 2009 report from Prescribing Observatory for Mental Health, the ideal levels for lithium as prophylactic treatment range from 0.6-0.75 mmol/L, while the therapeutic window is slightly wider, ranging from 0.4 mmol/L, normally preferred in older patients, to 1-1.2 mmol/L, usually referring to young patients in manic phase⁸⁰. Body Mass Index (BMI) and thyroid hormone are monitored regularly before and during lithium treatment, together with creatinine clearance and (Glomerular Filtration Rate) GFR which is an indicator of renal function, since renal dysfunction is the most severe and life threatening side-effect of lithium salts.

1.2.1 Mechanism of action

Despite being extensively studied, lithium's pharmacodynamic mechanism remains elusive. For a very long time, there have been two most prevalent theories:

Inositol monophosphatase (IMPase) inhibition within the phosphatidylinositol (PI) signalling pathway and glycogen synthase kinase 3 β (GSK3 β) inhibition. A schematic representation of the principal molecular pathways implicated in lithium's response is depicted in Figure 1. Lithium is presumed to block the action of these enzymes by competing with the cofactor magnesium. In fact lithium has similar radius and physical properties with magnesium. However, lithium has a low affinity for magnesium binding sites, and hence is not threatening vital cell functions.

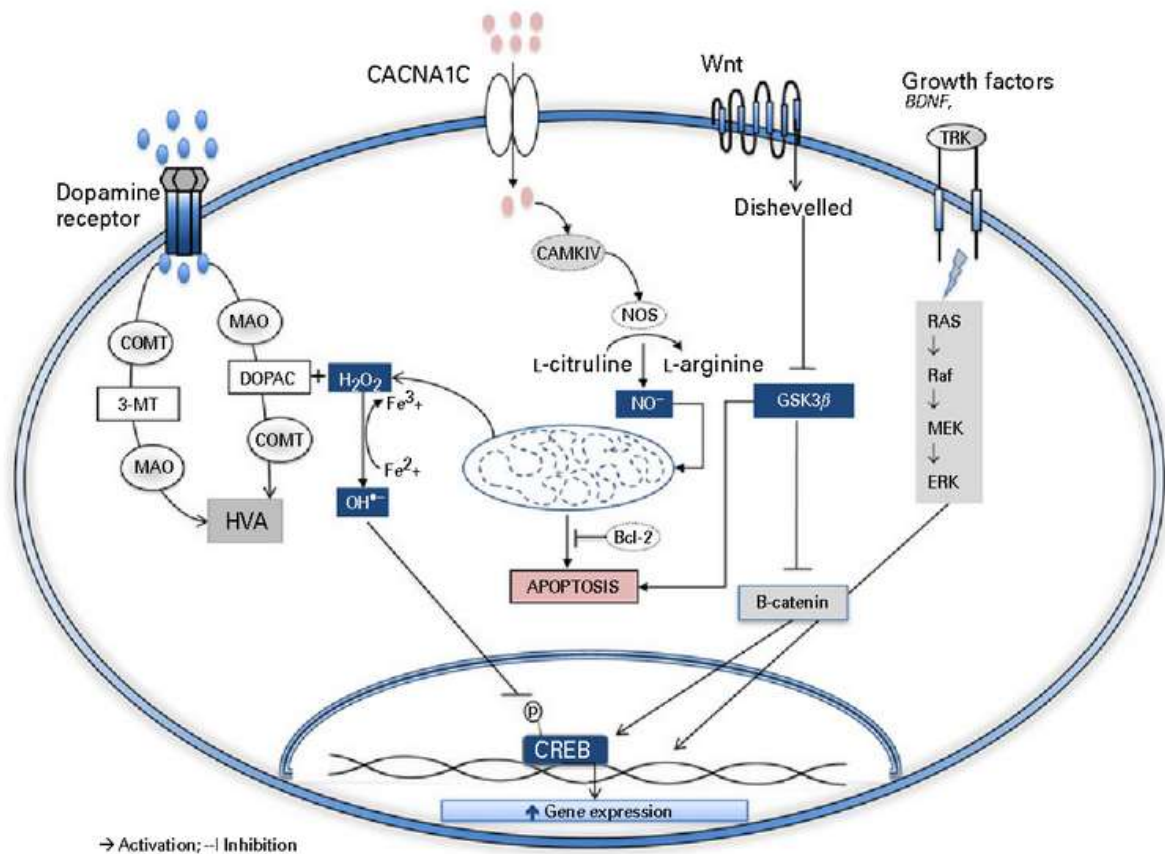


Figure 1: *Molecular pathways of action for lithium, in order from left to right: Dopamine neurotransmission, Calcium homeostasis mediated by Voltage-dependent calcium channels, Wnt pathway / GSK3β inhibition and subsequent β-catenin induction, BDNF neurotrophin and bcl-2 antiapoptotic factor induction. Many of these pathways are mediated by CREB transcription factor and phosphorylation which is reduced in the presence of lithium. Other pathways act through ROS production or nitric oxide induced stress, while lithium prevents intracellular stress by regulating neurotransmission, calcium homeostasis and regulating levels of pro-apoptotic, neurotrophic, proinflammatory and antiinflammatory factors.*

CACNA1C: Voltage-dependent calcium channel α-1 subunit, GSK3β: Glycogen Synthase Kinase 3β, Wnt: Wingless-related integrated site, BDNF: brain-derived neurotrophic factor, TRK: tyrosine kinase, COMT: catechol-O-methyltransferase, MAO: monoamine oxidase, 3-MT: 3-methoxytyramine, DOPAC: 3,4-dihydroxyphenylacetic acid, HVA: homovanillic acid, GSK3: glycogen synthase kinase 3, CREB: c reactive element, blue circles: dopamine, red circles: calcium calmoduline kinase IV (CAMKIV) ⁸¹.

The inositol pathway

Allison and Stewart's work first reported the ability of lithium to deplete myoinositol in vivo ⁸². Normally, an agonist binds to a receptor complex consisting of a receptor, Gq-protein and phospholipase (PLC). PLC hydrolyses the phospholipid phosphatidylinositol 4,5-bisphosphate (PIP₂) to form two second messengers: inositol-1,4,5 triphosphate (IP₃) and 1,2-diacylglycerol (DAG). IP₃ binds to specific receptors to help open the calcium (Ca²⁺) channel and DAG initiates activation of protein kinase C (PKC). IP₃ is sequentially broken down into inositol bisphosphates (IP₂) and then inositol monophosphates (IP). Myoinositol has a crucial role in PI signaling pathway, serving as a substrate for synthesis of phosphatidylinositol (PI) from IP, which is phosphorylated to form mono-, bis- and tris- phosphatidylinositol, closing in that way the cycle and resulting in the regeneration of this pathway. Within the PI signalling pathway the enzyme IMPase and other phosphoinositol phosphatases typically regenerate myo-inositol from IP ⁸³.

In BD patients, myoinositol levels are higher than normal ⁸⁴. Lithium, in therapeutic doses inhibits IMPase and other phosphoinositol phosphatases by binding on their catalytic core. These enzymes are involved in the metabolism of inositol, leading to myoinositol depletion, which in turn prevents the resynthesis of PIP₂ and subsequent formation of IP₃ and DAG, affecting cell signaling ^{83,85}.

Glycogen kinase synthase 3 beta (GSK3β) inhibition

It has been shown that lithium is able to modulate mechanisms involved in the development of *Drosophyla*, *Dictyostelium*, *Xenopus* etc, through GSK3β inhibition ^{86,87}. Lithium inhibition of purified GSK3β construct in sub-therapeutic concentrations confirmed that interaction. The mechanism is either direct by competing with Mg²⁺ cofactor, although such effect would require higher than therapeutic levels of Li, or the scenario implicates the indirect inhibition of GSK3β by increasing Ser21/Ser9 phosphorylation. Animal studies have shown that inhibition of GSK3β has antidepressant and antimanic effects, while high GSK3β levels lead to manic-like phenotypes ⁸⁸. GSK3β increases β-catenin levels, known to have antidepressant effects, and inactivates Wnt-related integration site (Wnt) pathway which plays a role in many cellular functions such as neural development, synapse formation, and neuronal plasticity. Furthermore, GSK3β seems to play a role in other neurodegenerative and psychiatric diseases and except for lithium, other neuropsychiatric drugs inhibit GSK3β and increase β-catenin levels as well. Through lithium and GSK3β/β-catenin pathway several neurotrophins including IGFII ^{89,90}, BDNF ²⁶ and VEGF ⁹¹ are increased. Closing the cycle, neurotrophins induce inhibitory Ser9-phosphorylation of GSK3β ⁹². Another neurotrophin, IGFI, that has been found upregulated in responders vs non-responders to lithium ³¹, increases β-

catenin levels ⁹³. as well as BDNF levels through a different pathway resulting in increased brain plasticity ⁹⁴. GSK3 function is also linked to (cAMP) response element binding protein (CREB) activity that is inhibited by GSK3 (and the inhibition is attenuated by lithium). CREB, a transcription factor with multiple targets, regulates among others BDNF neurotrophin and B-cell lymphoma 2 (bcl-2) apoptotic protein ⁹⁵. CREB and BDNF polymorphisms have been also associated with lithium response ⁹⁶. GSK3 activity is also subject to inhibitory regulation by protein kinase B (Akt). Akt activation leads to reduction of apoptotic mechanisms and this effect is mediated by β -arrestin.

Neuroprotection Theory

Neuroimaging studies have reported that lithium can increase the volume of grey matter in the human brain ^{97,98}. Moreover, lithium increases neurogenesis in rat hippocampus ⁹⁹ and is preferentially accumulated in neurogenic brain regions ¹⁰⁰. Several mechanisms have been proposed as responsible for lithium's neuroprotective actions. Extensive research in that direction has concluded that lithium prevents excitotoxicity, inhibits apoptosis, regulates autophagy, promotes cell survival and enhances neuronal plasticity ⁹⁵. Glutamate-induced excitotoxicity has been implicated in many neurodegenerative diseases. In this process, stimulation of N-methyl-D-aspartate (NMDA) receptors by glutamate causes an excessive influx of calcium into the cell, thus activating apoptotic mechanisms. Jakopec et al (2008) explored the effect of lithium pretreatment on glutamate induced excitotoxicity on human glioblastoma ¹⁰¹. Findings from this study showed that lithium promotes cell survival by activating anti-apoptotic factors. In other cases lithium prevented apoptotic-dependent cellular death through bcl-2 regulation and increase of SIX homeobox 1 (SIX1) transcription factor ^{102,103}. Bcl-2 is a key member of the best characterized family of proteins involved in apoptosis. It promotes cell survival by preventing the mitochondrial release of cytochrome C. In a study by Chen et al. (1999), lithium doubled levels of bcl-2 in the frontal cortex of rats ¹⁰⁴, suggesting possible involvement of lithium in mitochondria mediated neuroprotection.

Besides glutamergic neurotransmission, dopaminergic excitatory and GABAergic inhibitory neurotransmission are also affected in BD ¹⁰⁵. Glutamergic and dopaminergic pathways are thought to be involved in BD by inducing oxidative stress and NO production, respectively, while GABAergic neurotransmission is believed to have a beneficial effect.

It is likely that lithium exerts neuroprotective actions through modulating secondary signals regulated by the above neurotransmitters. These secondary messengers are most likely to be mechanistic Target of Rapamycin kinase (mTOR) and CREB. These mechanisms are involved in neurotrophin regulation; specifically, CREB's phosphorylation resulted in a decrease in the transcription of

important genes encoding for neurotrophins and it has been shown that lithium decreases the levels of phosphorylated and unphosphorylated CREB ¹⁰⁵⁻¹⁰⁷. An important neurotrophin regulated by lithium is BDNF. By influencing BDNF, lithium promotes neuronal survival and neural plasticity ¹⁰⁸. Moreover, Synapsin II (SYN2), upregulated by lithium and responsible for neuronal plasticity, is another candidate mediators of lithium's actions ¹⁰⁹. Finally, although the autophagy idea is still under debate regarding BD, lithium is known to regulate autophagy through the inositol pathway and GSK3 β inhibition in opposite directions ¹¹⁰. Lithium's neuroprotective actions can explain how lithium not only halts BD symptomatology but also might stall BD's progression and cognitive impairment. The evidence that support lithium's neuroprotective and neurogenerative actions are compelling and the most promising mediators of these actions are BDNF, bcl-2, CREB and GSK3 β , however, the exact mechanism and whether neuroprotective and neurogenerative actions of lithium are necessary for its therapeutic action remain to be resolved ¹¹¹.

1.2.2 Lithium Pharmacogenomics

A vast body of evidence correlates lithium response with a number of gene variations, thus supporting the strong genetic background of lithium response (reviewed in Alda, (2015) ⁹⁵ and Severino et al., (2013) ¹¹²). Moreover, excellent responders to lithium show similar clinical characteristics and heritability of response ¹¹³, advocating the notion that lithium response depends on genetic factors. The first indicator of lithium's response heritability was that offsprings of BD patients, responders to lithium had higher chances of responding to lithium when the disease was manifested. Apart from the genetic factors that determine response heritability, late onset of the disease, fewer hospitalizations, episodic course and a pattern of mania preceding depression ¹¹⁴ also predict a favorable response to lithium treatment. Since genetic heterogeneity reduces the power to identify significantly associated variants, studies focusing on homogeneous subgroups, such as lithium responders, may be more fruitful in identifying BD associated variants. This assumption led to several studies which proved that response to lithium is useful for the categorization of bipolar patients in more homogenous subgroups ^{31,51,63,113,115-118}. Initially, research in the field was based on linkage and candidate gene association studies. These studies were less informative than expected and gave plenty of negative results. Two linkage studies in Danish and Canadian populations indicated locus 18q23 and 7q11, respectively, as related to BD, but did not indicate any specific genes ¹¹⁹. On the contrary, association studies identified correlations with polymorphisms of genes belonging to several pathways, including neurotransmitter signaling, inositol pathway, circadian clock regulation, calcium homeostasis etc. These genes are dopaminergic receptor D1 (*DRD1*) ^{120,121}, tyrosine kinase *FYN* ^{121,122}, inositol

polyphosphate 1-phosphatase (*INPP1*)¹²³, *CREB1*¹²⁴, *Rev-Erba*^{125,126}, calcium channel gamma-2 subunit (*CACNG2*)¹²⁷, disrupted in schizophrenia 1 (*DISC1*) and glucocorticoid receptor (*NR3C1*)¹²⁸. One important finding from the association studies was that the combination of the short allele of the serotonin transporter gene (*5-HTTLPR*) and two Val alleles of the Val66Met polymorphism of *BDNF* gene are interpreted as 70% chances of non-response to lithium¹²⁹. Technology and GWAS studies gave the possibility to explore a wide range of common variant and overcome the limitation of candidate genes and family focused approaches. The most important GWAS studies regarding lithium response are presented on Table 1.

However, with the exception of Consortium for Lithium Genetics (ConLiGen) study, findings from

Gene or locus	SNP	p-value	pathway	phenotype	Sample origin	Sample size	Validation/Replication status	Reference
10p15	rs10795189	5.5×10^{-7}		lithium response	STEP-BD	458 treated with lithium	359 bipolar I or II University College London cohort	¹¹⁸
<i>ACCNI</i>	rs11869731	7.21×10^{-6}	cation channel	full responders vs non-responders	Sardinians	52 BD patients	validation group 204 BD	¹³⁰
<i>GADLI</i>	rs17026688 rs17026651	5.50×10^{-7} 2.52×10^{-7}	glutamergic	lithium response	Han Chinese	294 BPI characterized for response by alda scale	replication 100 patients, not replicated in european populations	¹³¹
<i>SESTD1</i>	rs116323614*	2.74×10^{-8}	phospholipids	responders vs controls	Swedish and British	1639 subjective responders and 8899 controls; 323 objective responders and 6684 controls	validated	⁶³
<i>AL157359.3</i> <i>AL157359.4</i>	<i>rs74795342*</i> <i>rs75222709*</i> <i>rs79663003*</i> <i>rs78015114*</i>	3.31×10^{-9} 3.5×10^{-9} 1.37×10^{-8} 1.31×10^{-8}	long non-coding RNAs (<i>lncRNAs</i>)	categorical and continuous ratings of lithium response	22 sites (US, Canada, Japan, Taiwan, Australia and Europe)	2935 patients	Independent study including 73 patients	¹³²

ACCNI: amiloride-sensitive cation channel 1 neuronal, *GADLI*: glutamate decarboxylase-like protein 1, *SESTD1*: *SEC14* and spectrin domains 1, STEP-BD: US -Systematic Treatment Enhancement Program for Bipolar Disorder, * genome wide significant

other GWAS did not surpass the genome wide significance level when confronting responders versus non-responders. Similarly, GWGE studies fail to capture the subtle differences in gene expression caused by lithium, suggesting the need of much larger samples and associations like ConLiGen. All

these suggest that, as for BD, SNPs and single transcripts involved in lithium response have small effect sizes, supporting the notion that many genes are involved and there is a significant contribution of environmental factors. This lead the latest research towards epigenetics. Epigenetics consist in the field that studies heritable post transcriptional regulators of gene expression that do not alter DNA sequence, yet can be influenced by environmental factors.

1.3 Epigenetics

1.3.1 Definition

Epigenetic mechanisms are responsible for the interaction between the environment and the genetic intracellular architecture, resulting in fine regulation of the gene expression. Epigenetics are referred to as the mechanisms involved in the regulation of gene expression by inducing inheritable genetic modifications without altering the DNA sequence; instead they consist in post-transcriptional modifications and regulators ¹³³. The epigenetic machinery is comprised of three highly interrelated pathways: the DNA methylation, histone modifications and chromatin remodeling, but also non-coding RNAs are now being considered as part of the epigenetic machinery ^{133,134}.

1.3.2 Epigenetics of mood stabilizers

Classical molecular biology methods and genetic studies have provided us with a vast body of knowledge around mechanisms involved in BD pathogenesis and treatment response; however, the incomplete heritability of the disease is expected to be explained through environmental factors and possibly through epigenetic modifications accumulated in ones genome. A growing body of evidence supports the involvement of epigenetic mechanisms in mood disorders ¹³⁵ and it is known now that psychotropic medications interfere with the epigenome as well ¹³⁶.

Mood stabilizers are also believed to be at least partly related to epigenetic modifications. For example, VPA, a mood stabilizer frequently used instead of lithium, is the most extensively investigated in regard to epigenetic effects. This drug is an inhibitor of class I and II histone deacetylases (HDAC) activity and thus increases acetylated histone H3 (H3ac) and acetylated histone H4 (H4ac) ¹³⁷. VPA has been suggested to act by reversing the downregulation of GABAergic genes observed in BD patients ¹³⁸. The interest is now being focused on the epigenetic effects of lithium after several failed attempts of replicating lithium associated genes, and the most prevalent

mechanisms (GSK3 β inhibition and inositol pathway) still have many gaps to be filled ¹³⁹. Animal studies showed that therapeutic lithium levels do not particularly effect global DNA methylation or histone marks, but can selectively regulate target genes associated with BD. As an example we have the BDNF promoter that is selectively demethylated by lithium and as a result the BDNF levels increase. This effect was held responsible for lithium's, neuroprotective actions ¹⁴⁰. This is only one of lithium's epigenetic actions. Recently, findings from the largest GWAS conducted so far on lithium response suggested the involvement of long non-coding RNAs in modulating lithium response ¹³². As a result interest of later epigenetic studies on lithium's response have turned towards non-coding RNAs and specifically microRNA regulation. Interestingly, Moreau et al, (2011) ¹⁴¹ found a general reduction of miRNAs in BD patients and changes on the genomic sequence in regions encoding miRNA biogenesis-related proteins, which evoke alterations of the expression of a large subset of miRNAs, that have been associated with an increased risk for psychiatric disorders ¹⁴². It has become clear that there is some effect of the treatment on these mechanisms but the exact mechanism, the direction and the impact of these changes remains to be explored.

1.4 microRNAs

Our genome consists of approximately 2% coding regions including their 5' and 3' untranslated regions (UTRs) and the rest is not coding for any proteins. That does not mean that non coding segments of the DNA do not possess important functions. In fact, many non-coding regions are transcribed into non-coding RNAs. MicroRNAs or miRNAs are the smallest non-coding RNAs.

MiRNAs are single stranded ribonucleic acid chains 19 - 30 nucleotides long, closely associated with Argonaute (AGO) family proteins. Usually, they are well conserved among species, especially when closely related species are considered. MiRNAs are present in most somatic tissues. Their most well-known and diffused function is the regulation of mRNA levels. Therefore, they are considered post transcriptional regulators of transcription. Moreover, findings demonstrate the inheritance of acquired traits through miRNAs. As a result, miRNAs are categorized and examined as epigenetic factors together with methylation of DNA and histone modifications.

1.4.1 Biogenesis

1. *miRNAs are transcribed as pri-miRNAs*

MiRNAs are originally transcribed in the nucleus of the cell like other RNAs, but from RNA polymerase II as part of primary polyadenylated transcripts folded into structures called pri-miRNAs.

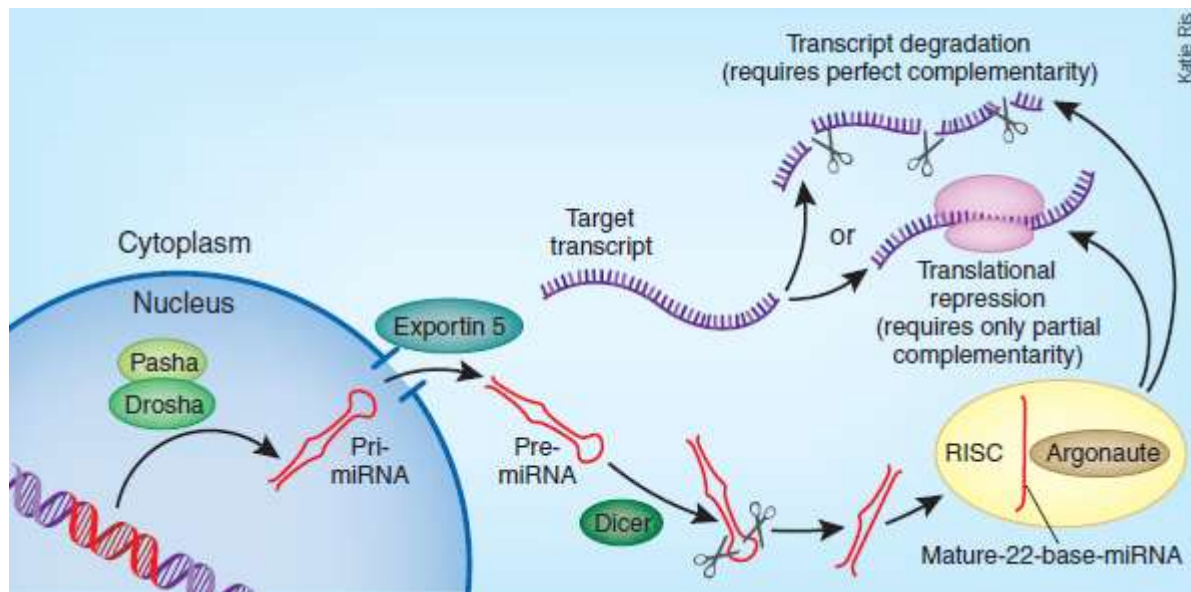


Figure 2: *miRNA biogenesis and function*¹.

Polymerase III is also a candidate enzyme possibly responsible for their transcription, but known miRNAs transcribed from introns of host genes are known to be transcribed by RNA polymerase II. The rest that are found close to host genes are believed to have their own regulatory elements and transcribed by polymerase III, because they do not possess the necessary polyadenylation signals. Pri-miRNAs are cleaved by Drosha enzyme (RNase III endonuclease).

2. Precursor miRNAs (pre-miRNAs) formation

Drosha recognizes the 2ndary structure of the primary stem loop and the elements flanking the stem loop generally within 125 nucleotides of the miRNA and cuts the RNA duplex pri-miRNA at one end forming 60 -70 nucleotides long hairpin shaped precursor miRNAs (pre-miRNAs) which have a 5' phosphate and 2 nucleotide 3' overhang.

3. Transportation out of the nucleus and mature miRNA formation

Subsequently, the Drosha processed products exit the nucleus with the help of the receptor Exportin-5 and Ran-GTP, which actively transport the pre-miRNAs from the nucleus to the cytoplasm. When ejected from the nucleus, pre-miRNAs are enzymatically cleaved by Dicer (RNase III endonuclease) to form mature miRNAs, which consist in the functional unit of miRNAs. Dicer actually cleaves the pre-miRNA two helical turns away from the base of the stem loop at the one end of the precursor, thus removes loop and terminal base pairs. Dicer cuts double stranded RNA but does not recognize

any specific sequence, for that reason Drosha, which determines the correct register of cleavage within the miRNA precursor, defines both mature ends of the miRNA (Figure 2).

4. *Mature miRNA and their function*

At this point the short lived double stranded miRNA:miRNA* is produced. The antisense miRNA star (miRNA*) is a single stranded RNA, complementary to the mature miRNA and soon after Dicer cuts the precursor it is separated from its complementary strand as a byproduct of this reaction¹⁴³⁻¹⁴⁶. According to Ko et al., (2008)¹⁴⁷ miRNA* can act as a miRNA as well. The RNA-induced silencing (RISC) complex is responsible for the enzymatic production of the mature miRNA as well as for the recognition and binding on the mRNA target. AGO proteins are the catalytic endonuclease components of RISC. Dicer–TARBP2 (TAR RNA-binding protein 2) loads the complex into a member of the AGO protein subfamily to form the RISC. The mature single stranded miRNA is bound to RISC complex and is believed to guide the complex to the complementary region of the targeted mRNA.

1.4.2 Functions

MiRNAs usually exert their regulatory actions by binding on the 3'UTR of the mRNA target through their seed region. The seed region consists in the nucleotides 2 to 8 of the mature sequence situated at the 5' end of the mature miRNA. The seed region complementarity can be either complete or containing mismatches leading to either degradation or to the cease of translation of the mRNA. As a result, in both cases we have decreased levels of translation with decreased or increased levels of mRNA, respectively. The mechanism of silencing is significantly associated with the complementarity of the miRNA to 3'UTR region of the mRNA and the incorporation of the miRNA to the RISC complex. High complementarities lead to degradation and lower complementarities to inhibition of the translation¹⁴⁶.

1.4.3 MicroRNAs as biomarkers

The overall importance of miRNAs in disease state and normal organism development and functions was first demonstrated through the genetic deletion of the miRNA biogenesis enzyme Dicer¹⁴⁸. We are aware of the existence of circulating nucleic acids in human plasma and serum since 1950s¹⁴⁹. Since then, the miRNAs have been characterized as biomarkers for various types of cancer, organ injury, metastasis, some conditions and psychiatric diseases. Differential miRNA expression using a

combination of next generation sequencing platforms with the gold standard quantitative Real Time PCR (qRT-PCR) have been successfully used for biomarker identification ^{150,151}. Circulating miRNAs show remarkable stability and demonstrate consistent expression profiles between healthy controls and patients. MiRNA biomarkers are becoming a useful tool for diagnosis and prognosis but also provide insight into disease pathogenesis and the mechanisms of action of the respective treatments.

1.4.4 MicroRNAs in BD

The failure of genetic association studies to shed significant light on missing heritability of BD led to the assumption that environmental factors play a defining role to the etiopathogenesis of the disorder. Epigenetic mechanisms are known to mediate the environmental influences through post transcriptional regulation.

Issler and Chen ¹⁴² and Kocerha et al. ¹⁵², in 2015 reviewed the impact of miRNAs in psychiatric research and Fries et al. (2017) ¹⁵³ in BD. In their reviews, numerous examples of experiments with human patients, animal and cellular models were presented, that investigated the role of miRNAs in the susceptibility to the disease and in the pathogenesis mechanism. For examples of experimental approaches see Figure 3. Studies conducted on either post-mortem or peripheral tissue of BD patients follow in general two basic approaches. The first one uses high throughput data or candidate regions to identify genomic loci (chromosomal deletions, insertions, duplications or copy number variations (CNVs)) or SNPs that affect miRNAs' levels and as a result, impede interactions with the mRNA target ¹⁵⁴ or inhibit the assembly of the miRNA-mRNA-Dicer complex.

Most studies on BD have identified SNPs that when present possibly lead to variable levels of the related miRNA in BD ^{155,156}. Some of these studies also indicate one or more inverse correlated targets ¹⁵⁵. The miRNAs and the respective SNPs and mRNA targets associated with BD are listed in Table 2. Most of the data in Table 2 come from GWAS. Exception in that list are Guella et al., (2013) ¹⁵⁷, Duan et al., (2014) ¹⁵⁸ and Fiorentino et al., (2016) ¹⁵⁹ studies which investigate previously correlated with BD candidate loci, and Kandaswamy et al., (2014) ¹⁵⁴ who found association between rs36175829 in the 3'UTR of Glutamate Metabotropic Receptor 7 (*GRM7*) and BD. This SNP is target for several miRNAs, however, the interactions were not confirmed experimentally.

Table 2: miRNA polymorphisms associated with BD and Lithium response and/or action					
miRNA	mRNA target	Method	Phenotype	Variant	Reference

miR-137	<i>TCF4</i>	Candidate SNP associated with BD and SCZ	Controls	rs1625579 (TT)	157
miR-137		GWAS	BD (mixed sample: BD, SCZ, MDD, ASD, ADHD)	rs1625579	156
miR-182		RNA-Seq	BD	rs76481776 T	160
miR-137/miR-2682		Sequencing 6.9 kb MIR137/MIR2682 regions	BD	1:g.98515539A>T	158
miR-708	<i>NRAS and CREB1</i>	GWAS	BD	rs7108878	155
miR-640		GWAS	BD	rs2965184	155
miR-644		GWAS	BD	rs7269526	155
miR-135a-1		GWAS	BD	rs9311474	155
miR-581		GWAS	BD	rs697112	155
miR-611		GWAS	BD	rs174535	155
let-7g		GWAS	BD	rs6445358	155
miR-499	<i>GPC6, C16orf72, WDR82 and CACNB2</i>	GWAS	BD	rs3818253	155
miR-1908	<i>KLC2</i>	GWAS	BD	rs174575	155
miR-708		HRM, candidate miRNA from GWAS	BD and SC Z	rs754333774	159
BD: Bipolar Disorder, SCZ: Schizophrenia, MDD; Major Depressive Disorder, ASD: Autism Spectrum Disorders, ADHD: Attention-Deficit/Hyperactivity Disorder, <i>TCF4</i> : Transcription factor 4, <i>NRAS</i> : NRAS Proto-Oncogene, <i>CREB1</i> : cAMP Responsive Element Binding Protein 1, <i>GPC6</i> : Glypican 6, <i>C16orf72</i> :Chromosome 16 open reading frame 72, <i>WDR82</i> : WD Repeat Domain 82, <i>CACNB2</i> : Calcium Voltage-Gated Channel Auxiliary Subunit Beta 2, <i>KLC2</i> : Kinesin Light Chain 2					

The second approach focuses on the expression profiles of candidate genes (eg. involved in neural system functions, specifically expressed in human brain, associated with psychiatric disease etc.), or high throughput methods searching for differences between two cohorts. These studies usually use peripheral tissues or post-mortem brain samples. This approach has been widely applied for BD and its findings are listed in Table 3.

miRNA	Up/Down Regulation	Phenotype	Tissue/Cells	mRNA target	Detection Method miRNA/mRNA	Reference
-------	--------------------	-----------	--------------	-------------	-----------------------------	-----------

miR-720 miR-140-3p miR-1973 miR-30d-5p miR-3158-3p miR-330-5p, miR-378a-5p miR-4521 miR-21-3p	↑	BD	Whole blood	-	miRNA array/in silico mRNA prediction	161
miR-1915-5p miR-1972 miR-4793-3p miR-4440	↓	BD	Whole blood	-	miRNA array/in silico mRNA prediction	161
miR-504	↑	BD	Postmortem brain (PFC)	-	Taqman Low Density Array	162
miR-140-3p miR-29a miR-454* miR-520c-3p	↓	BD	Postmortem brain (PFC)	-	Taqman Low Density Array	162
miR-33 miR-330 miR-192 miR-193a miR-193b miR-545 miR-138 miR-151 miR-210 miR-324-3p miR-22 miR-425 miR-181a miR-106b miR-301 miR-27b miR-148b miR-338 miR-639 miR- 15a miR-186 miR-99a miR-190 miR-339	↓	BD	Postmortem brain (PFC)	-	qPCR	141
miR-29c	↑	BD	Postmortem brain (PFC extracellular vesicles)	-	miRNA arrays	163
miR-383 miR-32 miR-490-5p miR-196b miR-513-5p miR-876-3p miR-449b	↑	BD	Postmortem brain	-	miRNA array	164

miR-297 miR-188-5p miR-187						
miR-145-5p, miR-485-5p, miR-370, miR-500a-5p, miR-34a-5p	↓	BD	Postmortem brain (PFC)	-	high throughput RT-PCR plates	165
miR-17-5p, miR-579, miR-106b-5p, miR-29c-3p;	↑	BD	Postmortem brain (PFC)	-	high throughput RT-PCR plates	165
miR-182	↑	BD, SCZ, MDD	Hippocampal dentate gyrus granule cells	-	RNA-Seq	160
miR-34a	↑	BD	Postmortem brain (cerebellum) and patient derived neurons	<i>ANK3</i> , <i>CACNB3</i>	qPCR and target prediction using BD GWAS genes	166
miR-34a	↓	BD	Postmortem brain (anterior cingulate cortex)	<i>PDE4B</i> , <i>NCOA1</i>	qPCR/luciferase assay	167
miR-184	↓	BD	Postmortem brain (anterior cingulate cortex)	<i>NCOR2</i> , <i>PDE4B</i>	qPCR/luciferase assay	167
miR-132, miR-133a, miR-212	↓	BD	Postmortem brain (anterior cingulate cortex)	-	qPCR	167
miR-499 miR- 708 miR-1908	↓	BD, depression vs remission	Peripheral blood	-	qPCR	168
miR-149	↑	BD	Postmortem brain anterior cingulate cortex (glial cells)	-	qPCR	169

BD: Bipolar Disorder, ↑: upregulated, ↓: downregulated, RT-PCR: Real Time PCR, MDD: Major Depressive Disorder, SCZ: Schizophrenia, qPCR: quantitative PCR, PFC: Prefrontal Cortex, *ANK3*: ankyrin-3, *CACNB3*: voltage-dependent L-type calcium channel subunit beta-3, *PDE4B*: Phosphodiesterase 4B, *NCOA1*: Nuclear Receptor Coactivator 1, *NCOR2*: Nuclear Receptor Corepressor 2

Besides miRNA as susceptibility marker we are often interested in the cellular effects of miRNA dysregulation. This usually translates into a mechanism of action and explains how the miRNA under study exerts its actions. For that reason, some of the studies also investigated the expression of mRNA targets by performing in vitro functional experiments. The interaction between miRNA and its target was investigated using either the gold standard luciferase assay¹⁶⁷ and/or qPCR using available cell lines, like HEK293. Bavamian et al., (2015)¹⁶⁶ were the only one to search for the miRNA-mRNA inverse correlation in BD patients derived neurons, reporting miR-34a over-expression that negatively regulates candidate genes for BD, namely *ANK3* and *CACNB3*; the miRNA-mRNA

interaction was confirmed with luciferase assay. Other studies combined bioinformatic approaches and pathway analysis to predict possible pathways regulated by the dysregulated miRNA ¹⁶¹.

1.4.5 MicroRNAs in lithium response

Indirect evidence of an association between miRNAs and BD also comes from a few studies suggesting an effect of medications typically used for the treatment of patients, such as mood stabilizers ¹⁷⁰, antipsychotics ^{171,172} and antidepressants (miR-1202: Lopez e al., 2014, miR-355: Li et al., 2015 and miR-124: He et al., 2016) ¹⁷³⁻¹⁷⁵ on miRNA expression.

In the last decades, the involvement and importance of miRNAs in drug response has drawn the interest of many researchers ¹⁷⁶. It is now becoming clear that alterations to miRNA levels may be one of the therapeutically relevant downstream effects of psychotropic drugs.

One of the first studies to examine miRNAs as potential targets of psychoactive drugs investigated if chronic treatment with the mood stabilizers lithium and valproate could influence hippocampal miRNA levels in rats ¹⁷⁷. Later studies focused on cell lines of human origin for expression studies

Table 4: miRNA dysregulated in lithium response

miRNA	Up/Down Regulation	Phenotype	Model	mRNA target	Detection Method miRNA/mRNA	Reference
miR-134	↓	BD drug naive, increasing after treatment	plasma	-	qPCR	178
miR-34a	↑	Li in vitro D4 and 16	LCLs	<i>VCL</i>	qPCR	179
miR-221	↑	Li in vitro D4 and 16	LCLs	<i>SRAED3NL</i> , <i>YWHAG</i> , <i>PRPF18</i>	qPCR	179
miR-152 miR-155	↑	Li in vitro D4 and 16	LCLs	-	qPCR	179
let-7b let-7c miR-30c miR-221	↓	Chronic Li or VPA in vivo	Rat hippocampus	-	miRNA arrays	177
miR-144	↑	Chronic Li or VPA in vivo	rat hippocampus	-	miRNA arrays	177
miR-34a miR-24 miR-128a	↓	Chronic Li or VPA in vivo	rat hippocampus	<i>GRM7</i> , <i>THRb</i> , <i>DPP10</i>	miRNA arrays/Western blot	177
miR-182 miR-147	↑	Li and VPA combined in vitro	rat CGCs	Reversing glutamate	miRNA arrays	180

miR-222				induced excitotoxicity		
miR-690 miR-34a miR-495	↓	Li and VPA combined in vitro	rat CGCs	Reversing glutamate induced excitotoxicity	miRNA arrays	180
miR-27b miR-125a-3p miR-324-3p	↓	R vs nR	PBMCs	<i>VNN3</i>	miRNA arrays / microarray + target prediction	181
miR-129-5p miR-125a-3p	↓	R vs nR	PBMCs	<i>FBXL13</i>	miRNA arrays / microarray + target prediction	181
miR-143 miR-125a-3p	↓	R vs nR	PBMCs	<i>PRRG4</i>	miRNA arrays / microarray + target prediction	181
miR-1270 miR-125a	↓	R vs nR	PBMCs	<i>ITGAX</i>	miRNA arrays / microarray + target prediction	181
miR-1908-5p	↑	BD, VPA, not Li	NPCs	<i>DLGAP4, GRIN1, STX1A, CLSTN1 and GRM4</i>	qPCR / Luciferase assay	182

BD: Bipolar Disorder, ↑: upregulated, ↓: downregulated, Li: lithium, VPA: Valproate, CGCs: cerebellar granule cells, R: responders, nR: non-responders, LCLs: Lymphoblastoid cell lines from BD patients, PBMCs: Peripheral Blood Mononuclear Cells from BD patients, NPCs: Neural Progenitor Cells from BD patients, D: Day, *VCL*: Vinculin, *ZDHHC11*: Zinc Finger DHHC-Type Containing 11, *YWHAG*: Tyrosine 3-Monooxygenase/Tryptophan 5-Monooxygenase Activation Protein Gamma, *PRPF18*: Pre-mRNA Processing Factor 18, *GRM7*: metabotropic glutamate receptor 7, *DPP10*: Dipeptidyl-peptidase 10, *THRb*: thyroid hormone receptor beta, *VNN3*: Vanin 3, *FBXL13*: F-Box And Leucine Rich Repeat Protein 13, *PIGB*: Phosphatidylinositol Glycan Anchor Biosynthesis Class B, *PRRG4*: Proline Rich And Gla Domain 4, *ITGAX*: Integrin Subunit Alpha X, *DLGAP4*: DLG Associated Protein 4, *GRIN1*: Glutamate Ionotropic Receptor NMDA Type Subunit 1, *STX1A*: Syntaxin 1, *CLSTN1*: Calsyntenin 1, *GRM4*: metabotropic glutamate receptor 4

- peripheral blood mononuclear cells (PBMCs), lymphoblastoid cell lines (LCLs), and neural progenitor cells (NPCs).

Hardly any differentially expressed miRNAs were consistent between studies with the exception of miR-34a. This miRNA was found altered both in patients' LCLs treated with lithium¹⁷⁹ and in the rats' brain^{177,180} but in different directions.

Furthermore, in 2013, Hunsberger et al., (2013) showed that miR-34a increase has apoptotic effects for neuroblastoma cell lines. The same study identified a number of miRNAs that are regulated from the combination of Li and valproate in cells under glutamate induced excitotoxicity. Only one of these miRNAs, miR-609, was altered by the glutamate toxicity induction and returned to normal levels after treatment ¹⁸⁰. Only one study had longitudinal prospective character and was conducted by Rong et al. in 2011, using patients' plasma. Drug naïve patients were sampled before and after treatment and revealed a decrease in miR-134 levels ¹⁷⁸. MiRNAs differentially expressed under lithium influence are listed in Table 4.

In 2016, the largest GWAS on lithium response conducted by ConLiGen resulted in two genome wide significant SNPs located nearby two non-coding transcripts ¹³². This gave GWAS on lithium response a new perspective and some researchers focused on non-coding RNAs and specifically miRNAs, whose functions have been more widely described in comparison with other non-coding transcripts. A recent study, screened candidate miRNA genes associated with BD in previous GWAS and selected more miRNA genes by performing a miRNA gene based analysis of the larger GWAS dataset regarding lithium response (ConLiGen dataset), and discovered SNPs near these miRNAs possibly associated with lithium response: miR-633, miR-607 and miR-499a ¹⁸³ (Table 5). A few years earlier, investigating the hypothesis that miR-206 regulates BDNF, a neurotrophic factor repeatedly associated with BD and lithium response, Ehret et al., (2013) ¹⁸⁴ discovered that interaction of two SNPs, one in miR-206 and one in BDNF, predicts BDI manifestation, as well as treatment response (Table 5).

miRNA	mRNA target	Phenotype	Variant	Reference
miR-633	-	R vs nR (continuous phenotype)	rs1588368	183
miR-607	-	R vs nR (dichotomous phenotype)	rs111682442	183
miR-499a	-	R vs nR	rs117616040	183
miR-206	<i>BDNF</i>	BD and treatment response (Li and VPA)	MIR206 rs16882131 and BDNF rs6265 interaction	117

BD: Bipolar Disorder, Li: lithium, VPA: Valproate R: responders, nR: non-responders

So far there are very few studies investigating miRNA variations with respect to lithium response and mechanism of action and none in regard to adverse reactions. In our study, we used patient derived cell lines and combined Next Generation Sequencing (NGS) of miRNA profiles, microarrays of mRNA expression and bioinformatic methods to detect miRNAs and targets associated with lithium response, as it will be explained in the next sections.

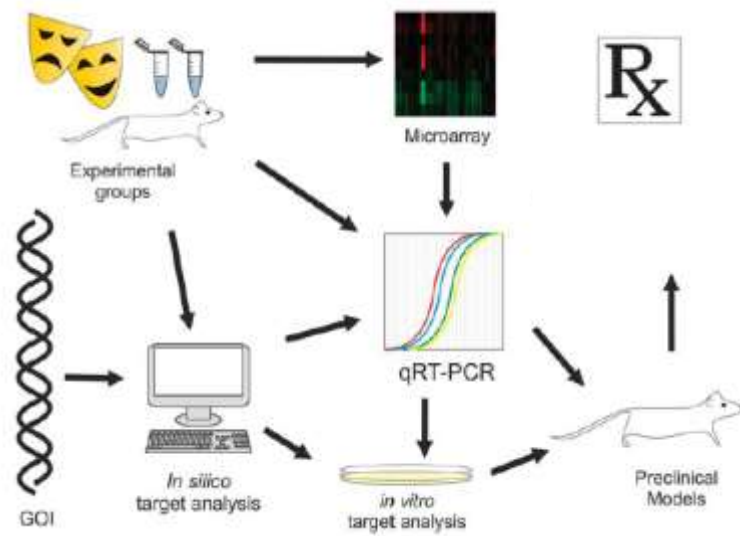


Figure 3: *Methods for the discovery of disease associated miRNAs for pharmacological use. GOI: Gene Of Interest, qRT-PCR: quantitative Real Time –PCR* ².

2. Aim of the study

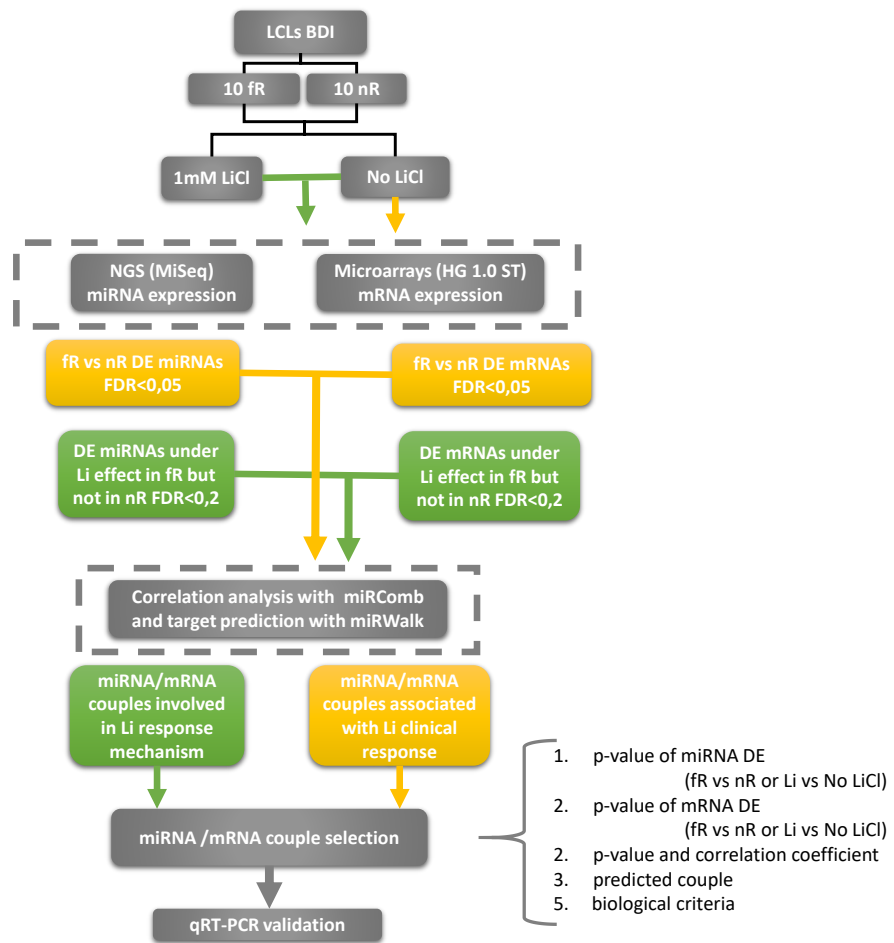


Figure 4: Workflow of the study. LCLs: Lymphoblastoid Cell Lines, fR: full-Responders, nR: non-Responders, LiCl: Lithium Chloride, NGS: Next Generation Sequencing, DE: Differentially expressed, FDR: p corrected False Discovery Rate, Li: Lithium, qRT-PCR: quantitative Real Time PCR

BD is a chronic, recurrent disorder, frequent in general population, which causes functional problems to the patients and high risk of suicide. Lithium salts are first line treatment for BD, yet only 70% of the patients treated respond adequately. The remaining 30% is nevertheless exposed to the risks for severe side effects. These facts underlie the need of predictive biomarkers of response to lithium. Pharmacogenomics is the field that studies the genetic factors responsible for these interpatient differences. So far, several genes have been identified as differentially expressed between responders and non-responders and thus, possibly involved in lithium's mechanism of response. However, lately, epigenetics have been gaining interest as gene regulators in BD and thus, being indirectly involved in the response to lithium. In our study we performed NGS of miRNAs isolated from BDI patients'

LCLs, fR or nR to lithium, treated or untreated with lithium in vitro. The aim of our study was to combine miRNA and mRNA expression data from fR vs nR and identify miRNA-mRNA couples that could help us better understanding the mechanistic link between lithium molecular effects and its clinical efficacy. The miRNA-mRNA couples may also constitute potential biomarkers of lithium response and, as such, their identification may help future implementation of pharmacogenomics for a better management of bipolar disorder.

For this purpose (full workflow shown in Figure 4), we performed genome wide expression profiling of miRNAs and mRNAs using NGS and expression microarrays, respectively, of LCLs from 20 BD patients characterized as fR or nR to lithium. To test the molecular effects of lithium that might be specifically correlated to its clinical efficacy, we split each cell line into two aliquots: one was grown in medium with LiCl 1mM, while the other one was grown in regular medium for one week. This approach allowed us to select miRNAs and mRNAs on which lithium had an effect exclusively in fR and not in nR. We then created lists of differentially regulated miRNAs and mRNAs between fR and nR (untreated LCLs), and between lithium treated vs untreated LCLs from fR (excluding targets influenced by lithium in nR). The list of miRNAs was matched with the list of mRNAs to identify significantly inversely correlated couples. Correlated mRNAs were also checked for in-silico evidence of their regulation by the specific miRNA using publicly available databases. Based on the differential expression p-values, correlation strength, in silico prediction and biological plausibility we selected miRNA-mRNA couples for further validation with qRT-PCR.

3. Materials and methods

3.1 Sample

Our sample consists of 20 BD patients (9 male and 11 females) with diagnosis of BDI, recruited at the Lithium Clinic of the Clinical Psychopharmacology Centre of the University Hospital of Cagliari, Italy. Patients were diagnosed according to Research Diagnostic Criteria (RDC) ¹⁸⁵ and DSM-IV ⁷ criteria, using personal semi-structured interviews [Schedule for Affective Disorder and Schizophrenia Lifetime Version (SADS-L)] ¹⁸⁶ and a systematic review of their medical records. A detailed description of the clinical and demographic characteristics of the subjects can be found in Table 6. The mean age of the sample at sampling was 44 (± 14.2).

Table 6: Demographic and Clinical characteristics of the sample

	fR	nR
Subjects (M/F)	10 (5/5)	10 (4/6)
Age at sampling: years(\pm SD)	45.25 (± 16.14)	44.5 (± 14.10)

To evaluate lithium response, we used the “Retrospective Criteria of Long-Term Treatment Response in Research

Subjects with Bipolar Disorder” (Alda scale), a 11 points-rating scale that measures the degree of improvement in the course of treatment (Criterion A) and weights clinical factors considered relevant for determining whether or not the observed improvement is due to the treatment (Criteria B1–B5). The extensive list of criteria A and B can be found in Table 7 ¹¹³. The scale was developed to evaluate the response to long-term treatment in subjects treated according to routine clinical practice. The combined rating from A and B criteria (Total Score, TS) ranges from 0 to 10, obtained by subtracting the criterion B from criterion A. Criterion A is determined as a change in frequency of affective episodes in the course of treatment on a scale from 0 to 10. The Criteria B1–B5 are rated as 0, 1 or 2 score. The first 2 items of Criteria B represent the recurrence risk, number (B1) and frequency (B2) of episodes before treatment, the third criterion (B3) is based on the length of treatment and the last two B Criteria concern compliance (B4) and use of additional medication (B5) during periods of stability. The scale has been used successfully before for such analysis. In previous studies that used the Alda scale, investigators adopted a total score of 7 as the best cutoff point between patients with no response to lithium treatment (0 to 6) and those with a response (7 to 10). The interrater reliability of the scale was good, with substantial Cohen’s kappa value of 0.66 among different population groups ¹⁸⁷.

For the purposes of our study we only considered patients with TS at the two extreme ends of the Alda scale assuming this translates into a more homogenous sample. Specifically, our sample consisted in 10 full-responders (fR), with $TS \geq 8$ and 10 non-responders (nR), with a $TS = 0$.

Table 7: Retrospective Criteria of Lithium Response in Research Subjects ^a
Criterion A is used to determine an association between clinical improvement and lithium treatment. Criteria B1–B5 establish whether there is a causal relationship between the improvement and the treatment.
A:Rate the degree of response (activity of the illness while on adequate lithium treatment) on the following 10-point scale:
10 Complete response; no recurrences during the course of adequate treatment; full functional recovery at work and at home, no residual symptoms
9 Very good response; no recurrences, but there may be minimal residual symptoms that could include transient anxiety, sleep disturbance, dysphoria, irritability; these symptoms have not required intervention
8 Very good response; illness activity reduced by more than 90%
7 Good response; illness activity reduced by 80%–90%
6 Good response; reduction in the activity of illness by 65%–80%
5 Moderate response; greater than 50% reduction (50%–65%) in illness activity
4 Moderate (35%–50%) improvement, i.e., more than one third reduction of illness activity
3 Mild improvement, reduction of illness activity by 20%–35%
2 Mild improvement (10%–20%)
1 Minimal improvement (0%–10%)
0 Non-response; the frequency, duration, and severity of episodes are unchanged or increased in the course of prophylactic treatment
B: Rate the degree of confidence about the response—subtract 0, 1, or 2 points for each of the following items:
B1: Number of episodes before lithium treatment
0 4 or more
1 2 or 3
2 1
B2: Frequency of episodes before lithium

<p>0 Average to high, including rapid cycling</p> <p>1 Low, spontaneous remissions of 3 or more years on average</p> <p>2 1 episode only; risk of recurrence cannot be established</p>
<p>B3: Duration of lithium treatment</p>
<p>0 2 or more years</p> <p>1 1–2 years</p> <p>2 Less than 1 year</p>
<p>B4: Compliance during period(s) of stability</p>
<p>0 Excellent; documented by serum lithium levels in the therapeutic range</p> <p>1 Good; more than 80% of serum lithium levels in the therapeutic range</p> <p>2 Poor; repeated periods of more than 1 week off lithium treatment; fewer than 80% of serum lithium levels in the therapeutic range</p>
<p>B5: Use of additional medication during the period of stability</p>
<p>0 None, except infrequent sleep medication (1 dose per week or less); no other mood stabilizers, antidepressants, or antipsychotics for control of mood disorder</p> <p>1 Low-dose antidepressants or antipsychotics as an “insurance” or prolonged use of sleep medication</p> <p>2 Systematic use of antidepressant or antipsychotic medications or additional mood stabilizers</p>
<p>C: Ascertain diagnosis of a mood disorder</p>
<p>a. This scale should be applied to the period of treatment closest to optimal, i.e., adequate dosage and least use of medications interfering with the effect of lithium. Martin Alda, M.D.</p>

3.2 Cell cultures and treatment

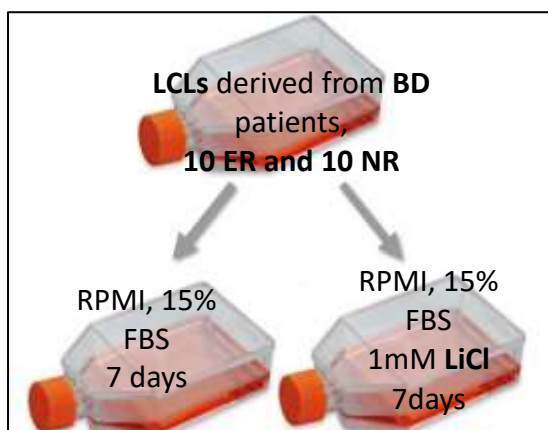


Figure 5: Cell culture and treatment plan

Lymphoblastoid cell lines (LCLs) were established from fresh blood by transforming B lymphocytes with Epstein–Barr virus (EBV) following standard procedures¹⁸⁸. The procedure includes cultivation of PPLO free B96 – 8 cells. At the reaching of 1×10^6 cells in RPMI 1640, supplemented with 10% fetal bovine serum (FBS), 2mM L-glutamine, 100 μ g/ml streptomycin and 100IE/ml penicillin, EBV is isolated from the supernatant by removing all the cells from the marmoset cell line, first by centrifugation and then by

filtering. In parallel patient's heparinized whole blood was mixed 1/1 with RPMI 1640 and mononuclear leukocytes were separated with Ficoll - Hypaque gradient. 2×10^6 leukocytes were resuspended in 1/1 B95-8 supernatant/fresh medium. After 24h, Cyclosporine A (final concentration 1 μ g/ml) was added to the medium and selectively inhibited non B lymphocytes. At the reaching of the confluence state, each cell line was adequately prepared for storage in liquid nitrogen.

For the present study, LCLs were thawed and regrown in RPMI-1640 medium, supplemented with 15% FBS, 1% penicillin/streptomycin, 1%L-glutamine 200 mM and 1% sodium pyruvate 100 mM (Sigma–Aldrich, St. Louis, MO, USA) inside T25 flasks. When they were confluent they were transferred in T75 flasks. Once LCLs reached the required cell count ($6-9 \times 10^6$ cells), they were transferred into 50mL falcons and centrifuged for 10 minutes at 1500 RPM. After having discarded the supernatant we split the cells in two equivalent aliquots by reconstituting the cell pellet in 10mL of full medium and transferred the 5mL of the cell suspension into one separate flask with drug free medium the rest of the cells were re-centrifuged as before, re-suspended in 5mL of medium containing 1 mM LiCl and transferred in a second flask of the same volume. We added drug free or 1mM LiCl medium to each flask, respectively, to achieve a final volume of 15mL. Each flask was cultured at 37°C in a humidified incubator with 6% CO₂ (Figure 5). The medium was changed every two days, this way continuous presence of 1 mM LiCl was warranted, and the volume gradually increased up to 40mL as the number of cells increased. After 1 week of treatment, cells were harvested for total RNA isolation in 750 μ l of QIAzol Lysis Reagent (QIAGEN GmbH - Hilden, Germany). The cells were re-suspended and incubated in QIAzol Lysis Reagent for 5 minutes before stored at -80°C until total RNA extraction.

3.3 Total RNA extraction

For total RNA extraction from the cell pellet of LCLs we used the miRNeasy Mini Kit (Catalog no. 217004) (QIAGEN GmbH - Hilden, Germany). The miRNeasy Mini Kit combines phenol/guanidine-based lysis of samples with QIAzol Lysis Reagent and silica membrane-based purification columns for total RNA extraction, including RNA molecules smaller than ~200 nucleotides (nt) such as miRNAs.

QIAzol Lysis Reagent is a monophasic solution of phenol and guanidine thiocyanate, designed to facilitate lysis of tissues, to inhibit RNases, and also to remove most of the cellular DNA and proteins from the lysate by organic extraction. Homogenization of the cell pellet is achieved simply by vortexing after QIAzol Lysis Reagent addition. We used approximately 1×10^6 cells at this step. The addition of chloroform to the lysate leads to the separation of the organic and the aqueous phase after centrifugation. RNA partitions gather to the upper, aqueous phase, while DNA partitions to the interphase and proteins to the lower, organic phase or the interphase. The upper, aqueous phase was extracted, and ethanol was added to provide appropriate binding conditions to the silica membranes of the columns for all RNA molecules from 18 nucleotides upwards. The sample was then applied to the RNeasy Mini spin column, where the total RNA bound to the membrane and phenol and other contaminants were efficiently washed away. After DNase I digestion and several washing steps total RNA was eluted in RNase-free water. The workflow is depicted in Figure 6.

In the miRNeasy procedure, genomic DNA is removed by organic extraction, but we also used a DNase I digestion step to ensure uncontaminated samples. For the DNase digestion we used the RNase-Free DNase Set (cat. no. 79254) (QIAGEN GmbH - Hilden, Germany) which contains RDD buffer optimized for on column digestion. The RNase-Free DNase Set is not provided in the miRNeasy Mini Kit. DNase was efficiently removed in subsequent wash steps.



miRNeasy Mini Handbook 12/2014

Figure 6: miRNeasy Mini kit workflow for total RNA extraction from cell pellet.

3.4 RNA Quantitation and Quality Control

Total RNA Quantitation

Nucleic acid concentration was measured with Qubit 2.0 Fluorometer. Catalog no. Q32866 (Invitrogen) (Figure 7). The Qubit® 2.0 Fluorometer is a benchtop fluorometer for the quantitation of DNA, RNA, and protein, using the highly sensitive and accurate fluorescence-based Qubit™ quantitation assays. The fluorogenic dyes used in these assays emit signals only when bound to specific target molecules, even at low concentrations, thus minimizing the effects of contaminants, including degraded DNA or RNA.



Figure 7: Qubit 2.0 Fluorometer (Invitrogen)

For the quantitation of total RNA we used the Qubit RNA BR (Broad-Range) Assay Kit. The assay is accurate for initial sample concentrations from 1 ng/μL to 1 μg/μL, providing an assay range of 20–1000 ng.

The kit included:

1. concentrated assay reagent
2. dilution buffer
3. two RNA standards
4. Plastic container (disposable) for mixing the Qubit® working solution
5. Qubit® assay tubes 0.5mL

The standards are actually nucleic acid RNA standards of low emission (standard 1) and high emission (standard 2) that are used by Qubit software to create a standard curve and at the same time they set the minimum and maximum range detected by the fluorometer.

Protocol

- a) Set up 2 assay tubes for the standards and 1 tube for each user sample.
- b) Prepared 200μL of Qubit® Working Solution for each standard and sample by diluting the Qubit® RNA BR Reagent 1:200 in Qubit® RNA BR Buffer.
- c) Prepared the assay tubes (use 0.5-mL PCR tubes) according to the following table:

Volume	Standards	Samples
Working Solution (from step 2)	190 μL	199μL

Standard (from kit)	1 μ L	—
User Sample	—	1 μ L
Total in each Assay Tube	200 μ L	200 μ L

- d) Vortexed standards and samples for 2–3 seconds and incubated at room temperature for 2 minutes.
- e) Selected RNA Broad Range Assay on the Qubit® 2.0 Fluorometer to calibrate with standards and read the samples.

Fragment Analyzer

For the initial quality and quantity control of the total RNA we utilized the Fragment Analyzer™ system. It is a multiplexed capillary electrophoresis (CE) instrument for performing automated, high throughput separation and quantification of nucleic acids (DNA and/or RNA). Separation is achieved by applying an electric field through a capillary array filled with gel matrices designed to separate DNA/RNA molecules by size. Smaller sized fragments are eluted faster than larger sized fragments. Detection is achieved by fluorescence of a sensitive intercalating dye present in separation gel matrix, which fluoresces when bound to double stranded DNA or RNA molecules. The Fragment Analyzer™ system utilizes a high intensity light emitting diode (LED) excitation light source that is focused across the capillary array detection window and imaged onto a sensitive, charge-coupled device (CCD) detector. By monitoring the relative fluorescence unit (RFU) intensity as a function of time during the CE separation, digital electropherogram traces representative of the DNA/RNA content.

For the initial estimation of the quantity of miRNAs in our total RNA samples we used the Small RNA Analysis Kit (DNF-470) which can measure effectively small RNAs, including miRNAs. Capillaries were prepared with intercalating dye and the Small RNA Separation Gel (DNF-262) at 1 μ L/10mL ratio and rinsed according to the manufacturer's protocol. The RNA samples and Small RNA Ladder (DNF-361) were denatured at 70°C for 10 minutes and 2 μ L of each sample was mixed thoroughly with 18 μ L of the Diluent Marker. Samples were loaded on the 12 Capillary Short Array (A2300-1250-3355; 33 cm effective length, 55 cm overall length).

For the Small RNA Libraries' products qualitative and quantitative validation we used the High Sensitivity Small DNA Fragment Analysis Kit (DNF-477) which is most accurate in the range of 50 bp – 1,500 bp. This analysis is possible due to the HS Small Fragment DNA Ladder (DNF-372) and the Small Fragment Separation Gel (DNF-230). To this end samples were denatured and 2 μ L of each

library was mixed thoroughly with 22µl of the Diluent Marker before being loaded on the array (prepared as mentioned to the previous paragraph).

3.5 Next Generation Sequencing (NGS) with MiSeq

3.5.1 Library Preparation and Sequencing

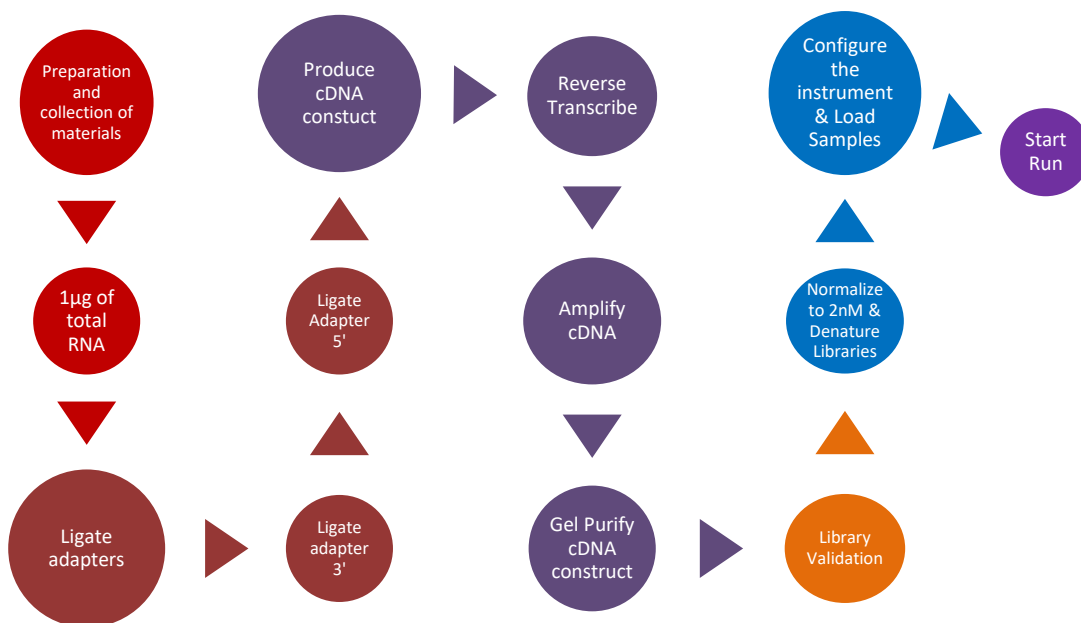


Figure 8: NGS Workflow

For the Library preparation we used the TruSeq Small RNA Library Prep Kit (Illumina, San Diego, CA, US) which contains a core solutions box and the Indices boxes. We followed the Illumina® TruSeq® Small RNA Library Prep protocol for miRNAs and other small RNAs as suggested by the manufacturer for the following steps (workflow on Figure 8; full protocol found in Appendix B):

1. Adapter ligation
2. Production of cDNA construct
3. Purification of cDNA construct
4. Library Validation
5. Normalization and denaturation

6. Run conditions

1. Adapter Ligation

This process describes the sequential ligation of the RNA 3' and RNA 5' RNA adapters to the 3' hydroxyl end and subsequently to the 5'-phosphate group of the mature miRNAs and other Dicer produced species in the sample. First we introduced 3' Adapter to **1µg of total RNA** as measured with Qubit® Fluorometer and heated at 70°C for 2 minutes. Then we added the T4 RNA Ligase and incubated at 28°C. We followed the same procedure to ligate 5' Adapter. After every ligation we kept samples on ice to avoid the formation of secondary structures.

2. Production of cDNA construct

Reverse transcription followed by PCR is used to create cDNA constructs based on the small RNA ligated with 3' and 5' adapters. This process selectively enriches those fragments that have adapter molecules on both ends. PCR is performed with 2 primers that anneal to the ends of the adapters.

The first step in this procedure is to dilute the 25 mM dNTP Mix and prepare 12.5 mM dNTP Mix for all samples. We incubated the 5' and 3' adapter-ligated RNA at 70°C for 2 minutes. We prepared the Reverse Transcription reaction as seen in the following table and added the 5' and 3' adapter-ligated RNA from the previous step.

Reverse Transcription reaction composition

Reagent Volume	(µl)
5X First Strand Buffer	2
12.5 mM dNTP mix	0.5
100 mM DTT	1
RNase Inhibitor	1
SuperScript II Reverse Transcriptase	1
Total Volume	5.5

The reaction is performed at 50°C for 1 hour and then placed on ice. Subsequently, we prepared one PCR amplification reaction for each index. During this step the cDNA construct will be amplified for 11 cycles and indices will be added to each sample. **For each reaction, only 1 out of the 48 RNA**

PCR Primer indices was used during the PCR step (single indexing). We used 12 different index sequences to single index our samples.

3. Purification of cDNA construct

This process gel purifies the amplified cDNA construct in preparation for subsequent cluster generation. After gel purification, the cDNA is recovered, purified further and concentrated using the AMPure XP beads.

Our cDNA constructs were quantified with Qubit 2.0 and equal molar amounts of 12 samples at a time were pooled together before gel purification. The pooled samples were electrophoresed using a Novex TBE gel, 6% in 1X Novex TBE running buffer. The gel was run for 60 minutes at 145 V. When the electrophoresis was finished the gel was stained with 0.5 µg/ml ethidium bromide for 3 minutes and visualized in a UV transilluminator. At the end of the electrophoresis the Custom RNA Ladder (CRL) and a High Resolution Ladder (HRL) were used to locate the miRNAs on the gel. The Custom RNA Ladder consists of 3 dsDNA fragments 145 bp, 160 bp, and 500 bp. After the adapter and index additions the band that contains mature microRNA is 147 nucleotides long. This band is generated from approximately 22 nucleotide small RNA fragments. A second band, generated from approximately 30 nucleotide RNA fragments, including piwi-interacting RNAs, as well as some miRNAs and other regulatory small RNA molecules has 157 nucleotides length (Figure 9). **Both bands were cut off together with a razor blade and loaded to the gel breaker, to recover the pooled and purified cDNA constructs.**

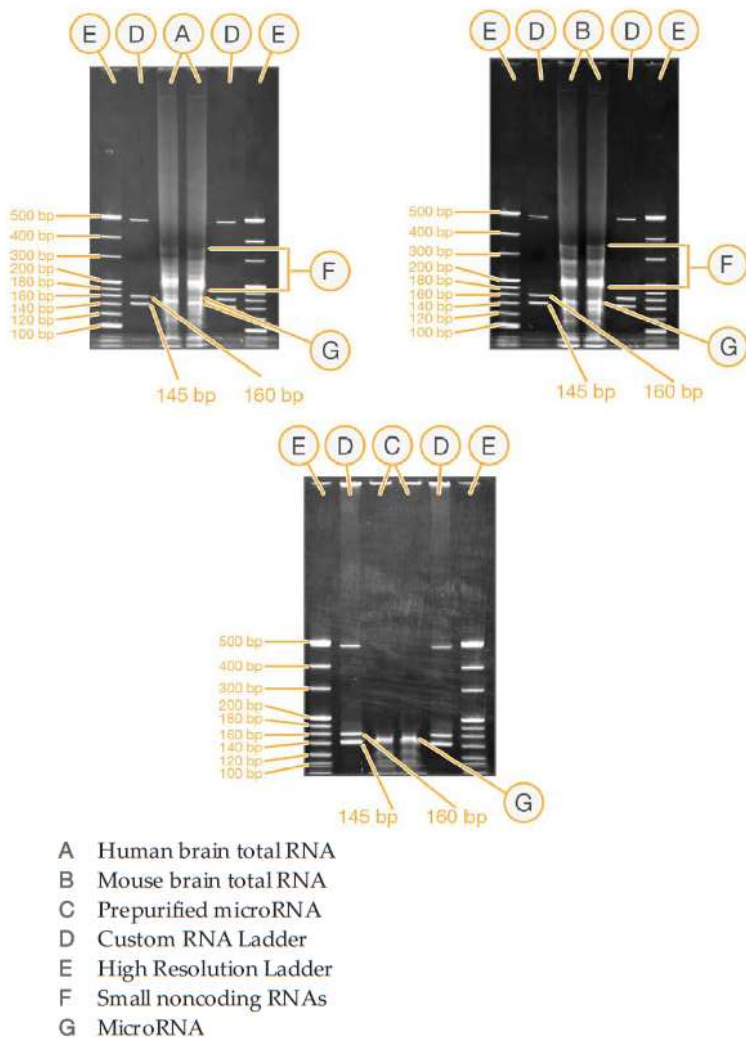


Figure 9: Example of miRNA bands observed under the UV transilluminator light

We did not perform the optional step of ethanol precipitation found in the TruSeq Small RNA Library Prep Kit manual. Instead we used AMPure XP beads (Beckman Coulter, Brea, CA, US) to further purify and concentrate our pooled samples' libraries. AMPure XP beads separate RNA fragments based on size (Workflow in Figure 10). The extended protocol can be found in Appendix C.

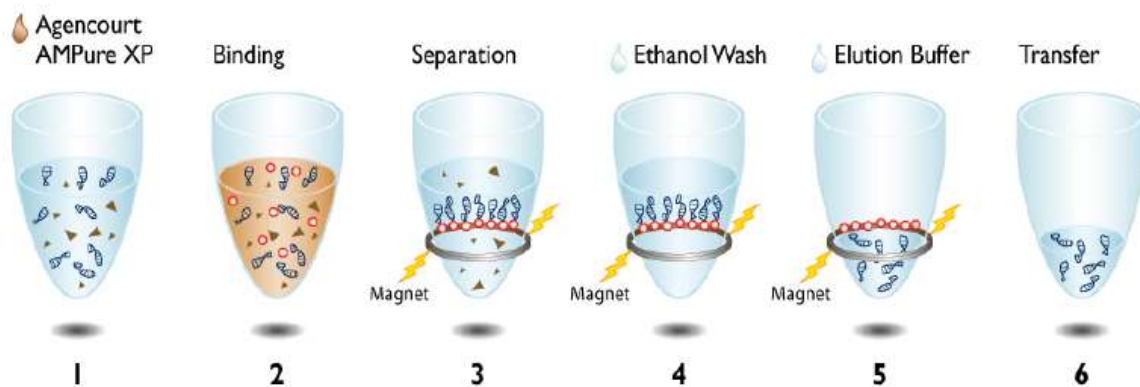


Figure 10: AMPure XP beads workflow

4. Validation of Libraries

For quality control analysis of the produced libraries:

1. We loaded 2 μ l of the resuspended construct on Fragment Analyzer™ Automated CE System (Advanced Analytical, Technologies, IA, USA).
2. We checked the purity, and concentration of the sample with Qubit® 2.0 Fluorometer (Thermo Fisher Scientific, Waltham, MA, USA).

5. Library Normalization and Denaturation

1. Normalized the concentration of the library to 2 nM using Tris-HCl 10 mM, pH 8.5.
2. Denatured with NaOH 0.1M for 5 minutes before loading on the instrument.

6. Run Conditions

For the Sequencing we used the MiSeq® System instrument (Illumina, San Diego, CA, USA). The instrument was loaded with MiSeq® Reagent Kit v3 and the samples were loaded on Standard Flow Cells with a single lane and 19 tiles on the top and 19 tiles on the bottom surface. In each side of the flow cell were loaded 12 samples, indexed and pooled as described in the previous steps. To set up the instrument for the run, we followed the workflow presented in Appendix A, Figure 3. The input information needed for the run were uploaded to the machine in the form of a *.csv file (comma-separated values file), referred to as the “SampleSheet.csv”. The sample sheet was prepared on

excel. Our Sample Sheet was designed using the Illumina Experiment Manager Guide (part # 15031335) and consulted the MiSeq Sample Sheet Quick Reference Guide (document # 5028392). This file contains all the information needed to set up the run and analyze it, including a list of the samples and their index sequences.

The .csv file contained information useful for the user (name of the experiment, the date of the experiment etc), but also necessary for the run, the analysis and the output expected from the instrument software. The latter included the workflow, the assay, the chemistry, the adapter sequences, the number of cycles, the samples list etc.

- We used the Small RNA Workflow and the default settings.
- We used the adapter reads default for this application:
TGG AATTCTCGGGTGCCAAGGC
- The total number of cycles in a paired-end read was 151. The read length was 2x75bp.

The file contained information about the sample IDs, the indices etc.

3.5.2 Data analysis

Preliminary data analysis

MiSeq system imaging of the clusters depends on LED and filter combinations specific for each labeled nucleotide. After imaging is complete for one tile, the flow cell is moved to the next tile and the process is repeated. The information produced from the image analyses is saved in *.bcl files that contain the real-time analyses base calling and base quality scoring for 1 cycle and 1 tile. The quality of base calling and consequently, the efficiency of the run at this stage are estimated by Phred Quality Scores, the Q scores. Q scores are defined as a property that is logarithmically related to the base calling error probabilities (P). The equation that gives us Q score is: $Q = -10 \log_{10} P$. The default threshold is Q30, which means that the called base has 1 chance in 1.000 to be wrong or in other words 99.9% probability to be correctly called.

1. The first step in all MiSeq workflows is demultiplexing which was automatically performed by the instrument software (Figure 11). MiSeq Reporter software confronts the index reads of all samples per flow cell to the index sequences specified in the sample sheet. According to the index sequence one FASTQ file was generated for each sample and index sequences were removed. Each FASTQ file contained reads for one sample. FASTAQ files we used for the

alignment had the default settings, therefore, index sequences and clusters not passing the filter were excluded.

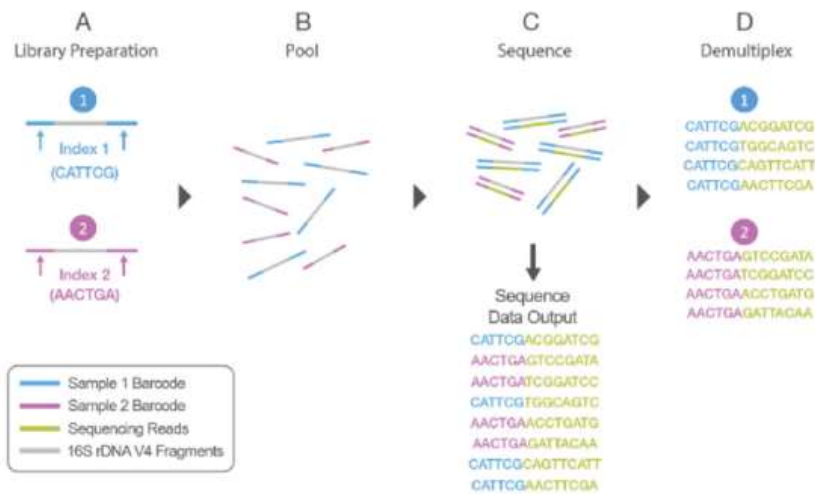


Figure 11: Demultiplexing

2. Reads were preprocessed before alignment for adapter removal using cutadapt¹⁸⁹ and shorten to a max length of 28 bp.
3. FASTQ file reads were then aligned to a reference of mature miRNAs using bowtie¹⁹⁰.

Statistical analysis of miRNAs data

Before modelling miRNAs were filtered keeping only those with at least 2 reads per million in all samples within at least one experimental group (fR vs nR or lithium treated vs untreated). Data were normalized based on effective library size as well as computation of dispersion. Expression values of mature miRNA were expressed as counts per million (CPM). Differential expression was computed using a negative binomial model after application of the normalization factors. Different constructs were tested and miRNAs with unadjusted p-value < 0.05 were reported. All modelling was performed based on edgeR framework¹⁹¹ in R¹⁹² and bioconductor¹⁹³. Correction for multiple testing was conducted according to BH procedure, a false discovery rate (FDR) based correction, using a threshold of < 0.05 (fR vs nR) or < 0.20 (Li+ fR vs Li- fR). The miRNAs surviving this threshold were used for further analyses.

3.6 Microarrays

3.6.1 Microarrays Experiment

Total RNA was extracted from cell pellets using TRIreagent solution (Ambion, Austin, TX, USA) and quantified with a NanoDrop ND-1000 spectrophotometer (Thermo Fisher, Waltham, MA, USA). Quality was considered adequate when the A260/280 ratio was in the range of 1.8–2.0. RNA integrity was checked by the Agilent 2100 Bioanalyzer (Agilent, Santa Clara, CA, USA) using a RNA 6000 Nano Chip and expressed as RNA Integrity Number (RIN), considered acceptable within the range of 7–10. We used 100 ng of total RNA from each sample to generate a purified sense-strand cDNA with incorporated dUTP, by using the Ambion® WT Expression Kit (Applied Biosystems, Foster City, CA, USA) following manufacturer's protocols. Samples were fragmented and labeled using the Affymetrix GeneChip WT Terminal Labeling Kit and hybridized to GeneChip® Human Gene 1.0 ST Arrays (Affymetrix, CA, USA), according to the manufacturer's instructions. This chip interrogates 28,869 well annotated genes with 764,885 distinct probes distributed across the full length of each gene. After 17 h at 45°C in the hybridization oven, arrays were washed and stained in GeneChip Fluidics Station 450 (Affymetrix, CA, USA) and scanned using GeneChip Scanner 3000 7G AutoLoader (Affymetrix, CA, USA). The .CEL files were generated and checked using the Affymetrix GeneChip® Command Console Software (AGCC) starting from the .DAT files. Samples were hybridized randomly by a technician blind to the clinical outcome and in vitro lithium treatment.

3.6.2 Statistical analysis of mRNAs data

GeneChip data quality control was performed using Expression Console Software (Affymetrix, CA, USA). Raw data were preprocessed based on the Robust Multi-array Average algorithm (RMA) for normalization and summarization¹⁹⁴. Data were filtered to remove duplicated or missing Entrez IDs. Genes were tested for differential expression between fR and nR both at basal and after in vitro lithium treatment using linear models. Significance was defined based on a FDR threshold of 0.05¹⁹⁵. The analyses were performed using the bioconductor¹⁹³ and the limma¹⁹⁶ packages implemented in R software¹⁹². We carried out pathway analysis using genes showing statistically significant difference in the comparison of fR versus nR. The FDR threshold of 0.05 allowed us to compare the microarray data with the miRNA sequencing data.

3.7 miRComb correlation analysis and Gene target prediction

miRComb

miRComb v0.9.1¹⁹⁷ (<http://mircomb.sourceforge.net>) is an R package designed to analyse miRNA – mRNA interactions. This package combines biological information (expression data) with theoretical information (miRNA target prediction databases) in order to obtain a curated list of potential miRNA-mRNA interaction pairs.

The workflow of the correlation analysis is reported in Figure 12. Expression data of miRNAs and mRNAs were log₂ transformed. Targets showing differential expression between fR and nR at the FDR threshold < 0.05 were then uploaded in miRComb. Negative correlations were considered significant if the FDR was < 0.05. The same procedure was applied to data from the experiments on lithium effect, but since none passed the < 0.05 FDR threshold we set a less stringent FDR threshold of 0.2. In this case we selected miRNAs and mRNAs on which lithium treatment in vitro had an effect only in fR but not in nR with FDR < 0.2 and negative correlations were considered significant if the nominal p value was < 0.05.

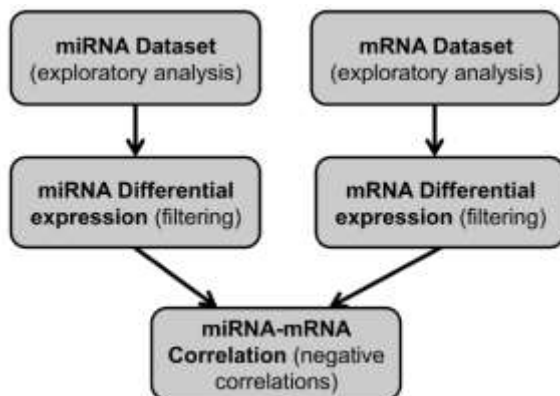


Figure 12: MiRComb workflow

MiRWalk

MiRWalk¹⁹⁸ (<http://mirwalk.uni-hd.de/>) is a comparative platform that interrogates different miRNA-mRNA interaction prediction databases and contains also an algorithm that predicts all the possible miRNA binding sites in the gene region. miRWalk is a comprehensive database that provides predicted as well as experimentally verified miRNA binding site information. We used miRWalk algorithm and 6 more integrated databases (DIANA-microTv4.0, miRanda-rel2010, miRDB4.0, RNA22v2, RNAhybrid2.1 and Targetscan6.2) The probability of the predicted miRNA-mRNA

interaction to be true is expressed as a score. The score is calculated from a random-forest based approach by executing TarPmiR algorithm for miRNA target site prediction.

3.8 Validation with qRT-PCR

3.8.1 Introduction to qRT-PCR

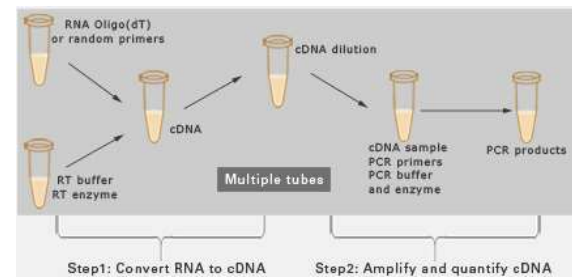


Figure 13: two-step qRT-PCR

Retrotranscription

MiRNA and mRNA levels were quantified with a two-step RT-PCR (Figure 13). Retrotranscription of the RNA was performed using specific primers with stem loop structure for the miRNAs and Random (hexamer) primers for the mRNAs as starting point for the reverse transcriptase that produced the cDNA eligible for the qRT-PCR reaction (Figure 14).

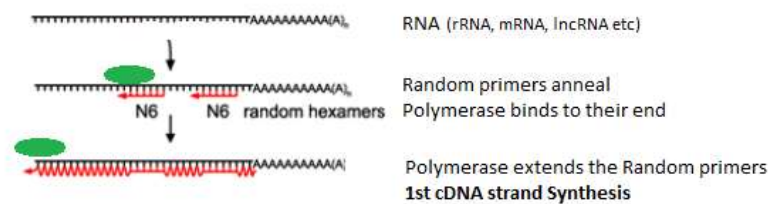



Figure 14: Retrotranscription with Random Hexamer Primers,  reverse transcriptase enzyme

qRT-PCR

TaqMan Gene Expression Assays were used for the relative quantification of mRNAs¹⁹⁹ and miRNAs with the Comparative Ct Method. These assays are based on the 5' nuclease chemistry, and each one contains primer and probe set specific for the target of interest (Figure 15). The probe is also double labelled with a fluorescent reporter and a quencher. The polymerase uses the primers to initiate the polymerization and during the polymerization of the target the 5' nuclease activity of the polymerase degrades the probe and as a result the quencher is separated from the fluorescent reporter which now is able to emit fluorescence. This procedure is repeated for several cycles and as the quantity of the initial template is increased exponentially due to the PCR conditions the fluorescence is increased. The detailed procedure can be found in Appendix D.

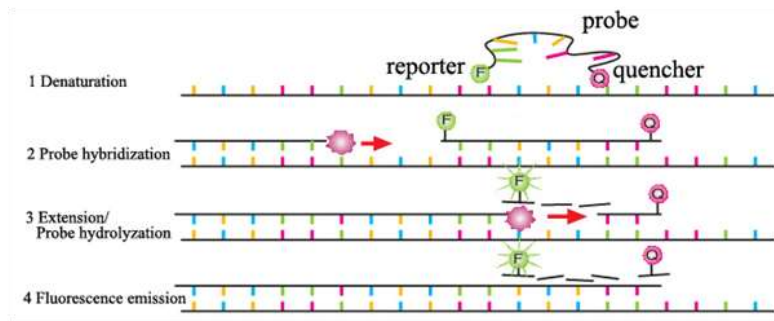


Figure 15: Taqman Chemistry

3.8.2 miRNA quantification by qRT-PCR

For the validation via qRT-PCR of the selected miRNA we used TaqMan® Small RNA Assays (Applied Biosystems, Foster City, CA, US). These assays include a stem-looped primer for reverse transcription and a sequence specific TaqMan® assay to accurately detect mature miRNAs in a two-step RT-PCR ²⁰⁰.

Each TaqMan® Small RNA Assay includes:

- One tube containing small RNA-specific RT primer
- One tube containing a mix of:
 - Small RNA-specific forward PCR primer
 - Specific reverse PCR primer
 - Small RNA-specific TaqMan® MGB probe

The list of the TaqMan® Small RNA Assays used:

Assay ID	Assay Name
002287	hsa-miR-155*
002284	hsa-miR-138
000408	hsa-miR-27a
002277	hsa-miR-320

001093	RNU6B
--------	-------

Quantification using the TaqMan® Small RNA Assays is done using two-step qRT-PCR:

1. For the retrotranscription we used as input 10ng of total RNA and the TaqMan® MicroRNA Reverse Transcription Kit (Applied Biosystems, Foster City, CA, US). This kit is using MultiScribe™ RT enzyme, dNTPs and the miRNA specific RT primer from the TaqMan Small RNA Assay to convert the total miRNA of the sample into cDNA. Using the thermal cycler, PCR system 9700 we performed the retrotranscription under the following

Temperature (°C)	Time (minutes)	Step
16	30	Hold
42	30	Hold
85	5	Hold
4	∞	Hold

conditions:

2. In the PCR step, PCR products were amplified from cDNA samples using the TaqMan® Small RNA Assay together with the TaqMan® Universal PCR Master Mix, no AmpErase™ UNG (4324018) according to the manufacturer's protocol. The RT-PCR was performed in StepOnePlus instrument (Applied Biosystems, Foster City, CA, US) using MicroAmp® Fast Optical 96-Well Reaction Plates (4346907) covered with MicroAmp® Optical Adhesive Film (4360954). Each reaction contained 0.9 ng di cDNA from the previous step and final volume of 10µl and was performed in triplicate. As endogenous control we used RNU6B TaqMan™ microRNA Control Assays 20× (4427975) which was retrotranscribed and PCR amplified following the same two step procedure. As calibrator we retrotranscribed a pool of all the RNA samples.

The instrument is set to use TaqMan chemistry and the comparative Ct relative quantification method and the reaction conditions are the following:

Temperature (°C)	Time	Step
50	2 (minutes)	Hold
95	10 (minutes)	Hold
95	15 (seconds)	40 cycles
60	1 (minute)	

3.8.3 mRNA quantification by qRT-PCR

RT-PCR was performed in two steps. During the first step of reverse transcription, cDNA was synthesized from 2 µg of total RNA with the High-capacity cDNA Reverse Transcription Kit (Life Technologies Corporation, Carlsbad, USA). This kit uses MultiScribe™ Reverse Transcriptase and Random Primers (hexamers) to synthesize the first strand cDNA of most mRNA and other RNA species. MultiScribe™ Reverse Transcriptase works more efficiently at 37°C therefore the reaction took place in the thermo cycler, PCR system 9700 and the conditions were the following:

Temperature (°C)	Time (minutes)	Step
25	10	Hold
37	120	Hold
85	5	Hold
4	∞	Hold

TaqMan chemistry was chosen for the qRT-PCRs and each reaction was run in triplicate using:

1. StepOnePlus™ instrument (Applied Biosystems, Foster City, CA, US)
2. TaqMan Gene Expression Master Mix 2X (Applied Biosystems, Foster City, US)
3. TaqMan Gene Expression Assays 20X (primers and probe for gene target)

Human GAPD (GAPDH) Endogenous Control (FAM™/MGB probe, non-primer limited)
(Assay: NM_002046.3)

4. AXYGEN® PCR MICROPLATE PCR-96-LP-AB-C, for ABI (321-70-51)
5. MicroAmp® Optical Adhesive Film (4360954)

GAPDH was used as a housekeeping gene to normalize target genes and a pool of all samples was used as calibrator in all the plates.

List of targets:

Assay ID	Gene Symbol
Hs00162095_m1	SP4
Hs00186419_m1	BHLHE40
Hs00998426_m1	CAPNS1
Hs01051295_m1	RHOA

Hs00892674_m1	RGS16
Hs01688766_m1	AUTS2
Hs00187858_m1	KYAT1

The quantity of cDNA of the assay and endogenous control per reaction was 1) 20ng or 2) 40ng. The master mix was prepared using TaqMan Gene Expression Master Mix 2X (Applied Biosystems, Foster City) and TaqMan Gene Expression Assays 20X (Primers and probe for gene target) or Human GAPDH Endogenous Control 20X (FAM / MGB Probe, Non-Primer Limited) (4333764F) as recommended by the company, with a final volume of 10µl per reaction and was distributed in 96 well plates AXYGEN® PCR MICROPLATE PCR-96-LP-AB-C, for ABI (321-70-51) covered with MicroAmp® Optical Adhesive Film (4360954) which are compatible with RT-PCR in StepOnePlus™ instrument (Applied Biosystems, Foster City, CA, US). RT-PCR was performed under the following conditions:

Temperature (°C)	Time	Step
50	2 (minutes)	Hold
95	10 (minutes)	Hold
95	15 (seconds)	42 cycles
60	1 (minute)	

qRT-PCR data analysis

Relative expression levels were measured by means of the comparative Ct method using as endogenous control for the calculation of $\Delta\Delta C_t$ RNU6B for miRNAs and GAPDH for mRNAs. As calibrator we used a pool of all the samples. For the statistical analysis we used the Relative Quantity (RQ) values as calculated with the $2^{-\Delta\Delta C_t}$ equation. The tests for the statistical analysis (parametric or non-parametric) were selected based on the normality of the data distribution and the homogeneity of variance for each target separately. To estimate whether the data deviate significantly from the normal distribution we used the Shapiro Wilk test. Levene's test was used to estimate the equality of variance of the means. When normal distribution was followed differences between fR and nR were analyzed with the independent sample t-test. When the variances of means were not equal we chose the SPSS option "equal variances not assumed". When at least one of the confronted groups did not follow the normal distribution, we used the non-parametric Mann–Whitney U-test. The differences

between lithium treated and untreated LCLs were tested with a paired samples parametric t-test. Pearson's correlation coefficients and p-values of the association between miRNAs and their predicted mRNA targets were calculated. The results of the association are presented in graphs generated by Microsoft Excel. The significance threshold was set at $p < 0.05$. Statistical tests were carried out using SPSS statistical software package v20 (SPSS, Inc., Chicago, IL, USA).

4. Results

4.1 Next Generation Sequencing (NGS) of miRNAs

4.1.1 NGS dysregulated miRNAs in full-Responders (fR) vs non-Responders (nR) to lithium

Quality control initiates immediately after base call by the instrument software. Sequencing base call quality was automatically calculated by the MiSeq Control Software and presented as a Q score distribution as seen in Figure 16. At base calling 96.4% of the bases had score > Q30 (Figure 16). The reads were extracted as FASTAQ files by the MiSeq Reporter Software and processed with cut adapt and bowtie to remove the adapter sequences and align to known miRNAs, respectively. In total, 998 miRNAs were aligned in our sample, out of approximately 2500 reference miRNAs used for the alignment.

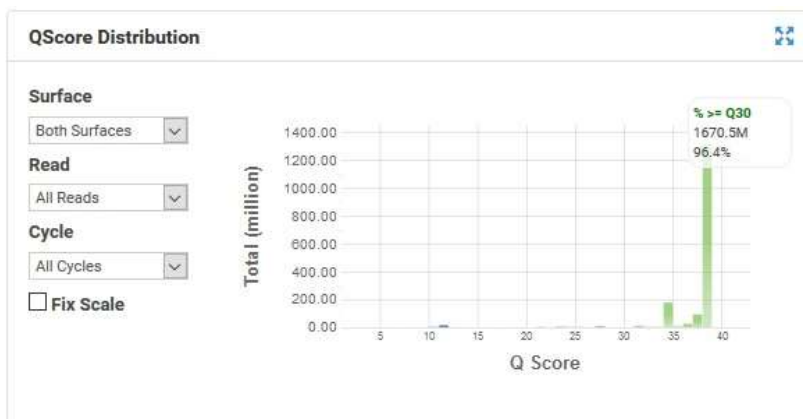


Figure 16: Automatic base calling Q scores from MiSeq instrument.

Initially we controlled for miRNAs differentially expressed between fR and nR. The initial filtering of 2 reads per million (RPM) in all samples within at least one experimental group resulted in 194 miRNAs. Statistical analysis between the two groups resulted in 52 significantly differentially expressed miRNAs between fR and nR with a FDR < 0.05 (Table 8).

Table 8: Mature miRNAs differentially expressed between fR and nR with FDR < 0.05

	miRNA	logFC	logCPM	p-value	FDR	FC
1	hsa-miR-320a	-0,87159	10,30874	3,21E-10	3,81E-08	0,546545
2	hsa-miR-125a-5p	-2,6339	8,747585	6,57E-08	3,9E-06	0,161108

3	hsa-miR-148a-3p	1,157969	15,05057	1,24E-07	4,92E-06	2,231431
4	hsa-miR-574-3p	-1,63656	7,569793	5,35E-07	1,59E-05	0,321622
5	hsa-miR-1273h-3p	-1,01753	7,379623	3,48E-05	0,000826	0,493962
6	hsa-miR-22-3p	0,837128	14,4139	7,25E-05	0,001433	1,78649
7	hsa-miR-9-5p	-0,81807	10,74986	0,000115	0,001869	0,5672
8	hsa-miR-26b-5p	0,830558	9,887388	0,000126	0,001869	1,778372
9	hsa-miR-378a-5p	-1,2176	6,858434	0,00023	0,002974	0,429997
10	hsa-miR-223-3p	2,047295	5,884447	0,000251	0,002974	4,133303
11	hsa-miR-155-3p	1,185132	7,708617	0,000284	0,003059	2,273842
12	hsa-miR-505-3p	-1,01443	6,802691	0,000474	0,004254	0,495024
13	hsa-miR-744-5p	0,665581	8,159317	0,00048	0,004254	1,586207
14	hsa-let-7e-5p	-1,62222	7,510987	0,000502	0,004254	0,324836
15	hsa-miR-138-5p	-1,66643	10,47137	0,000554	0,004382	0,315031
16	hsa-miR-181a-3p	1,381639	9,36691	0,000626	0,004395	2,605642
17	hsa-miR-15a-5p	0,691987	10,72931	0,00063	0,004395	1,615507
18	hsa-miR-941	-0,87732	10,66932	0,000694	0,004532	0,544376
19	hsa-miR-148b-3p	1,217073	8,999277	0,000726	0,004532	2,324746
20	hsa-miR-652-3p	-1,11507	6,84613	0,000832	0,004937	0,461668
21	hsa-miR-130b-3p	-0,53224	10,35912	0,000889	0,005019	0,69148
22	hsa-miR-15b-3p	0,855417	7,236825	0,001252	0,006752	1,809281
23	hsa-miR-345-5p	-0,84076	9,337964	0,001354	0,006984	0,558348
24	hsa-miR-454-5p	1,099163	6,317823	0,001934	0,009561	2,142303
25	hsa-miR-4677-3p	1,325574	6,048634	0,002143	0,010166	2,506326
26	hsa-miR-374a-3p	0,800033	7,815446	0,002442	0,011141	1,741141
27	hsa-miR-19b-3p	0,669348	10,52238	0,002869	0,012504	1,590354
28	hsa-let-7d-3p	-0,49312	9,258785	0,002952	0,012504	0,710485
29	hsa-miR-181d-5p	-0,86579	7,492878	0,003413	0,013637	0,548745
30	hsa-miR-101-3p	0,817671	8,577526	0,003484	0,013637	1,762558
31	hsa-miR-629-5p	-1,11416	6,860233	0,003564	0,013637	0,461961
32	hsa-miR-574-5p	-1,01807	7,149769	0,003881	0,014387	0,493777
33	hsa-miR-378a-3p	-0,54957	13,75491	0,004164	0,014966	0,683224

34	hsa-miR-148a-5p	0,683302	10,65283	0,004371	0,015165	1,605811
35	hsa-miR-142-3p	0,554845	11,34566	0,004475	0,015165	1,469011
36	hsa-miR-454-3p	0,531824	8,625445	0,005024	0,016281	1,445756
37	hsa-miR-142-5p	0,660187	14,28279	0,005123	0,016281	1,580287
38	hsa-miR-598-3p	-0,97865	7,232469	0,005216	0,016281	0,507454
39	hsa-let-7f-5p	0,414577	16,38311	0,005372	0,016338	1,332908
40	hsa-miR-27a-5p	0,734097	7,616572	0,008375	0,024086	1,663356
41	hsa-let-7a-5p	0,368051	15,70205	0,008512	0,024086	1,290608
42	hsa-miR-210-5p	0,498983	9,005094	0,008662	0,024086	1,413217
43	hsa-miR-30e-3p	0,515521	10,35189	0,008732	0,024086	1,429511
44	hsa-miR-146a-5p	0,963063	16,26544	0,011687	0,031506	1,949444
45	hsa-miR-23a-3p	-0,4542	9,522637	0,013126	0,0346	0,729913
46	hsa-miR-15b-5p	0,476958	10,32102	0,014947	0,038543	1,391806
47	hsa-miR-425-5p	-0,45873	11,31229	0,017051	0,043031	0,727628
48	hsa-miR-197-3p	-0,49361	9,57574	0,018221	0,045027	0,710244
49	hsa-miR-335-3p	1,755321	8,3273	0,020426	0,048893	3,376013
50	hsa-miR-421	0,417253	8,6018	0,020782	0,048893	1,335383
51	hsa-miR-26a-5p	0,425191	14,89959	0,021022	0,048893	1,34275
52	hsa-miR-194-5p	-0,73191	7,204028	0,021488	0,049015	0,602104
<i>LogCPM: logarithm of 2 of Counts per Million (CPM), FC: Fold Change, logFC: logarithm of 2 of Fold Change, FDR: p corrected for False Discovery Rate (FDR)</i>						

4.1.2 Correlation analysis between mRNA and miRNA expression data and software prediction of miRNA-mRNA couples dysregulated in fR vs nR

We identified 146 total negative correlations with a FDR < 0.05. The minimum absolute value of the correlation coefficient included was 0.7 and only the negative correlations were taken into account. 125 genes and 24 miRNAs were included in these inverse correlations, showing that each miRNA was negatively correlated with more than one gene. The list of the statistically significant correlations (ranked solely based on the adjusted p-value of the correlation) is found in Table 9.

The miRNAs with the largest number of correlations were **hsa-miR-320a**, involved in 18 correlations, **hsa-miR-378a-3p** with 13 correlations and **hsa-miR-155-3p** and **hsa-miR-1273 h-3p** with 9 negative correlations each.

Table 9 : List of the significant correlations (Adj. p-value of cor < 0.05)

miRNA	mRNA	Cor.	Adj. p-value of cor.	FDR	FC	FDR	FC	Score
				miRNA	miRNA	mRNA	mRNA	
hsa-miR-1273h-3p	PEX14	-0,84	0,025	0,00083	0,49396	0,03180	1,08471	1
hsa-miR-138-5p	ZBTB45	-0,85	0,025	0,00438	0,31503	0,01369	1,16162	2
hsa-miR-155-3p	RP2	-0,84	0,025	0,00306	2,27384	0,00610	0,73240	1
hsa-miR-320a	BHLHE40	-0,83	0,025	0,00000	0,54655	0,00023	1,37037	6
hsa-miR-320a	PBLD	-0,83	0,025	0,00000	0,54655	0,01090	1,16900	2
hsa-miR-320a	LSP1	-0,83	0,025	0,00000	0,54655	0,00003	1,48312	1
hsa-miR-345-5p	STRA6	-0,83	0,025	0,00698	0,55835	0,00513	1,20864	1
hsa-miR-421	PLCXD1	-0,87	0,025	0,04889	1,33538	0,01899	0,74408	1
hsa-miR-9-5p	PARP4	-0,83	0,025	0,00187	0,56720	0,03154	1,12772	1
hsa-miR-138-5p	GABARAP	-0,82	0,03	0,00438	0,31503	0,00562	1,13855	2
hsa-miR-378a-3p	ATF7	-0,81	0,041	0,01497	0,68322	0,01501	1,14348	2
hsa-miR-1273h-3p	ISCU	-0,81	0,042	0,00083	0,49396	0,01928	1,18871	3
hsa-miR-155-3p	SP4	-0,81	0,042	0,00306	2,27384	0,00096	0,67680	4
hsa-miR-155-3p	DNASE1L3	-0,81	0,042	0,00306	2,27384	0,00046	0,28877	1
hsa-miR-15a-5p	SMARCA2	-0,81	0,042	0,00440	1,61551	0,00709	0,73536	1
hsa-miR-374a-3p	PTPMT1	-0,81	0,042	0,01114	1,74114	0,01309	0,91122	1
hsa-miR-1273h-3p	EDF1	-0,79	0,045	0,00083	0,49396	0,02135	1,12852	2
hsa-miR-130b-3p	GFOD2	-0,79	0,045	0,00502	0,69148	0,01900	1,11655	1
hsa-miR-155-3p	ZC3HC1	-0,79	0,045	0,00306	2,27384	0,00315	0,87884	1
hsa-miR-27a-5p	DNAJB4	-0,8	0,045	0,02409	1,66336	0,00327	0,72788	1
hsa-miR-320a	PARD6G	-0,79	0,045	0,00000	0,54655	0,00025	2,01292	4
hsa-miR-320a	C9	-0,8	0,045	0,00000	0,54655	0,00863	1,12540	2
hsa-miR-320a	FSTL3	-0,8	0,045	0,00000	0,54655	0,00000	1,64234	1
hsa-miR-320a	RHOA	-0,79	0,045	0,00000	0,54655	0,00101	1,10800	1
hsa-miR-345-5p	CYB5D2	-0,79	0,045	0,00698	0,55835	0,00004	1,24419	3
hsa-miR-345-5p	RER1	-0,79	0,045	0,00698	0,55835	0,02557	1,10580	2
hsa-miR-374a-3p	PIR	-0,79	0,045	0,01114	1,74114	0,00069	0,73394	2
hsa-miR-374a-3p	ENGASE	-0,79	0,045	0,01114	1,74114	0,00138	0,83901	1
hsa-miR-374a-3p	PLXNA1	-0,79	0,045	0,01114	1,74114	0,00581	0,75747	1

hsa-miR-374a-3p	TNS3	-0,79	0,045	0,01114	1,74114	0,03671	0,73357	1
hsa-miR-378a-3p	PPP1CA	-0,79	0,045	0,01497	0,68322	0,00415	1,15026	2
hsa-miR-378a-3p	DCAF11	-0,79	0,045	0,01497	0,68322	0,00127	1,16646	1
hsa-miR-378a-3p	SIRT2	-0,79	0,045	0,01497	0,68322	0,00718	1,13547	1
hsa-miR-421	SFRP1	-0,79	0,045	0,04889	1,33538	0,00541	0,51236	2
hsa-miR-574-3p	TCEB3	-0,79	0,045	0,00002	0,32162	0,00007	1,24905	2
hsa-miR-574-3p	RNF31	-0,79	0,045	0,00002	0,32162	0,00594	1,16625	1
hsa-miR-138-5p	BCL2L1	-0,78	0,047	0,00438	0,31503	0,00041	1,38919	4
hsa-miR-27a-5p	SELL	-0,78	0,047	0,02409	1,66336	0,00746	0,43554	2
hsa-miR-378a-3p	ZBTB45	-0,78	0,047	0,01497	0,68322	0,01369	1,16162	1
hsa-miR-125a-5p	STS	-0,77	0,05	0,00000	0,16111	0,00030	1,85648	4
hsa-miR-1273h-3p	TRAF4	-0,76	0,05	0,00083	0,49396	0,00023	1,26310	2
hsa-miR-1273h-3p	FPGS	-0,77	0,05	0,00083	0,49396	0,02437	1,10102	2
hsa-miR-1273h-3p	MAPK8IP3	-0,78	0,05	0,00083	0,49396	0,02536	1,10486	2
hsa-miR-1273h-3p	BOD1	-0,77	0,05	0,00083	0,49396	0,01538	1,11397	1
hsa-miR-1273h-3p	PDZD2	-0,76	0,05	0,00083	0,49396	0,01719	1,35845	1
hsa-miR-1273h-3p	UPP1	-0,75	0,05	0,00083	0,49396	0,00006	1,44816	1
hsa-miR-138-5p	POM121	-0,75	0,05	0,00438	0,31503	0,00218	1,14674	3
hsa-miR-142-3p	BDH1	-0,76	0,05	0,01516	1,46901	0,03388	0,87971	2
hsa-miR-148a-3p	EIF2AK2	-0,76	0,05	0,00000	2,23143	0,00060	0,83809	2
hsa-miR-155-3p	BICD2	-0,76	0,05	0,00306	2,27384	0,01014	0,88586	4
hsa-miR-155-3p	COG5	-0,78	0,05	0,00306	2,27384	0,03329	0,79895	2
hsa-miR-155-3p	AUTS2	-0,77	0,05	0,00306	2,27384	0,00203	0,42915	1
hsa-miR-155-3p	RNF168	-0,78	0,05	0,00306	2,27384	0,00235	0,73176	1
hsa-miR-155-3p	CCBL1	-0,76	0,05	0,00306	2,27384	0,00001	0,75325	1
hsa-miR-15a-5p	WDR48	-0,76	0,05	0,00440	1,61551	0,00582	0,82470	3
hsa-miR-15a-5p	DIABLO	-0,77	0,05	0,00440	1,61551	0,01591	0,89632	1
hsa-miR-181a-3p	CD59	-0,75	0,05	0,00440	2,60564	0,00059	0,84467	1
hsa-miR-194-5p	ST8SIA2	-0,76	0,05	0,04901	0,60210	0,02804	1,14368	1
hsa-miR-26b-5p	LDLR	-0,77	0,05	0,00187	1,77837	0,01369	0,84947	2
hsa-miR-27a-5p	KMO	-0,75	0,05	0,02409	1,66336	0,02953	0,82018	2
hsa-miR-320a	GPATCH8	-0,76	0,05	0,00000	0,54655	0,00683	1,12791	5
hsa-miR-320a	PLSCR3	-0,78	0,05	0,00000	0,54655	0,00052	1,31047	4

hsa-miR-320a	ADD1	-0,76	0,05	0,00000	0,54655	0,00571	1,14940	4
hsa-miR-320a	HNRNPUL1	-0,77	0,05	0,00000	0,54655	0,01671	1,07813	4
hsa-miR-320a	ASB2	-0,76	0,05	0,00000	0,54655	0,00000	4,48596	3
hsa-miR-320a	CA5B	-0,77	0,05	0,00000	0,54655	0,00005	1,42334	3
hsa-miR-320a	CAPNS1	-0,76	0,05	0,00000	0,54655	0,00213	1,21409	3
hsa-miR-320a	CA13	-0,76	0,05	0,00000	0,54655	0,02003	1,35930	3
hsa-miR-320a	GPR132	-0,76	0,05	0,00000	0,54655	0,00003	1,50357	2
hsa-miR-320a	PAPSS2	-0,78	0,05	0,00000	0,54655	0,00001	2,59282	1
hsa-miR-320a	RGS16	-0,77	0,05	0,00000	0,54655	0,00056	1,52099	1
hsa-miR-345-5p	RAP2C	-0,76	0,05	0,00698	0,55835	0,02057	1,08515	2
hsa-miR-345-5p	TSPYL1	-0,77	0,05	0,00698	0,55835	0,00052	1,20721	1
hsa-miR-345-5p	GRHL3	-0,76	0,05	0,00698	0,55835	0,00109	1,18455	1
hsa-miR-345-5p	PLEKHG5	-0,75	0,05	0,00698	0,55835	0,01744	1,08328	1
hsa-miR-378a-3p	DUSP4	-0,77	0,05	0,01497	0,68322	0,00457	1,50335	5
hsa-miR-378a-3p	RPS6KA1	-0,76	0,05	0,01497	0,68322	0,00447	1,18544	4
hsa-miR-378a-3p	ZNF70	-0,76	0,05	0,01497	0,68322	0,00117	1,22485	3
hsa-miR-378a-3p	SH2B3	-0,77	0,05	0,01497	0,68322	0,00073	1,30565	2
hsa-miR-378a-3p	ARPC4	-0,77	0,05	0,01497	0,68322	0,00370	1,17813	2
hsa-miR-378a-3p	DAP	-0,76	0,05	0,01497	0,68322	0,02661	1,17454	2
hsa-miR-378a-3p	ASCC1	-0,77	0,05	0,01497	0,68322	0,00066	1,23626	1
hsa-miR-378a-3p	TMEM8A	-0,75	0,05	0,01497	0,68322	0,01776	1,23271	1
hsa-miR-421	ANGPTL2	-0,77	0,05	0,04889	1,33538	0,00876	0,77161	4
hsa-miR-454-5p	KIF6	-0,77	0,05	0,00956	2,14230	0,03027	0,75199	2
hsa-miR-454-5p	SIRT4	-0,78	0,05	0,00956	2,14230	0,02944	0,88233	1
hsa-miR-505-3p	VAPB	-0,76	0,05	0,00425	0,49502	0,00226	1,13882	4
hsa-miR-574-3p	UFD1L	-0,76	0,05	0,00002	0,32162	0,00644	1,17731	2
hsa-miR-574-3p	ISG20L2	-0,77	0,05	0,00002	0,32162	0,00059	1,33933	1
hsa-miR-574-3p	CREM	-0,76	0,05	0,00002	0,32162	0,00059	1,33936	1
hsa-miR-574-3p	SLC25A44	-0,76	0,05	0,00002	0,32162	0,02495	1,21874	1
hsa-miR-9-5p	EDEM1	-0,76	0,05	0,00187	0,56720	0,00035	1,25436	5
hsa-miR-9-5p	DCAF11	-0,76	0,05	0,00187	0,56720	0,00127	1,16646	2
hsa-miR-9-5p	IL2RA	-0,77	0,05	0,00187	0,56720	0,00776	2,45678	2
hsa-miR-9-5p	CD40LG	-0,77	0,05	0,00187	0,56720	0,03218	1,14119	2

Cor.: correlation coefficient, adj. p-value of cor.: corrected p value referring to the correlation analysis, FC: Fold Change, score: miRWalk score

Our next step was to filter the list of correlations keeping only the miRNA-mRNA couples that were predicted from at least 1 out of 7 target prediction software interrogated by miRWalk. The in silico analysis ruled out only three miRNAs, resulting in 21 miRNAs inversely correlated with one or more bioinformatically predicted targets. In total, 95 interactions were predicted. Only two gene were correlated with more than one miRNA (*DCAF11* and *TBTB45*).

4.1.3 NGS dysregulated miRNAs due to in vitro lithium treatment

The statistical analysis of miRNA's expression under lithium effects resulted in 2 lists of nominally differentially expressed miRNAs. The first list consisted of 18 miRNAs differentially expressed under lithium treatment in fR (unadjusted p-value < 0.05); 15 of them were upregulated and 3 downregulated. The second list consisted of the miRNAs differentially expressed under lithium effect in nR (unadjusted p-value < 0.05); in this list we found 16 miRNAs, 9 upregulated and 7 downregulated (Table 11).

Subsequently, we implemented an FDR controlling procedure to correct for multiple testing and we included only the differentially expressed miRNAs with FDR < 0,2 in further analysis.

- 1) All the miRNAs differentially expressed in fR under Li treatment that survived FDR < 0.2 threshold are presented in Table 10.
- 2) The miRNAs differentially expressed in nR under Li treatment that had a FDR < 0.2 are also presented in Table 10.

We considered only miRNAs surpassing our threshold (FDR < 0.2) in fR but not in nR. As can be seen in Table 10 none of the miRNAs is in overlap between the two groups, as a result, all 5 miRNAs differentially expressed in fR were used at the next step.

Table 10: miRNAs differentially expressed under lithium's effect, FDR < 0.2				
Group	miRNA	p	FDR	FC
	hsa-miR-29b-3p	0,000977	0,100307	1,408753

Lithium effect on fR	hsa-miR-374a-5p	0,002525	0,129651	1,544458
	hsa-miR-27a-3p	0,003981	0,13627	1,176038
	hsa-miR-23a-3p	0,00585	0,150169	1,249623
	hsa-miR-106b-5p	0,00856	0,175786	1,282124
Lithium effect on nR	hsa-miR-27a-5p	1,77E-05	0,003185	1,783326
	hsa-miR-151a-5p	0,000296	0,026642	0,68359
<i>FC: Fold Change, FDR: p corrected for False Discovery Rate (FDR)</i>				

4.1.4 Correlation analysis of genome wide expression data and miRNA expression data and software prediction of miRNA-mRNA couples regulated by lithium in vitro

Table 11: Cumulative table of differentially expressed genes and miRNA along different experimental groups.

High Throughput Platform	Experimental Group	No of DEGs
<i>MiSeq, small RNA Seq</i>	<i>fR vs nR (FDR<0.05)</i>	52
<i>Microarray (HG 1.0 ST)</i>	<i>fR vs nR (FDR<0.05)</i>	2060
<i>MiSeq, small RNA Seq</i>	<i>Li effect fR (unadjusted p-value < 0.05)</i>	18
<i>MiSeq, small RNA Seq</i>	<i>Li effect nR (unadjusted p-value < 0.05)</i>	16
<i>MiSeq, small RNA Seq</i>	<i>Li effect fR only (FDR<0.2)</i>	5
<i>Microarray (HG 1.0 ST)</i>	<i>Li effect fR only (FDR<0.2)</i>	66
<i>fR: full - Responders, nR: non – Responders, DEGs: Differentially Expressed Genes, FDR: p corrected for False Discovery Rate, Li: Lithium, RPM: reads per million</i>		

As was done before for the fR vs nR experimental groups, we also performed a miRNA-mRNA correlation analysis on lithium effect. The 5 miRNAs that fulfilled the criteria (Table10: Lithium effect in fR only) were implicated in 15 inverse correlations but only half of them were predicted in silico. Table 12 reports all the miRNA-mRNA inverse correlated couples predicted by miRWalk.

Table 12: List of the miRNA-mRNA couples altered by Lithium in vitro in fR

miRNA	mRNA	Cor.	p-cor.	p-miRNA	FC miRNA	p-mRNA	FC mRNA	Score
hsa-miR-29b-3p	RFX7	-0,49	0,016	0,000977	1,41	0,000275	0,93	6
hsa-miR-27a-3p	ZNF493	-0,41	0,040	0,003981	1,18	4,61E-05	0,84	6
hsa-miR-29b-3p	ZNF577	-0,49	0,015	0,000977	1,41	3,91E-05	0,88	5
hsa-miR-374a-5p	B4GALT6	-0,59	0,004	0,002525	1,54	6,07E-08	0,82	5
hsa-miR-106b-5p	ZNF493	-0,47	0,021	0,00856	1,28	4,61E-05	0,84	2
hsa-miR-23a-3p	FFAR2	-0,42	0,036	0,00585	1,25	0,000343	0,84	1
hsa-miR-27a-3p	IKBIP	-0,40	0,046	0,003981	1,18	0,000875	0,87	1

Cor.: correlation coefficient, p-cor.: Uncorrected p value referring to the correlation analysis, FC: Fold Change, score: miRWalk score

4.2 Choice of targets for validation

Due to the large number of data generated by high throughput methods, results typically require replication with an alternative, targeted gold standard approach, such as qRT – PCR.

MiRNA – mRNA couples to be validated were prioritized based on the following criteria:

1. p-value of miRNA differential expression between fR and nR
2. p-value of mRNA differential expression between fR and nR
3. p-value and correlation coefficient of correlation analysis
4. At least one out of 7 target prediction software predicted the correlation
5. biological criteria: Pubmed articles supporting the involvement of the miRNA and the possible mRNA target in:
 - a. central nervous system related processes
 - b. psychiatric disorders
 - c. pharmacological effects of lithium or other psychotropic drugs

Table 13: miRNA – mRNA couples selected for validation in fR vs nR and the biological criteria supporting the choice

<i>miRNA</i>	<i>Biological evidence</i>	<i>mRNA</i>	<i>Biological evidence</i>
miR-320a	<ul style="list-style-type: none"> expressed in the brain over-expressed by fluoxetine in neuroblastoma cells ²⁰¹ under-expressed in serum from Autistic patients ²⁰² downregulated in plasma from depressed patients ²⁰³ involved in AD and dementia ²⁰⁴ 	<i>BHLHE40</i>	<ul style="list-style-type: none"> associated with circadian rhythms, BD ²⁰⁵ and lithium response ²⁰⁶
		<i>RHOA</i>	<ul style="list-style-type: none"> Ras homolog gene family, member A neuronal development, neuronal survival, and neurodegeneration ²⁰⁷ part of pathway affected by CNV associated with BD, SCZ, autism and intellectual ability ²⁰⁸
		<i>CAPNS1</i>	<ul style="list-style-type: none"> Calcium dependent cysteine proteases involved in autophagy, apoptosis, migration, etc ²⁰⁹ Involved in dendritic branching, spine density, hippocampal long term potentiation ²¹⁰ Hypermethylated in SCZ prefrontal cortex ²¹¹
		<i>RGS16</i>	<ul style="list-style-type: none"> Regulator of G-protein signaling 16 Indispensable protein for the circadian regulation of cAMP in the superchiasmatic nucleus: variants associated with chronotypes ²¹²
miR-155-3p	<ul style="list-style-type: none"> involved in post-transcriptional gene regulation of the immune system ²¹³ increased by LiCl in LCLs ¹⁷⁹ 	<i>SP4</i>	<ul style="list-style-type: none"> associated with BD ¹⁷⁷ and regulated by Li ²¹⁴ SP4 transcription factor. Involved in the development of the hippocampus ²¹⁵ Associated with SCZ ²¹⁶, MDD ²¹⁷
		<i>AUTS2</i>	<ul style="list-style-type: none"> Autism Susceptibility Candidate 2 Regulates neuronal expression through epigenetic mechanisms ²¹⁸ Implicated in neurodevelopmental processes ²¹⁹
		<i>CCBL1 (KYATI)</i>	<ul style="list-style-type: none"> kynurenine aminotransferases involved in the inhibition of glutamergic neurotransmission in SCZ ²²⁰

miR-138-5p	<ul style="list-style-type: none"> involved in memory performance in humans ²²¹ chronic stress raises its levels in the rat ²²² 	<i>BCL2L1</i>	<ul style="list-style-type: none"> involved in apoptosis and lithium response ¹⁰³
<p>BD: Bipolar Disorder, CNV: Copy Number Variants AD: Alzheimer Disease, SCZ: Schizophrenia, MDD: Major Depressive Disorder, LiCl: Lithium Chloride, LCLs: Lymphoblastoid Cell Lines, <i>SP4</i>: Specific protein 4, <i>BCL2L1</i>: B-Cell CLL/Lymphoma 2 (BCL2) Like 1 , <i>BHLHE40</i>: Basic Helix-Loop-Helix Family Member E , <i>CCBL1</i>: Kynurenine Aminotransferase 1, <i>AUTS2</i>: Autism Susceptibility Candidate 2, <i>CAPNS1</i>: Calpain Small Subunit 1, <i>RGS16</i>: Regulator Of G Protein Signaling 16</p>			

Finally, we came up with 4 miRNAs in total from both experimental groups and their possible mRNA targets, three of which were selected from the fR vs nR experimental group (Table 13) and one from fR with lithium vs fR without lithium group (Table 14). In Table 13 and 14 is reported the biological relevance of the selected miRNAs and targets.

Table 14: Biological evidence supporting the following miRNA - mRNA couple selected for validation for Lithium's effects on fR			
<i>miRNA</i>	<i>Biological Evidence</i>	<i>mRNA</i>	<i>Biological Evidence</i>
miR-27a-3p	<ul style="list-style-type: none"> involved in vulnerability to stress ²²³ cognitive impairment ²²⁴ 	<i>ZNF493</i>	<ul style="list-style-type: none"> Differentially expressed in BD patients' derived neurons ²²⁵ and in Li response ²²⁶

Using the expression data from NGS and microarrays we reproduced some statistically significant (adjusted p-value of correlation < 0.05) representative correlations in the following graphs. As seen in Figure 17 there is a negative slope that correlates the miRNA and its possible gene target. The negative correlation coefficient indicates that there is an inverse correlation and as the correlation coefficient approaches 1, it means that the two groups are more strongly correlated. The FDR adjusted p-value (adj. pval.) is significant when < 0.05. The nR are indicated as 0 (blue) and the fR as 1 (pink). In Figure 17 and 18, hsa-miR-320a is downregulated in fR in comparison with nR, at the same time the miRNA's possible targets, *CAPNS1* and *RGS16*, levels are increased. As the miRNA levels increase in nR the gene levels decrease. The opposite effects are observed between hsa-miR-155-3p and *SP4* gene (Figure 19).

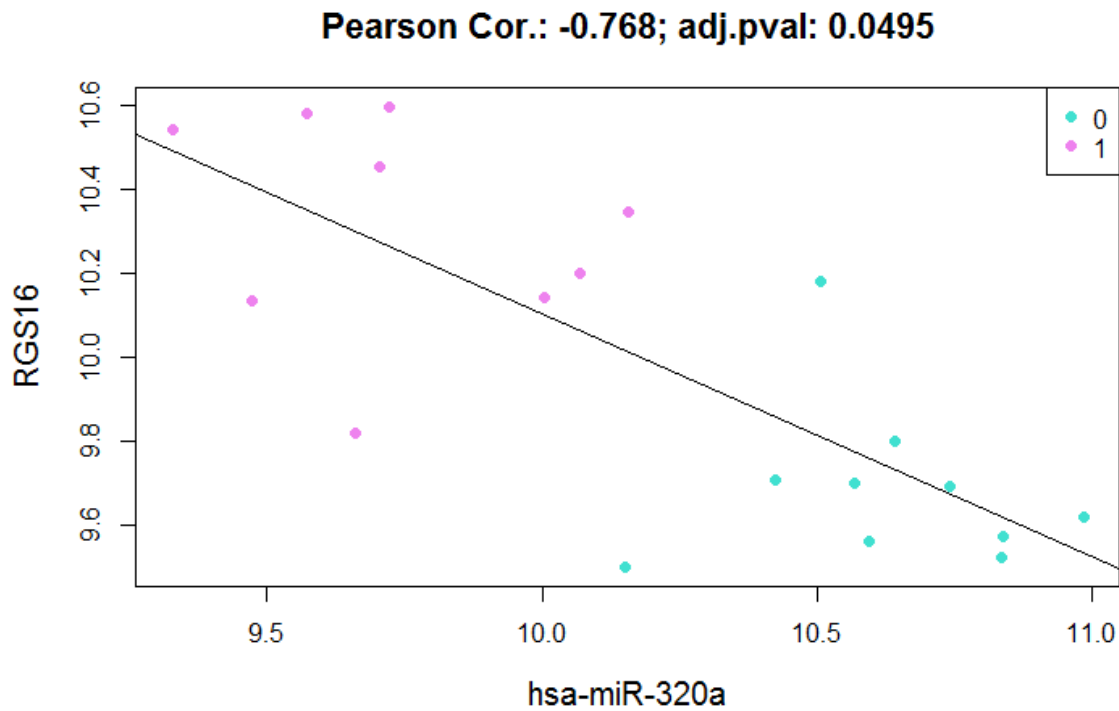


Figure 17: Correlation graph between *hsa-miR-320a* (x axon) and *RGS16* gene (y axon). The slope of the line and the negative correlation coefficient indicate that the correlation is negative and the FDR corrected p-value that it is statistically significant. The nR are indicated as 0 and the fR as 1. *hsa-miR-320a* is downregulated in fR while *RGS16* gene levels are increased, as the miRNA levels increase in nR the gene levels decrease. (produced by miRComB)

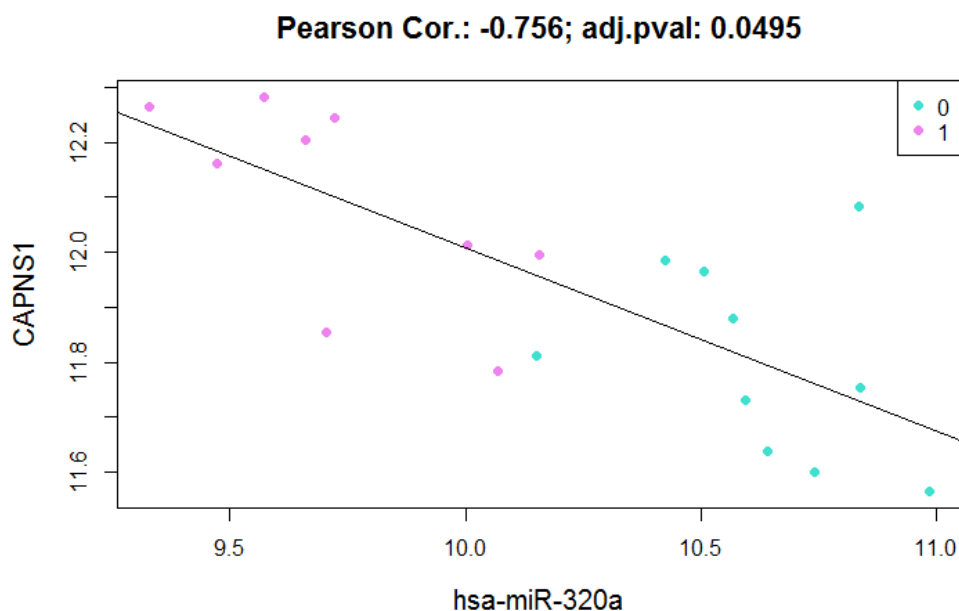


Figure 18: Correlation graph between *hsa-miR-320a* (x axon) and *CAPNS1* gene (y axon). The slope of the line and the negative correlation coefficient indicate that the correlation is negative and the FDR corrected p-value that it is statistically significant. The nR are indicated as 0 and the

fR as 1. hsa-miR-320a is downregulated in fR while CAPNS1 gene levels are increased, as the miRNA levels increase in nR the gene levels decrease. (produced by miRComb)

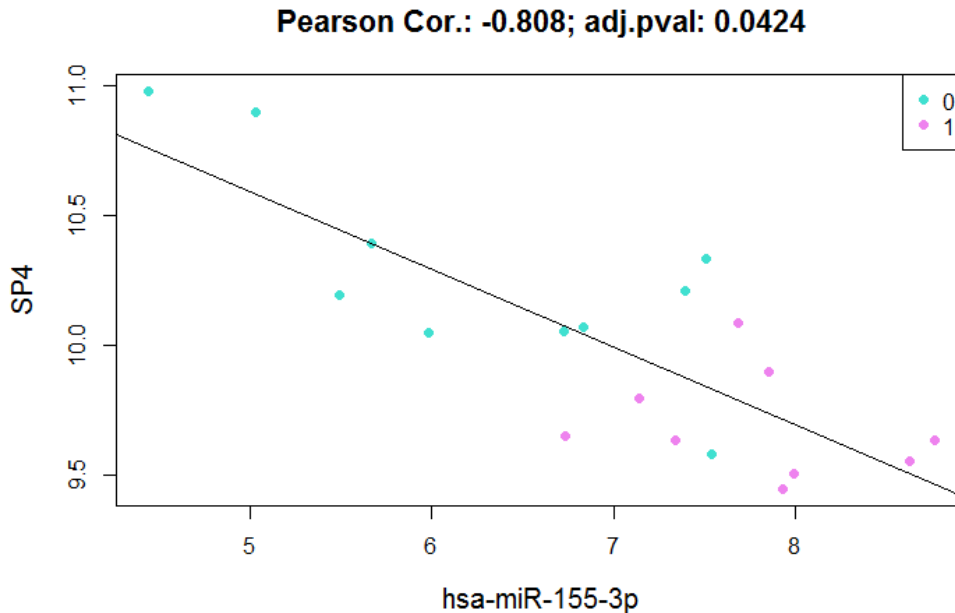


Figure 19: Correlation graph between hsa-miR-155-3p (x axon) and SP4 gene (y axon). The slope of the line and the negative correlation coefficient indicate that the correlation is negative and the FDR corrected p-value of 0.0424 is statistically significant. The nR are indicated as 0 and the fR as 1. hsa-miR-155-3p is upregulated in fR and less expressed in nR. SP4 gene levels move in the opposite direction, decreased in fR and upregulated in nR. (produced by miRComb)

4.3 Validation of selected miRNAs and targets with qRT-PCR

1. miRNA quantification

The validation was performed on the initial sample that was used for the correlation analysis (10 fR and 10 nR). Shapiro Wilk test and histograms showed that the Relative Quantities (RQ) distribution was not significantly different from the normal distribution and Levene's test for the equality of variances was not significant either. Therefore, we performed a two tailed independent samples t-test to compare the means between the group of fR and that of nR. The statistical analyses of the RQ values confirmed the differential expression between fR and nR of miRNA hsa-miR-320a (p=0.001) and hsa-miR-155-3p (p=0.001) but not for hsa-miR-138-5p (p=0.128).

Similarly, in order to control for lithium effects we performed qRT-PCR using material extracted from the LCLs of fR and confronted those treated with lithium with those cultured in normal medium. In order to estimate hsa-miR-27a-3p differential expression we performed a paired samples parametric t-test. The test showed no statistically significant differences between the two groups

(fR+Li vs fR-Li; p=0.233). As a result, our only candidate as lithium mechanism's element was excluded.

2. mRNA targets quantification

qRT-PCR was performed for the selected targets of the validated miRNAs (7 in total). In total, only 3 targets were validated **CAPNS1** (hsa-miR-320a), **RGS16** (hsa-miR-320a) and **SP4** (hsa-miR-155-3p).

The RQ values for genes *RGS16*, *RHOA* and *CAPNS1* did not differ significantly from the normal distribution (Shapiro Wilk test). Thus, for these genes we performed an Independent samples t-test to compare means between our two groups (fR vs nR). Levene's test showed that the means were not significantly variable for *RGS16* and *RHOA*. The t-test confirmed the significant differential expression for *RGS16* (p=0.017) but not for *RHOA* (p=0.561). However Levene's test showed that the means were significantly variable for *CAPNS1*, thus, we did not assume equality of variances. Nevertheless, the difference of means between fR and nR remained significant for *CAPNS1* with p=0.040. Also the direction of the expression was confirmed to be the same with the microarrays experiment, overexpressed in fR for *CAPNS1* and *RGS16*.

Genes *AUTS2*, *KYAT1* and *SP4* (possible miR-155-3p targets) and *BHLHE40* (possible target of miR-320a) deviated from normal distribution, according to the Shapiro-Wilk normality test. Outliers were found only among *KYAT1* and *SP4* genes' RQ and were excluded, resulting in 9 fR vs 10 nR, which underwent subsequent analysis. Means were compared using non-parametric Mann-Whitney U-test. The resulting p-value was not significant for *BHLHE40* (p=0.529), *AUTS2* (p=0.089), *KYAT1* (p=0.447) and showed a trend for association with response for *SP4* (p=0.053), in accordance with the direction of the expression found in the microarrays (dowregulated in fR and upregulated in nR). For the statistical analysis results for all the tested genes see Table 15.

Table 15: SPSS analysis of qRT-PCR results			
Group Statistics		Lithium Response	
Gene		<i>fR</i>	<i>nR</i>
<i>RGS16</i> ¹	<i>N</i>	10	10
	<i>Mean</i>	0.94	0.66
	<i>Standard Deviation</i>	0.28	0.19
	<i>p-value (two-tailed)</i>	0.017*	
<i>CAPNS1</i> ¹	<i>N</i>	10	10

	<i>Mean</i>	<i>1.78</i>	<i>1.20</i>
	<i>Standard Deviation</i>	<i>0.86</i>	<i>0.19</i>
	<i>p-value (two-tailed)</i>	<i>0.040*</i>	
<i>RHOA¹</i>	<i>N</i>	<i>10</i>	<i>10</i>
	<i>Mean</i>	<i>1.19</i>	<i>1.13</i>
	<i>Standard Deviation</i>	<i>0.27</i>	<i>0.14</i>
	<i>p-value (two-tailed)</i>	<i>0.561</i>	
<i>BHLHE40²</i>	<i>N</i>	<i>10</i>	<i>10</i>
	<i>Mean</i>	<i>2.17</i>	<i>1.35</i>
	<i>Standard Deviation</i>	<i>1.67</i>	<i>0.46</i>
	<i>p-value (two-tailed)</i>	<i>0.529</i>	
<i>SP4²</i>	<i>N</i>	<i>9</i>	<i>10</i>
	<i>Mean</i>	<i>0.60</i>	<i>1.82</i>
	<i>Standard Deviation</i>	<i>0.37</i>	<i>1.40</i>
	<i>p-value (two-tailed)</i>	<i>0.053**</i>	
<i>AUTS2²</i>	<i>N</i>	<i>10</i>	<i>10</i>
	<i>Mean</i>	<i>3.53</i>	<i>1.68</i>
	<i>Standard Deviation</i>	<i>3.04</i>	<i>2.02</i>
	<i>p-value (two-tailed)</i>	<i>0.089</i>	
<i>KYAT1²</i>	<i>N</i>	<i>9</i>	<i>10</i>
	<i>Mean</i>	<i>1.19</i>	<i>3.13</i>
	<i>Standard Deviation</i>	<i>0.34</i>	<i>2.63</i>
	<i>p-value (two-tailed)</i>	<i>0.447</i>	
<i>1 independent samples t-test, 2 Mann Whitney U test, *statistically significant differences when comparing the means of the two groups, **there is a trend towards significance</i>			

For the validated targets and *SP4* we performed a correlation analysis using the qRT-PCR data to explore whether also the correlation was validated. The inverse correlation was validated between

SP4 and *hsa-miR-155-3p* (correlation coefficient -0.457 and $p=0.021$; Figure 20).

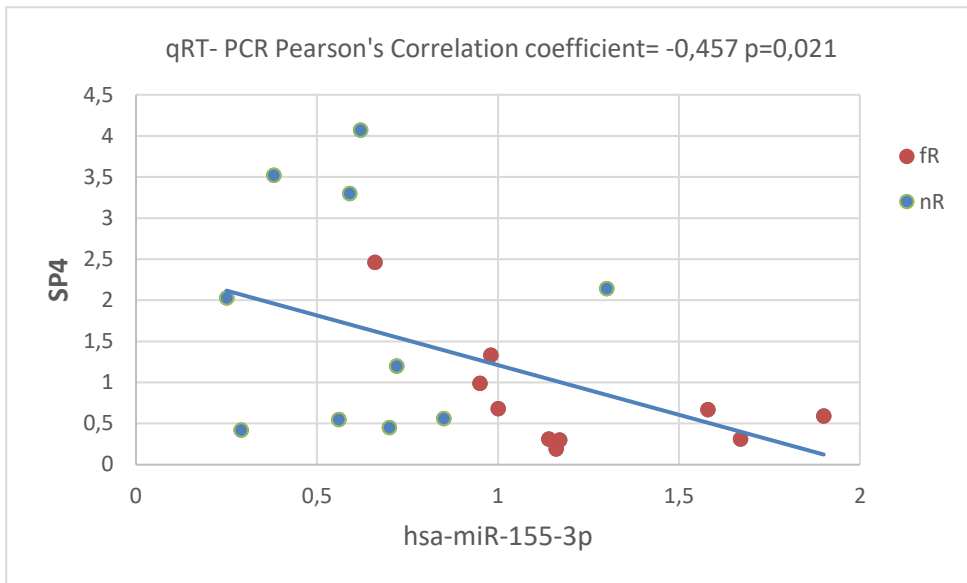


Figure 20: Pearson's correlation analysis for validated gene *SP4* and *hsa-miR-155-3p*. *fR*: full-responders, *nR*: non-responders

As we can see in Figure 21 and 22 the correlation analysis was not statistically significant for the rest of the validated targets (*CAPNS1* and *RGS16*) but the slope between transcript levels and miRNA levels was negative, suggesting a negative correlation, in agreement with the NGS findings presented in Figure 17 and 18).

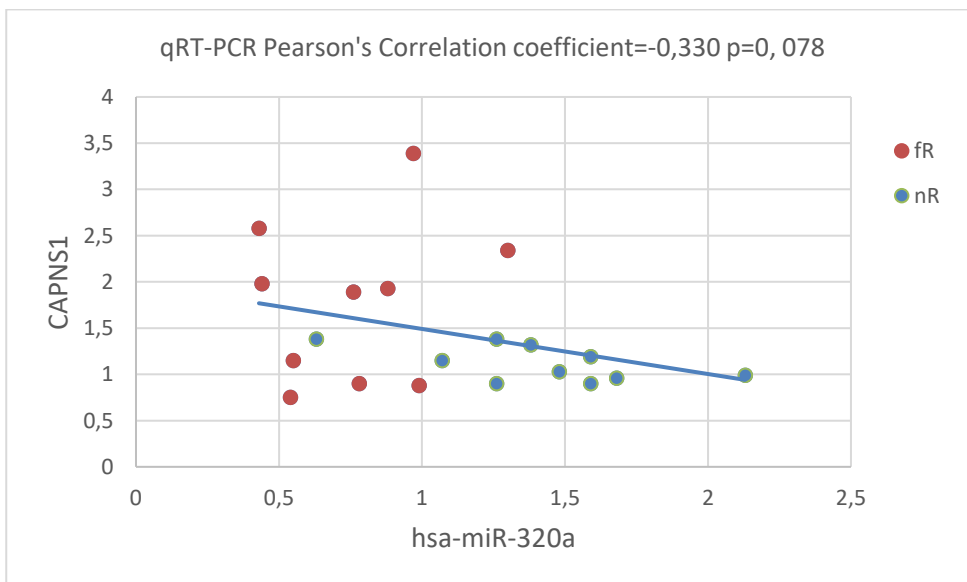


Figure 21: Pearson's correlation analysis for validated gene *CAPNS1* and *hsa-miR-320a*. *fR*: full-responders, *nR*: non-responders

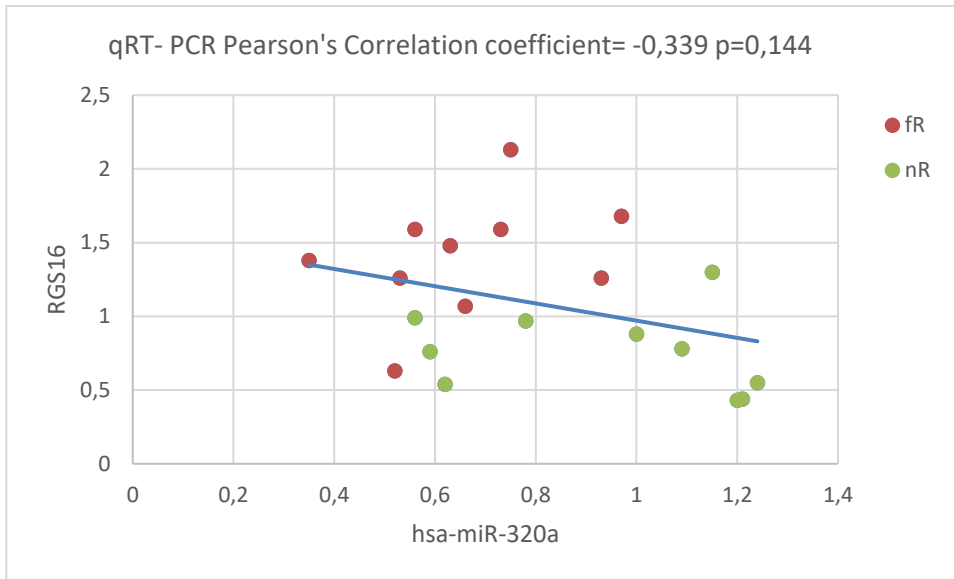


Figure 22: Pearson's correlation analysis for validated gene RGS16 and hsa-miR-320a. fR: full-responders, nR: non-responders

5. Discussion and Future Directions

In this study, we report the findings from the 1st genome wide investigation of miRNAs using NGS conducted on patient derived cell lines characterized for response in lithium treatment. The NGS data from 20 BDI patients were combined with microarray expression data from the same sample and after in silico analysis we obtained two lists of miRNAs and their inversely correlated mRNAs: one list of differentially expressed miRNA/mRNA between fR and nR (FDR < 0.05) and another list with miRNA/mRNA differentially regulated by in vitro lithium treatment in fR but not affected in nR (FDR < 0.2). The above lists were filtered for targets predicted by at least one of the seven target-prediction databases interrogated. After prioritization of the resulting miRNA-mRNA couples, we validated the selected ones via qRT-PCR. The principal findings of this study summarize in 3 miRNA-mRNA couples, namely miR-155-3p - *SP4*, miR-320a – *CAPNS1* and miR-320a – *RGS16*. The discovery of miRNA biomarkers and the correlation of the detected couples with mechanisms involved in BD and lithium response are the principal aims of this study thus in this section we will discuss the existing knowledge around the miRNAs and mRNAs indicated by our study and whether they are supported by previous studies.

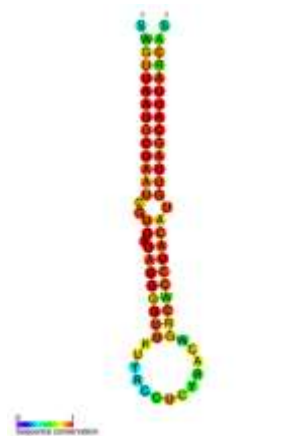


Figure 23: miR-155 is a highly conserved miRNA with red we can see the conserved bases

MiR-155 is a highly conserved miRNA. The MIR155HG gene is transcribed by RNA polymerase II and the resulting ~1,500 nucleotide RNA pri-miRNA is cleaved by Drosha to produce a 65 nucleotide stem-loop precursor miRNA (pre-mir-155). One of the two precursor strands holds the "passenger miRNA" (miR-155*). MiR-155* is released and degraded while the other strand, designated to be the "guide strand" or "mature miRNA" (miR-155), is retained within the RISC²²⁷. Recent data suggest that both arms of the pre-miRNA hairpin can give rise to mature miRNAs. The mature miRNA is considered the miR-155-5p. In contrast to miR-155-5p, the miRNA miR-155-3p is produced from the complementary strand but 20-200 times less frequently²²⁸ and the concentration in hematopoietic cells is very low²²⁹. In addition, much less sequence data is available regarding the level of conservation of miR-155-3p across species²³⁰ (miRBase; www.mirbase.org).

Concerning miR-155-5p, we know that it is specific for hematopoietic cells, including B-cells, T-cells, monocytes and granulocytes²²⁹, and a variety of physiological functions have been attributed to miR-155 gene including hematopoiesis, development and maturation of lymphocytes, immunity, inflammation, cancer and cardiovascular disease²³¹.

In disease conditions, miR-155 is overexpressed in autoimmune disorders²³²⁻²³⁴, B cell lymphomas²³⁵ and viral infections²³⁶⁻²³⁸. Findings suggesting a role for miR-155 in the immune system and inflammation are in accordance with the normalization of proinflammatory cytokines by mood stabilizers^{41,239} and the largely discussed hypothesis of altered inflammatory response in BD³⁹. Several independent studies have demonstrated that miR-155 regulates the inflammation in various disease as a proinflammatory miRNA, by upregulating proinflammatory cytokines and downregulating anti-inflammatory cytokines in macrophages^{213,240,241} and microglia²⁴².

Moreover, in autoimmune disease miR-155 induces inflammatory responses. In particular, increased miR-155 promotes inflammation²³². In accordance to that, Prajapati et al., (2015) suggested that this miRNA is upregulated due to the proinflammatory cytokine TNF- α ²⁴³. On the contrary, miR-155 inhibition had the opposite effects^{233,234}. Surprisingly, miR-155 levels increase due to glucocorticoids (dexamethasone) commonly used to treat autoimmune conditions²⁴⁴.

MiR-155 is expressed in B cells and regulates immune response also in viral infections, such as encephalitis²³⁶. MiR-155 seems to mediate the innate immune response and could be negative regulator of the viral load^{237,245}.

An increasing body of evidence supports that miR-155 levels have a key role in neuroprotection. MiR-155 involvement in neuroinflammation and in extension to oxidative stress and apoptosis has been initially demonstrated by models of induced neuronal damage. In microglia, the cells in charge of the immune defense of the central nervous system, lipopolysaccharide (LPS) induced inflammation, increased the levels of miR-155 in comparison to controls. Induction of miR-155 increased the oxidative activity, activated Toll-like receptor 4 (TLR4), increased levels of pro-inflammatory cytokines²⁴² and decreased the suppressor of cytokine signaling (SOCS1)²⁴⁶. In contrast, depletion of miR-155-5p promoted neural regeneration, regulated the levels of proinflammatory and anti-inflammatory cytokines, and decreased the extent of inflammation in mice macrophages²⁴⁰ and rat brain tissue²⁴⁷. In addition, antiapoptotic effects have been attributed to miR-155, mediated by IL-17 pro-inflammatory cytokine²⁴⁸. The neuroprotective and neuroregenerative functions of this miRNA were later confirmed by Harrison et al., (2017)²⁴⁹. Several studies investigated the involvement of miR-155 in neuronal conditions like neuropathic pain²⁵⁰ and neurodegenerative diseases, namely AD and ALS, by regulating inflammation in neuron supporting cells^{251,252} and indirectly by regulating T lymphocytes function²⁵³.

Moreover, administration of miR-155 antagonist also significantly increased the level of BDNF^{254,255}, a well-studied neurotrophin and key protein of the neurotrophin theory for BD²⁰ and mediator of lithium therapeutic responses²⁶.

However, it is not known if miR-155-3p plays a role in the above processes because few studies have investigated the expression levels of miR-155-3p due to the fact that miR-155-5p is the principally expressed mature miRNA^(256 ; miRmine; <http://guanlab.ccmb.med.umich.edu/mirmine/>). With the exception that miR-155-3p is found in astrocytes²⁵⁷ and plasmacytoid dendritic cells²⁵⁸, is involved in hepatocellular carcinoma²⁵⁹, and the pathogenesis of autoimmune encephalomyelitis²⁶⁰ our knowledge regarding miR-155-3p is very limited. In our study hsa-miR-155-3p is upregulated in fR in comparison with nR. We are not sure if this means that during maturation of the precursor into miR-155-3p, the complementary strand, in this case the one bearing miR-155-5p is degraded due to the biosynthesis procedure described earlier in the Introduction section. That would mean lower levels of miR-155-5p, reduction of inflammatory responses, reduction of apoptosis, increment of BDNF levels and thus, better treatment response. Controversial could be considered the results from earlier studies that although not specified, they most likely refer to miR-155-5p expression. In these studies, miR-155 levels were significantly up-regulated in mice treated with lithium²⁵⁵ and in LCLs derived from BD patients treated with lithium in vitro¹⁷⁹.

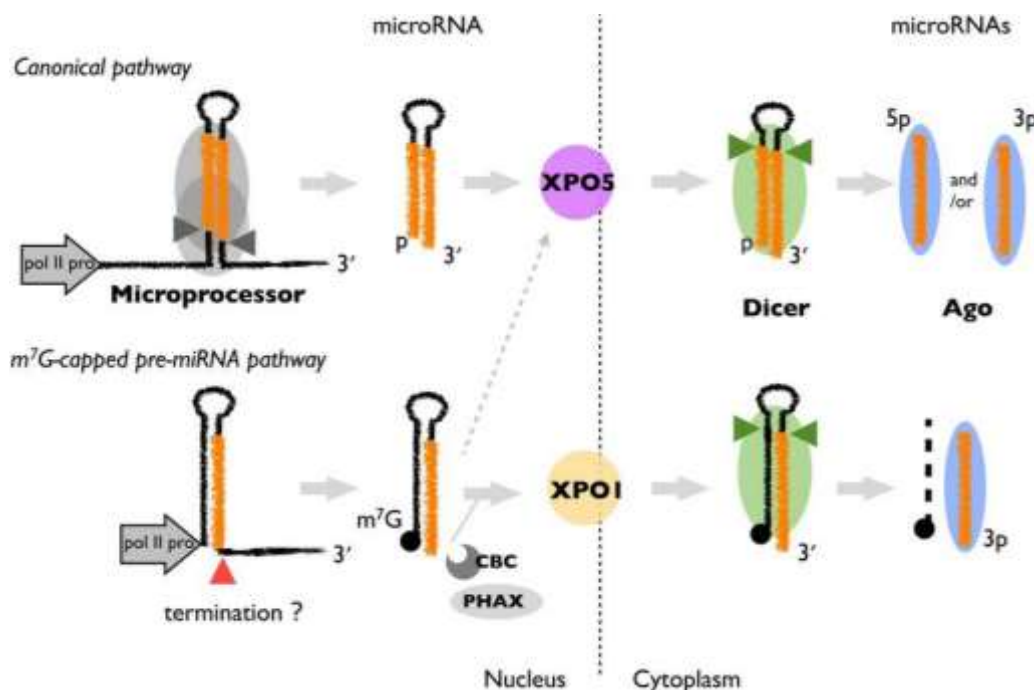


Figure 24: miRNA biosynthesis. Above is depicted the canonical biosynthesis pathway. Below is depicted the non-canonical pathway²⁶¹.

Our second candidate miRNA is miR-320a. MiR-320a and mir-320 family are ubiquitously expressed. The biogenesis of miR-320 is different from the canonical microprocessor-dependent miRNAs (Figure 24). The pre-miR-320 is transcribed directly as a precursor microRNA hairpin and contains a 5' m7G-cap. Pre-miR-320 is exported to cytoplasm preferentially from Exportin-1 instead of Exportin-5. The m7G-capped precursor is then loaded onto RISC complex in a way that only -3p miRNA matures and -5p strand is degraded ²⁶¹. As far as miR-320a functions are concerned, they converge towards an association of this miRNA with BD and lithium response. Post ischemic brain restoration ^{262,263} induced by miR-320a indicate a possible role of this miRNA as neuroprotective factor. In fact, according to White et al., (2012) ²⁶⁴ miR-320 induces neurite outgrowth by targeting cAMP-regulated phosphoprotein-19 kDa (*ARPP-19*). Moreover, many of miR-320a actions are attributed to Wnt/ β -catenin pathway by direct interaction with β -catenin ^{265,266}. B-catenin activation is a secondary messenger of GSK3 β inhibition, a mechanism strongly believed to mediate lithium's effects. In addition, miR-320a has been associated with several pathological conditions, including cardiomyopathy ²⁶⁷, neurodegenerative ^{204,268,269} and psychiatric disorders, ^{202,203,270-272}. We know that cardiovascular problems are common in BD ⁴, neurodegenerative diseases and BD share common pathogenesis mechanisms ⁵² and psychiatric disorders have an overlapping genetic background with BD.

In multiple sclerosis ²⁶⁸, miR-320a influences blood-brain barrier permeability and neurological disability through matrix metalloproteinase 9 (MMP-9) regulation in B lymphocytes ²⁶⁹. Previous studies by Rybakowski and coworkers reported that MMP-9 polymorphisms might be associated with lithium prophylactic effects, however, findings on this matter are controversial ^{121,273,274}. In AD a variant of another gene belonging in the miR-320 family is associated with increased susceptibility ²⁰⁴. In several occasions, miR-320 family members have been suggested as peripheral biomarkers of psychiatric disorders. Altered peripheral levels of miR-320a and other miR-320 family members consist in a good prognostic factor for schizophrenia ²⁷², autism ^{202,270} and depression ^{203,271}. In addition, miR-320a regulates Glutamate Ionotropic Receptor NMDA Type Subunit 2A (*GRIN2A*) and Disrupted in schizophrenia 1 (*DISC1*) genes that are known to be significant in the etiology of MDD ²⁰³ and is upregulated by the psychotropic drug fluoxetine in neuroblastoma cells ²⁰¹.

MiR-320 seems to be a useful biomarker for various neuropsychiatric disorders and would be interesting to evaluate the possibility of miR-320a being a biomarker of BD. However, we did not evaluate this miRNA as candidate biomarker for BD, but in lithium response. In our sample, fR had decreased levels of this miRNA in comparison with nR. It is possible that lithium acts more efficiently with lower levels of miR-320a since, as we saw, they both compete for Wnt/ β -catenin pathway.

The candidate target of miR-155-3p, as indicated by our study, is *SP4*. The protein encoded by *SP4* gene is a transcription factor from a family of transcription factors. SP4 can bind to the GC promoter region of a variety of genes. The encoded protein binds to many common sites in promoter CpG islands with the transcription factor SP1. Both transcription factors are important for epigenetic regulation not only because of their preference towards CpG islands but they also regulate DNA methyltransferase 3b (Dnmt3b), an enzyme responsible for the methylation of the DNA sequence²⁷⁵. Through the above mechanisms *SP4* and its homolog *SP1* possibly mediate the epigenetic effects of various environmental factors and medications. Mild stress and antidepressant treatment alter the methylation of promoter that are conserved binding sites of this transcriptional factor²⁷⁶. *SP4* shares many common actions with its homolog *SP1*. However, SP4 protein is not as ubiquitously expressed as SP1^{276,277}, SP4 is mostly brain specific and mainly expressed in hippocampus²¹⁵ and cerebellum²⁷⁸. SP4 protein is also found in lymph and kidneys²⁷⁹ (Human Protein Atlas available from www.proteinatlas.org). The brain specific nature of SP4 explains also that it is a crucial factor for brain maturation by regulating dendritic branching^{278,280} and may be involved in the development of the hippocampus²¹⁵.

At the molecular level, *SP4* and other members of the family regulate neurotrophin factor 3 (*NT-3*), a neurotrophin whose altered levels in serum have been associated with BD and is closely related to *BDNF*²⁷. It is known that impaired glutamatergic activity due to reduced NMDA neurotransmission is implicated in BD²⁸¹ and other psychiatric disorders²⁸². Partially silencing *SP4* led to decreased levels of NMDA receptor 1 (NMDAR1) subunits²⁸³. An N-Methyl-D-aspartate (NMDA) receptor antagonist restored Sp4 levels in mouse hippocampus²⁷⁷. The same antagonist inhibits the arachidonic acid pathway²⁸⁴, a pathway involved in mood stabilizer's beneficial actions.

SP4 is one of our more interesting candidates since it has been consistently correlated with neuropsychiatric disorders. Genomic studies associated common variants of *SP4* gene with MDD^{285,286}. Besides being associated with MDD²¹⁷ serotonin (5-HT1A) receptor promoter is one of SP4's targets²⁷⁶. The involvement of serotonin in depression and treatment of depression is well documented. In fact SSRIs, SNRIs, TCAs, tetracyclic antidepressants (TeCAs), and monoamine oxidase inhibitors (MAOIs) are common treatments of depression and their common feature is that they all increase the levels of serotonin and other neurotransmitters. Rare CNVs and deletions of *SP4* gene have been associated with SCZ²⁸⁷. Increased levels of this transcription factor were found in postmortem hippocampus of SCZ patients²⁷⁷ and PBMCs of schizophrenic postmenopausal women²¹⁶. However, antipsychotics did not affect the expression of this gene²⁷⁷. Even more interestingly, several studies focused on the involvement of *SP4* in BD²⁸⁸ and the response to mood stabilizers²¹⁴.

Specifically, levels of phosphorylated SP4 were increased²⁸⁹ and total protein levels reduced²⁹⁰ in peripheral cells of first episode BD patients. Moreover, the total level of *SP4* transcript was reduced in postmortem brains of BD patients²¹⁴. In addition, several polymorphisms on this gene were found to increase susceptibility to BD. The same studies also support the involvement of SP4 in the pharmacological actions of mood stabilizers. Lithium treatment, for example, depleted phosphorylated SP4 in rat primary cultured cerebellar granule neurons²⁸⁹. Moreover, mice missing one *Sp4* functional gene developed sensorimotor gating symptoms, an endophenotype of BD and SCZ, while lithium treatment led to partial remission^{177,215}. And finally, lithium stabilized the loss of SP4 protein in non-depolarizing neurons,²¹⁴ showing an actual mechanistic interaction between lithium and SP4, suggesting SP4 as possible mediator of lithium's pharmacological actions.

RGS16 is one of miR-320a possible targets, it codifies for the Regulator of G-protein signaling 16. The protein encoded by this gene belongs to the 'regulator of G protein signaling' family. It inhibits signal transduction by increasing the GTPase activity of G protein alpha subunits. Most neurotransmitters' receptors are linked with G-proteins. The G-protein coupled receptors are a category of receptors linked to enzymes that initiate signaling pathways. These receptors are widely studied in relation to BD not only because they mediate neurotransmitters' transduction signaling, but also because the levels²⁹¹ and the 5-hydroxytryptamine (5-HT) ligand mediated activation²⁹² of the stimulatory subtype of G-protein coupled receptors (Gas) were increased in the cortex of BD patients. Moreover, Gas levels tended to normalize under lithium treatment²⁹³. *RGS16* has been mostly cited for its involvement in insulin regulation and proliferation of β -cells in pancreas²⁹⁴ and related tumors²⁹⁵. Nonetheless, *RGS16* was upregulated during the day in rat hypothalamus²⁹⁶. Insights into the mechanism of *RGS16* showed that this protein is indispensable for the circadian regulation of cAMP in the superchiasmatic nucleus (SCN), variants in the gene are associated with chronotypes and deletion of the gene affects behavioral rhythms in animal models²¹². As we previously discussed in the introduction, remission in BD depends in a degree to circadian rhythm stability^{46,297} and lithium besides regulating many circadian genes²⁹⁸ also seems to stabilize the symptoms related to the disrupted rhythmicity of BD, such as sleep/wake cycle. Other members of the same family regulate neuroinflammation and neurodegeneration pathways²⁹⁹. *RGS16* protein is expressed in several brain regions, predominantly in the thalamic midline/intralaminar and principal relay nuclei, and the hypothalamic SCN³⁰⁰.

CAPNS1 is Calpain small subunit 1 and was also suggested as miR-320a target. Calpains are a ubiquitous, well-conserved family, implicated in neurodegenerative processes. They are involved in dendritic branching, spine density and hippocampal long term potentiation²¹⁰. Their activation can

be triggered by ROS^{301,302}, calcium influx, and endoplasmic reticulum (ER) stress^{301,303,304} and lead to cell death. Calcium dependent cysteine proteases, like CAPNS1, are involved in autophagy, apoptosis, migration, etc.^{209,305}. Marcassa E et al., (2017) showed that thapsigargin can induce autophagy through *CAPNS1* activation³⁰⁶. Thapsigargin is a drug used to induce ER stress by inhibiting ER Ca²⁺ ATPase. Lithium has been found to attenuate thapsigargin actions in LCLs by restoring Ca²⁺ levels³⁰⁷. Moreover, CAPNS1 seems to be involved in mechanisms associated with BD, such as ROS activity and inflammation and its expression profile clusters with oxidative stress and inflammation related genes³⁰². In addition, common variants of the gene are associated with IL-6 expression induction³⁰⁸. IL-6 is an important proinflammatory cytokine that plays critical roles in both innate and adaptive immunity and is vital in the transition from an acute to a sustained inflammatory response; IL-6 has also been considered as possible therapeutic target in BD³⁰⁹. At the molecular level, CAPNS1 upregulates β -catenin levels, an action mediated by GSK3b inhibition by lithium and correlated with lithium's therapeutic effects³¹⁰. CAPNS1, in turns, is regulated by epigenetic mechanisms and post transcriptional regulators. Several miRNAs target this gene³¹¹⁻³¹³ and in SCZ patients it is hypermethylated in the prefrontal cortex (PFC)²¹¹.

Although for some of our findings the biological evidence are compelling, the strength of our study is somehow limited by the size of the sample, the experimental model and the lack of functional validation. The miRNA profiles of 20 BDI fR and nR to lithium as well as the lithium effects on cell lines derived from the same subjects are valuable preliminary data. Our main findings originate all from the comparison between nR and fR, this is because our candidate miRNA differentially regulated by lithium in vitro in fR compared to nR was not validated. This in combination with the fact that we had to apply a less stringent criterion for statistical significance to select candidates for validation (FDR<0.2) undernotes the need of a larger detection sample and an appropriate replication sample to observe lithium effects. Unfortunately, our sample size was limited by several factors including the number of patients fitting the criteria of our study. As far as our validated miRNA-target couples are concerned, a replication sample, larger than the detection sample, composed of BD patients characterized for lithium response and preferably in monotherapy with lithium, would finely address the sample size problem and boost our discovery. Ideally, longitudinal prospective studies using peripheral samples from drug naïve BD patients before and after treatment with lithium monotherapy could give us a more clear idea of possible lithium biomarkers. However, this approach has some obvious difficulties: i) first episode patients rarely are treated in a controlled clinic environment ii) they usually present with depression consequently BD is not diagnosed at this early stage and they are initially treated for depression and iii) finally, due to the risks of severe adverse reactions and the requirement for constant monitoring of the patient, lithium is often not used in first

episode patients. In fact, there is one single study, conducted by Rong et al. in 2011, adopting a longitudinal prospective approach, using initially drug naïve BD subjects ¹⁷⁸.

Another weakness of our study is that our patient derived cell lines, in that case LCLs, are immortalized with Epstein-Bar virus. Expression levels and especially epigenetic marks are known to be altered by viral infections, like Epstein virus, thus, attention should be paid ³¹⁴. As an alternative to LCLs in the research for biomarkers of response we could use PBMCs which did not undergo the immortalization procedure. However this does not seem to be a major problem since PBMCs share 99% DNA sequence similarity with LCLS and our study design makes sure to overcome the immortalization barrier by confronting only responders with non-responders transformed with the same protocol and when we test for lithium's effects we make sure to do it in vitro. Besides, PBMCs have the disadvantage that they cannot be conserved for long periods in culture.

Another possible disadvantage of our model is that it originates from the peripheral system and it is not directly related to the brain. Most of the theories regarding the pathogenesis of BD start and end with the brain's chemical and molecular balance ¹². Nevertheless, peripheral samples (LCLs, PBMCs) have an approximately 22.9% co-expression with post mortem brain samples ³¹⁵ and LCLs have been used extensively for BD research and important findings can be attributed to their use ³¹⁶. In addition, expression data from blood preparations are more suitable as biomarkers, since they are more accessible than brain tissues. However they might not be so appropriate in deciphering the mechanisms involved in BD pathogenesis and lithium response. This can be compensated with additional functional studies using appropriate cellular and animal models as I will analyze later in the discussion section. As alternative to peripheral cells or additional functional studies a few groups used another approach that included olfactory neuronal epithelium cells. These cells have the advantage of being a patient derived neuronal model, however they are short living cells, usually obtained with methods considered invasive and compromising, and still are not the neural type involved in BD. As a result, only few studies chose this approach and are reviewed in Viswanath et al., (2015) ³¹⁶. The answer to BD cellular modeling might come from another growing field of induced Pluripotent Stem Cells (iPSCs) ³¹⁷. iPSCs produced from LCLs ³¹⁸ or more commonly from fibroblasts ³¹⁹ can be cryopreserved and put in culture when needed. With proper care iPSCs can be cultured for several passages and can be differentiated into neural progenitor cells (NPCs), neurons and other type of cells. NPCs and neurons derived from iPSCs are used more and more in research of neurodegenerative and psychiatric disorders ³²⁰. Existing studies on iPSCs have investigated lithium's effects on neurons from iPSCs ³²¹ lithium effects on neurons from iPSCs derived from BD patients ³²² and one study confronted neurons derived from iPSCs from BD patients, responders and non-

responders to lithium³²³ so far. An alternative to iPSCs are the iNeurons which are directly produced from human fibroblasts in vitro^{324,325} also applied to study BD patients characterized for lithium response¹¹⁷.

Besides targeted quantification, a functional analysis could also shed light into whether the suggested miRNA-mRNA interactions are actually taking place in a cellular environment. There is a large number of options for performing a functional analysis. Firstly, we would have to decide the type of model. For once, in vitro models are cheaper, faster and easier to handle than animal models, however, they provide less information regarding the phenotype and possible systemic responses that follow the miRNA overexpression or loss of function. In vitro approaches require the selection of an appropriate cellular model. This can be either related to the disease under study, like neuronal/glia cells, or any other tissue of origin that expresses or not the miRNA under study, depending on the study design¹⁴². For example, a gain of function approach requires low or no expression of the miRNA and expression of the candidate target. Such experiments can be performed using miRNA mimics (Figure 25), which are synthetic homologues of the actual miRNA, or with miRNA expression vectors. By increasing the levels of the miRNA we expect a decrease in the level of the target. On the contrary, a loss of function study design requires a model that expresses the miRNA of interest. Techniques used to inhibit a miRNA include transfection with i) anti-miRs (AMOs; Figure 25), constructs which hybridize to the mature miRNA or the precursor, thus, hindering its actions, ii) the sponges (Figure 25), they act in the same way but they can hybridize more miRNAs at the same time and iii) target inhibitors (or masks) (Figure 25), oligoribonucleotide sequences complementary to the 3'UTR of the target. MiRNA inhibitors (anti-miRs or sponges) can be introduced also in expression constructs leading to intracellular miRNA inhibition and as a result we would expect an increase in the levels of the mRNA target³²⁶. The implications of the miRNA alterations on gene and protein expression profiles are measured with qRT-PCR and Western blot respectively.

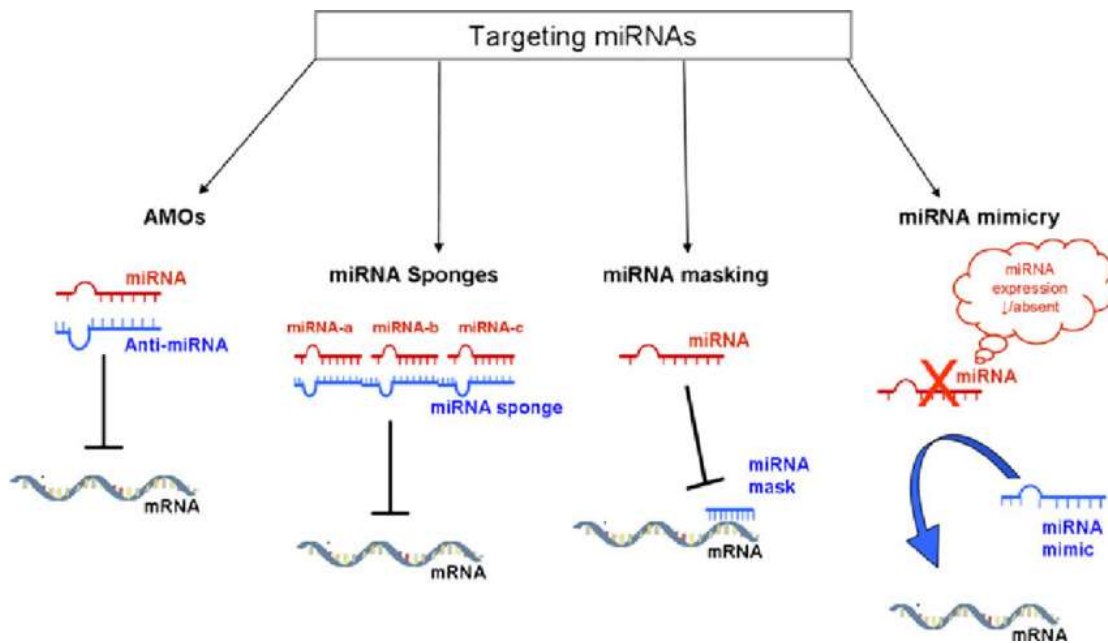


Figure 25: Different types of synthetic oligoribonucleotides used in miRNA interaction experiments that either increase (miRNA mimic) or inhibit (Anti-miRNA, sponges, target inhibitors or masks) endogenous miRNAs actions. AMOs: anti-miRNA or miRNA complementary inhibitors.

In vivo studies have the advantage that they permit us to observe behavioral and physiological effects. Regardless the different observations that permit us the in vivo and in vitro model, the approaches used to detect interactions are in principle the same. For example, in mouse models it is possible to introduce the miRNA (over)expression construct into almost any mouse tissue with the help of transgenic mice technology. Similarly, a loss of function approach can be adopted by producing knockout mice for the miRNA gene of interest or using a mutated target binding site. In the latter case, we can validate a direct miRNA-mRNA interaction and at the same time observe the implications from the inhibition of this interaction ³²⁶.

Gold standard among these methods is the luciferase assay. To perform the luciferase assay we clone the mRNA target's 3'UTR or a mutated version of it downstream of the reporter coding region in a DNA construct. Subsequently, by transfecting the construct into cells expressing the relevant miRNA, it is possible to see if the interaction takes place by measuring the signal of the reporter gene ³²⁷. Other approaches that allow us to detect direct interaction of the miRNA with the target 3'UTR, involve the use of target inhibitors in combination with the above mentioned reporter construct. Thus, when the target inhibitors bound to the target they attenuate miRNA action resulting in restoring higher levels of mRNA target ¹⁴².

In the context of this study we did not proceed with the approaches recommended earlier in the discussion, however, further investigation of the meaning and reproducibility of our findings is warranted.

To conclude, I would like to highlight the importance of our study. Our work is the first validated whole genome miRNA expression profiling study performed with NGS that not only confronted the cohorts of excellent responders and non-responders to lithium, but also investigated the effects of lithium on patient derived cell lines. Another very important aspect of the study is the combination of actual miRNA and mRNA expression data and, as such, we did not rely only on predictions to identify potential couples. Moreover, our subjects are followed by our lithium clinic “Clinical Psychopharmacology Centre of the University Hospital of Cagliari, Italy”, thus, we were able to obtain a thorough and detailed clinical description and characterization for lithium response. The miRNAs identified in this study and the mRNAs they regulate are interesting candidate biomarkers for lithium response and further research, following a careful study design as extensively discussed in this section, is highly recommended. In present days, the exploration of non – coding RNAs in the context of BD and lithium response has drawn the attention of several scientific groups. Our study, justifies this notion and highlights once more the importance of the non-coding portion of the genome in lithium response.

References

1. Mack GS. MicroRNA gets down to business. *Nat Biotechnol.* 2007;25(6):631-638.
2. O'Connor RM, Dinan TG, Cryan JF. Little things on which happiness depends: microRNAs as novel therapeutic targets for the treatment of anxiety and depression. *Mol Psychiatry.* 2012;17(4):359-376.
3. Kleine-Budde K, Touil E, Moock J, Bramesfeld A, Kawohl W, Rössler W. Cost of illness for bipolar disorder: a systematic review of the economic burden. *Bipolar Disord.* 2014;16(4):337-353.
4. Osby U, Brandt L, Correia N, Ekblom A, Sparén P. Excess mortality in bipolar and unipolar disorder in Sweden. *Arch Gen Psychiatry.* 2001;58(9):844-850.
5. Tondo L, Isacsson G, Baldessarini R. Suicidal behaviour in bipolar disorder: risk and prevention. *CNS Drugs.* 2003;17(7):491-511.
6. Pompili M, Innamorati M, Raja M, et al. Suicide risk in depression and bipolar disorder: Do impulsiveness-aggressiveness and pharmacotherapy predict suicidal intent? *Neuropsychiatr Dis Treat.* 2008;4(1):247-255.
7. Association AP. *Diagnostic and statistical manual of mental disorders IV* ed. Washington, DC: American Psychiatric Association; 2000.
8. World Health Organization sb. *International statistical classification of diseases and related health problems.* 10th revision, Fifth edition. ed. Switzerland: Geneva, Switzerland : World Health Organization, 2016.
9. Kupka RW, Altshuler LL, Nolen WA, et al. Three times more days depressed than manic or hypomanic in both bipolar I and bipolar II disorder. *Bipolar Disord.* 2007;9(5):531-535.
10. Merikangas KR, Jin R, He JP, et al. Prevalence and correlates of bipolar spectrum disorder in the world mental health survey initiative. *Arch Gen Psychiatry.* 2011;68(3):241-251.
11. Drevets WC, Frank E, Price JC, et al. PET imaging of serotonin 1A receptor binding in depression. *Biol Psychiatry.* 1999;46(10):1375-1387.
12. Manji HK, Quiroz JA, Payne JL, et al. The underlying neurobiology of bipolar disorder. *World Psychiatry.* 2003;2(3):136-146.
13. Baraban JM, Wang RY, Aghajanian G. Reserpine suppression of dorsal raphe neuronal firing: mediation by adrenergic system. *Eur J Pharmacol.* 1978;52(1):27-36.
14. Tellioglu T, Robertson D. Genetic or acquired deficits in the norepinephrine transporter: current understanding of clinical implications. *Expert Rev Mol Med.* 2001;2001:1-10.
15. Esler M, Alvarenga M, Pier C, et al. The neuronal noradrenaline transporter, anxiety and cardiovascular disease. *J Psychopharmacol.* 2006;20(4 Suppl):60-66.
16. Goodwin FK, Jamison KR. *Manic-depressive illness.* New York ; Oxford: Oxford University Press; 1990.
17. Manji PW. Monoaminergic mechanisms in bipolar disorder. In: Young LT JR, ed. *Bipolar disorder: biological models and their clinical application.* New York: Dekker1997:1-40.
18. Davies AM. The neurotrophic hypothesis: where does it stand? *Philos Trans R Soc Lond B Biol Sci.* 1996;351(1338):389-394.
19. Rattiner LM, Davis M, Ressler KJ. Brain-derived neurotrophic factor in amygdala-dependent learning. *Neuroscientist.* 2005;11(4):323-333.
20. Post RM. Role of BDNF in bipolar and unipolar disorder: clinical and theoretical implications. *J Psychiatr Res.* 2007;41(12):979-990.
21. Machado-Vieira R, Dietrich MO, Leke R, et al. Decreased plasma brain derived neurotrophic factor levels in unmedicated bipolar patients during manic episode. *Biol Psychiatry.* 2007;61(2):142-144.
22. Li Z, Zhang C, Fan J, et al. Brain-derived neurotrophic factor levels and bipolar disorder in patients in their first depressive episode: 3-year prospective longitudinal study. *Br J Psychiatry.* 2014;205(1):29-35.
23. Fernandes BS, Molendijk ML, Köhler CA, et al. Peripheral brain-derived neurotrophic factor (BDNF) as a biomarker in bipolar disorder: a meta-analysis of 52 studies. *BMC Med.* 2015;13:289.

24. Kauer-Sant'Anna M, Kapczinski F, Andreazza AC, et al. Brain-derived neurotrophic factor and inflammatory markers in patients with early- vs. late-stage bipolar disorder. *Int J Neuropsychopharmacol*. 2009;12(4):447-458.
25. Cunha AB, Frey BN, Andreazza AC, et al. Serum brain-derived neurotrophic factor is decreased in bipolar disorder during depressive and manic episodes. *Neurosci Lett*. 2006;398(3):215-219.
26. Manji HK, Moore GJ, Chen G. Clinical and preclinical evidence for the neurotrophic effects of mood stabilizers: implications for the pathophysiology and treatment of manic-depressive illness. *Biol Psychiatry*. 2000;48(8):740-754.
27. Tseng PT, Chen YW, Tu KY, et al. State-dependent increase in the levels of neurotrophin-3 and neurotrophin-4/5 in patients with bipolar disorder: A meta-analysis. *J Psychiatr Res*. 2016;79:86-92.
28. Walz JC, Magalhães PV, Giglio LM, et al. Increased serum neurotrophin-4/5 levels in bipolar disorder. *J Psychiatr Res*. 2009;43(7):721-723.
29. Walz JC, Andreazza AC, Frey BN, et al. Serum neurotrophin-3 is increased during manic and depressive episodes in bipolar disorder. *Neurosci Lett*. 2007;415(1):87-89.
30. Scola G, Andreazza AC. The role of neurotrophins in bipolar disorder. *Prog Neuropsychopharmacol Biol Psychiatry*. 2015;56:122-128.
31. Squassina A, Costa M, Congiu D, et al. Insulin-like growth factor 1 (IGF-1) expression is up-regulated in lymphoblastoid cell lines of lithium responsive bipolar disorder patients. *Pharmacol Res*. 2013;73:1-7.
32. Girshkin L, O'Reilly N, Quidé Y, et al. Diurnal cortisol variation and cortisol response to an MRI stressor in schizophrenia and bipolar disorder. *Psychoneuroendocrinology*. 2016;67:61-69.
33. Watson S, Gallagher P, Ritchie JC, Ferrier IN, Young AH. Hypothalamic-pituitary-adrenal axis function in patients with bipolar disorder. *Br J Psychiatry*. 2004;184:496-502.
34. Deshauer D, Duffy A, Alda M, Grof E, Albuquerque J, Grof P. The cortisol awakening response in bipolar illness: a pilot study. *Can J Psychiatry*. 2003;48(7):462-466.
35. Vieta E, Gasto C, Martinez de Osaba MJ, et al. Prediction of depressive relapse in remitted bipolar patients using corticotrophin-releasing hormone challenge test. *Acta Psychiatr Scand*. 1997;95(3):205-211.
36. Glavin GB, Paré WP, Sandbak T, Bakke HK, Murison R. Restraint stress in biomedical research: an update. *Neurosci Biobehav Rev*. 1994;18(2):223-249.
37. Schindler C, Levy DE, Decker T. JAK-STAT signaling: from interferons to cytokines. *J Biol Chem*. 2007;282(28):20059-20063.
38. Souza JA, Rossa C, Garlet GP, Nogueira AV, Cirelli JA. Modulation of host cell signaling pathways as a therapeutic approach in periodontal disease. *J Appl Oral Sci*. 2012;20(2):128-138.
39. Muneer A. Bipolar Disorder: Role of Inflammation and the Development of Disease Biomarkers. *Psychiatry Investig*. 2016;13(1):18-33.
40. Becking K, Boschloo L, Vogelzangs N, et al. The association between immune activation and manic symptoms in patients with a depressive disorder. *Transl Psychiatry*. 2013;3:e314.
41. Knijff EM, Breunis MN, Kupka RW, et al. An imbalance in the production of IL-1beta and IL-6 by monocytes of bipolar patients: restoration by lithium treatment. *Bipolar Disord*. 2007;9(7):743-753.
42. Rapaport MH, Guylai L, Whybrow P. Immune parameters in rapid cycling bipolar patients before and after lithium treatment. *J Psychiatr Res*. 1999;33(4):335-340.
43. Boufidou F, Nikolaou C, Alevizos B, Liappas IA, Christodoulou GN. Cytokine production in bipolar affective disorder patients under lithium treatment. *J Affect Disord*. 2004;82(2):309-313.
44. Padmos RC, Hillegers MH, Knijff EM, et al. A discriminating messenger RNA signature for bipolar disorder formed by an aberrant expression of inflammatory genes in monocytes. *Arch Gen Psychiatry*. 2008;65(4):395-407.
45. Powell TR, McGuffin P, D'Souza UM, et al. Putative transcriptomic biomarkers in the inflammatory cytokine pathway differentiate major depressive disorder patients from control subjects and bipolar disorder patients. *PLoS One*. 2014;9(3):e91076.
46. Geoffroy PA, Etain B, Sportiche S, Bellivier F. Circadian biomarkers in patients with bipolar disorder: promising putative predictors of lithium response. *Int J Bipolar Disord*. 2014;2(1):28.

47. Geoffroy PA, Bellivier F, Scott J, et al. Bipolar disorder with seasonal pattern: clinical characteristics and gender influences. *Chronobiol Int*. 2013;30(9):1101-1107.
48. Roybal K, Theobald D, Graham A, et al. Mania-like behavior induced by disruption of CLOCK. *Proc Natl Acad Sci U S A*. 2007;104(15):6406-6411.
49. Gonzalez R. The relationship between bipolar disorder and biological rhythms. *J Clin Psychiatry*. 2014;75(4):e323-331.
50. Boivin DB. Influence of sleep-wake and circadian rhythm disturbances in psychiatric disorders. *J Psychiatry Neurosci*. 2000;25(5):446-458.
51. Costa M, Squassina A, Piras IS, et al. Preliminary Transcriptome Analysis in Lymphoblasts from Cluster Headache and Bipolar Disorder Patients Implicates Dysregulation of Circadian and Serotonergic Genes. *J Mol Neurosci*. 2015;56(3):688-695.
52. Ng F, Berk M, Dean O, Bush AI. Oxidative stress in psychiatric disorders: evidence base and therapeutic implications. *Int J Neuropsychopharmacol*. 2008;11(6):851-876.
53. Axelson D, Goldstein B, Goldstein T, et al. Diagnostic Precursors to Bipolar Disorder in Offspring of Parents With Bipolar Disorder: A Longitudinal Study. *Am J Psychiatry*. 2015;172(7):638-646.
54. Smoller JW, Finn CT. Family, twin, and adoption studies of bipolar disorder. *Am J Med Genet C Semin Med Genet*. 2003;123C(1):48-58.
55. Craddock N, Sklar P. Genetics of bipolar disorder. *Lancet*. 2013;381(9878):1654-1662.
56. Tsuang M. The genetics of mood disorders. In: SV F, ed. Baltimore: The John Hopkins University Press; 1990.
57. Ferreira MA, O'Donovan MC, Meng YA, et al. Collaborative genome-wide association analysis supports a role for ANK3 and CACNA1C in bipolar disorder. *Nat Genet*. 2008;40(9):1056-1058.
58. Baum AE, Akula N, Cabanero M, et al. A genome-wide association study implicates diacylglycerol kinase eta (DGKH) and several other genes in the etiology of bipolar disorder. *Mol Psychiatry*. 2008;13(2):197-207.
59. Schulze TG, Detera-Wadleigh SD, Akula N, et al. Two variants in Ankyrin 3 (ANK3) are independent genetic risk factors for bipolar disorder. *Mol Psychiatry*. 2009;14(5):487-491.
60. Mühleisen TW, Leber M, Schulze TG, et al. Genome-wide association study reveals two new risk loci for bipolar disorder. *Nat Commun*. 2014;5:3339.
61. Xiao X, Wang L, Wang C, et al. Common variants at 2q11.2, 8q21.3, and 11q13.2 are associated with major mood disorders. *Transl Psychiatry*. 2017;7(12):1273.
62. Hou L, Bergen SE, Akula N, et al. Genome-wide association study of 40,000 individuals identifies two novel loci associated with bipolar disorder. *Hum Mol Genet*. 2016;25(15):3383-3394.
63. Song J, Bergen SE, Di Florio A, et al. Genome-wide association study identifies SESTD1 as a novel risk gene for lithium-responsive bipolar disorder. *Mol Psychiatry*. 2016;21(9):1290-1297.
64. Williams HJ, Norton N, Dwyer S, et al. Fine mapping of ZNF804A and genome-wide significant evidence for its involvement in schizophrenia and bipolar disorder. *Mol Psychiatry*. 2011;16(4):429-441.
65. Steinberg S, de Jong S, Mattheisen M, et al. Common variant at 16p11.2 conferring risk of psychosis. *Mol Psychiatry*. 2014;19(1):108-114.
66. Cichon S, Mühleisen TW, Degenhardt FA, et al. Genome-wide association study identifies genetic variation in neurocan as a susceptibility factor for bipolar disorder. *Am J Hum Genet*. 2011;88(3):372-381.
67. Green EK, Grozeva D, Forty L, et al. Association at SYNE1 in both bipolar disorder and recurrent major depression. *Mol Psychiatry*. 2013;18(5):614-617.
68. Group PGCBDW. Large-scale genome-wide association analysis of bipolar disorder identifies a new susceptibility locus near ODZ4. *Nat Genet*. 2011;43(10):977-983.
69. McMahon FJ, Akula N, Schulze TG, et al. Meta-analysis of genome-wide association data identifies a risk locus for major mood disorders on 3p21.1. *Nat Genet*. 2010;42(2):128-131.
70. Sklar P, Smoller JW, Fan J, et al. Whole-genome association study of bipolar disorder. *Mol Psychiatry*. 2008;13(6):558-569.

71. Mühleisen TW, Reinbold CS, Forstner AJ, et al. Gene set enrichment analysis and expression pattern exploration implicate an involvement of neurodevelopmental processes in bipolar disorder. *J Affect Disord.* 2018;228:20-25.
72. Swann AC. Practical Pharmacological Maintenance Treatment of Bipolar Disorder. In: *Bipolar disorder: Clinical and Neurobiological Foundations.*: John Wiley & Sons; 2010.
73. CADE JF. Lithium salts in the treatment of psychotic excitement. *Med J Aust.* 1949;2(10):349-352.
74. Garnham J, Munro A, Slaney C, et al. Prophylactic treatment response in bipolar disorder: results of a naturalistic observation study. *J Affect Disord.* 2007;104(1-3):185-190.
75. Tondo L, Baldessarini RJ. Reduced suicide risk during lithium maintenance treatment. *J Clin Psychiatry.* 2000;61 Suppl 9:97-104.
76. Yildiz A, Vieta E, Leucht S, Baldessarini RJ. Efficacy of antimanic treatments: meta-analysis of randomized, controlled trials. *Neuropsychopharmacology.* 2011;36(2):375-389.
77. Grandjean EM, Aubry JM. Lithium: updated human knowledge using an evidence-based approach: part III: clinical safety. *CNS Drugs.* 2009;23(5):397-418.
78. Movig KL, Baumgarten R, Leufkens HG, van Laarhoven JH, Egberts AC. Risk factors for the development of lithium-induced polyuria. *Br J Psychiatry.* 2003;182:319-323.
79. Livingstone C, Rampes H. Lithium: a review of its metabolic adverse effects. *J Psychopharmacol.* 2006;20(3):347-355.
80. Health POfM. Topic 7 baseline report. Monitoring of patients prescribed lithium: baseline. CRTU069 (data on file). In: Prescribing Observatory for Mental Health; 2009.
81. Andreatza AC, Young LT. The neurobiology of bipolar disorder: identifying targets for specific agents and synergies for combination treatment. *Int J Neuropsychopharmacol.* 2014;17(7):1039-1052.
82. Allison JH, Stewart MA. Reduced brain inositol in lithium-treated rats. *Nat New Biol.* 1971;233(43):267-268.
83. Berridge MJ, Irvine RF. Inositol phosphates and cell signalling. *Nature.* 1989;341(6239):197-205.
84. Silverstone PH, McGrath BM, Kim H. Bipolar disorder and myo-inositol: a review of the magnetic resonance spectroscopy findings. *Bipolar Disord.* 2005;7(1):1-10.
85. Haimovich A, Eliav U, Goldbourt A. Determination of the lithium binding site in inositol monophosphatase, the putative target for lithium therapy, by magic-angle-spinning solid-state NMR. *J Am Chem Soc.* 2012;134(12):5647-5651.
86. Stambolic V, Ruel L, Woodgett JR. Lithium inhibits glycogen synthase kinase-3 activity and mimics wingless signalling in intact cells. *Curr Biol.* 1996;6(12):1664-1668.
87. Klein PS, Melton DA. A molecular mechanism for the effect of lithium on development. *Proc Natl Acad Sci U S A.* 1996;93(16):8455-8459.
88. Prickaerts J, Moechars D, Cryns K, et al. Transgenic mice overexpressing glycogen synthase kinase 3beta: a putative model of hyperactivity and mania. *J Neurosci.* 2006;26(35):9022-9029.
89. Sinha D, Wang Z, Ruchalski KL, et al. Lithium activates the Wnt and phosphatidylinositol 3-kinase Akt signaling pathways to promote cell survival in the absence of soluble survival factors. *Am J Physiol Renal Physiol.* 2005;288(4):F703-713.
90. Bezchlibnyk YB, Xu L, Wang JF, Young LT. Decreased expression of insulin-like growth factor binding protein 2 in the prefrontal cortex of subjects with bipolar disorder and its regulation by lithium treatment. *Brain Res.* 2007;1147:213-217.
91. Guo S, Arai K, Stins MF, Chuang DM, Lo EH. Lithium upregulates vascular endothelial growth factor in brain endothelial cells and astrocytes. *Stroke.* 2009;40(2):652-655.
92. Wada A. Lithium and neuropsychiatric therapeutics: neuroplasticity via glycogen synthase kinase-3beta, beta-catenin, and neurotrophin cascades. *J Pharmacol Sci.* 2009;110(1):14-28.
93. Ye P, Hu Q, Liu H, Yan Y, D'ercole AJ. beta-catenin mediates insulin-like growth factor-I actions to promote cyclin D1 mRNA expression, cell proliferation and survival in oligodendroglial cultures. *Glia.* 2010;58(9):1031-1041.

94. McCusker RH, McCrea K, Zunich S, et al. Insulin-like growth factor-I enhances the biological activity of brain-derived neurotrophic factor on cerebrocortical neurons. *J Neuroimmunol.* 2006;179(1-2):186-190.
95. Alda M. Lithium in the treatment of bipolar disorder: pharmacology and pharmacogenetics. *Mol Psychiatry.* 2015;20(6):661-670.
96. Rybakowski JK, Suwalska A, Skibinska M, et al. Prophylactic lithium response and polymorphism of the brain-derived neurotrophic factor gene. *Pharmacopsychiatry.* 2005;38(4):166-170.
97. Moore GJ, Bebchuk JM, Wilds IB, Chen G, Manji HK, Menji HK. Lithium-induced increase in human brain grey matter. *Lancet.* 2000;356(9237):1241-1242.
98. Hajek T, Cullis J, Novak T, et al. Hippocampal volumes in bipolar disorders: opposing effects of illness burden and lithium treatment. *Bipolar Disord.* 2012;14(3):261-270.
99. Chen G, Rajkowska G, Du F, Seraji-Bozorgzad N, Manji HK. Enhancement of hippocampal neurogenesis by lithium. *J Neurochem.* 2000;75(4):1729-1734.
100. Zanni G, Michno W, Di Martino E, et al. Lithium Accumulates in Neurogenic Brain Regions as Revealed by High Resolution Ion Imaging. *Sci Rep.* 2017;7:40726.
101. Jakopc S, Karlović D, Dubravčić K, et al. Lithium effect on glutamate induced damage in glioblastoma cells. *Coll Antropol.* 2008;32 Suppl 1:87-91.
102. Chen RW, Chuang DM. Long term lithium treatment suppresses p53 and Bax expression but increases Bcl-2 expression. A prominent role in neuroprotection against excitotoxicity. *J Biol Chem.* 1999;274(10):6039-6042.
103. Lowthert L, Leffert J, Lin A, et al. Increased ratio of anti-apoptotic to pro-apoptotic Bcl2 gene-family members in lithium-responders one month after treatment initiation. *Biol Mood Anxiety Disord.* 2012;2:15.
104. Chen G, Zeng WZ, Yuan PX, et al. The mood-stabilizing agents lithium and valproate robustly increase the levels of the neuroprotective protein bcl-2 in the CNS. *J Neurochem.* 1999;72(2):879-882.
105. Berk M, Kapczinski F, Andreazza AC, et al. Pathways underlying neuroprogression in bipolar disorder: focus on inflammation, oxidative stress and neurotrophic factors. *Neurosci Biobehav Rev.* 2011;35(3):804-817.
106. Gould TD, Picchini AM, Einat H, Manji HK. Targeting glycogen synthase kinase-3 in the CNS: implications for the development of new treatments for mood disorders. *Curr Drug Targets.* 2006;7(11):1399-1409.
107. Böer U, Cierny I, Krause D, et al. Chronic lithium salt treatment reduces CRE/CREB-directed gene transcription and reverses its upregulation by chronic psychosocial stress in transgenic reporter gene mice. *Neuropsychopharmacology.* 2008;33(10):2407-2415.
108. Farah R, Khamisy-Farah R, Amit T, Youdim MB, Arraf Z. Lithium's gene expression profile, relevance to neuroprotection A cDNA microarray study. *Cell Mol Neurobiol.* 2013;33(3):411-420.
109. Cruceanu C, Alda M, Grof P, Rouleau GA, Turecki G. Synapsin II is involved in the molecular pathway of lithium treatment in bipolar disorder. *PLoS One.* 2012;7(2):e32680.
110. Sarkar S, Floto RA, Berger Z, et al. Lithium induces autophagy by inhibiting inositol monophosphatase. *J Cell Biol.* 2005;170(7):1101-1111.
111. Goodwin GM, Martinez-Aran A, Glahn DC, Vieta E. Cognitive impairment in bipolar disorder: neurodevelopment or neurodegeneration? An ECNP expert meeting report. *Eur Neuropsychopharmacol.* 2008;18(11):787-793.
112. Severino G, Squassina A, Costa M, et al. Pharmacogenomics of bipolar disorder. *Pharmacogenomics.* 2013;14(6):655-674.
113. Grof P, Duffy A, Cavazzoni P, et al. Is response to prophylactic lithium a familial trait? *J Clin Psychiatry.* 2002;63(10):942-947.
114. Tighe SK, Mahon PB, Potash JB. Predictors of lithium response in bipolar disorder. *Ther Adv Chronic Dis.* 2011;2(3):209-226.
115. Grof P, Duffy A, Alda M, Hajek T. Lithium response across generations. *Acta Psychiatr Scand.* 2009;120(5):378-385.

116. Alda M, Grof P, Rouleau GA, Turecki G, Young LT. Investigating responders to lithium prophylaxis as a strategy for mapping susceptibility genes for bipolar disorder. *Prog Neuropsychopharmacol Biol Psychiatry*. 2005;29(6):1038-1045.
117. Wang JL, Shamah SM, Sun AX, Waldman ID, Haggarty SJ, Perlis RH. Label-free, live optical imaging of reprogrammed bipolar disorder patient-derived cells reveals a functional correlate of lithium responsiveness. *Transl Psychiatry*. 2014;4:e428.
118. Perlis RH, Smoller JW, Ferreira MA, et al. A genomewide association study of response to lithium for prevention of recurrence in bipolar disorder. *Am J Psychiatry*. 2009;166(6):718-725.
119. Rybakowski JK. Genetic influences on response to mood stabilizers in bipolar disorder: current status of knowledge. *CNS Drugs*. 2013;27(3):165-173.
120. Rybakowski JK, Dmitrzak-Weglaz M, Suwalska A, Leszczynska-Rodziewicz A, Hauser J. Dopamine D1 receptor gene polymorphism is associated with prophylactic lithium response in bipolar disorder. *Pharmacopsychiatry*. 2009;42(1):20-22.
121. Rybakowski JK, Czerski P, Dmitrzak-Weglaz M, et al. Clinical and pathogenic aspects of candidate genes for lithium prophylactic efficacy. *J Psychopharmacol*. 2012;26(3):368-373.
122. Szczepankiewicz A, Rybakowski JK, Skibinska M, et al. FYN kinase gene: another glutamatergic gene associated with bipolar disorder? *Neuropsychobiology*. 2009;59(3):178-183.
123. Steen VM, Løvlie R, Osher Y, Belmaker RH, Berle JO, Gulbrandsen AK. The polymorphic inositol polyphosphate 1-phosphatase gene as a candidate for pharmacogenetic prediction of lithium-responsive manic-depressive illness. *Pharmacogenetics*. 1998;8(3):259-268.
124. Mamdani F, Alda M, Grof P, Young LT, Rouleau G, Turecki G. Lithium response and genetic variation in the CREB family of genes. *Am J Med Genet B Neuropsychiatr Genet*. 2008;147B(4):500-504.
125. Campos-de-Sousa S, Guindalini C, Tondo L, et al. Nuclear receptor rev-erb- α circadian gene variants and lithium carbonate prophylaxis in bipolar affective disorder. *J Biol Rhythms*. 2010;25(2):132-137.
126. McCarthy MJ, Nievergelt CM, Shekhtman T, Kripke DF, Welsh DK, Kelsoe JR. Functional genetic variation in the Rev-Erba pathway and lithium response in the treatment of bipolar disorder. *Genes Brain Behav*. 2011;10(8):852-861.
127. Silberberg G, Levit A, Collier D, et al. Stargazin involvement with bipolar disorder and response to lithium treatment. *Pharmacogenet Genomics*. 2008;18(5):403-412.
128. Czerski PMK, S & Maciukiewicz, Malgorzata Margaret & Hauser, Joanna & Karlowski, W & Cichon, Sven, & Rybakowski J. P.1.003 Multiple single nucleotide polymorphisms of schizophrenia-related DISC1 gene in lithium-treated patients with bipolar affective disorder. *European Neuropsychopharmacology*. 2011;21.
129. Rybakowski JK, Suwalska A, Skibinska M, Dmitrzak-Weglaz M, Leszczynska-Rodziewicz A, Hauser J. Response to lithium prophylaxis: interaction between serotonin transporter and BDNF genes. *Am J Med Genet B Neuropsychiatr Genet*. 2007;144B(6):820-823.
130. Squassina A, Manchia M, Borg J, et al. Evidence for association of an ACCN1 gene variant with response to lithium treatment in Sardinian patients with bipolar disorder. *Pharmacogenomics*. 2011;12(11):1559-1569.
131. Chen CH, Lee CS, Lee MT, et al. Variant GADL1 and response to lithium therapy in bipolar I disorder. *N Engl J Med*. 2014;370(2):119-128.
132. Hou L, Heilbronner U, Degenhardt F, et al. Genetic variants associated with response to lithium treatment in bipolar disorder: a genome-wide association study. *Lancet*. 2016;387(10023):1085-1093.
133. Ivanov M, Barragan I, Ingelman-Sundberg M. Epigenetic mechanisms of importance for drug treatment. *Trends Pharmacol Sci*. 2014;35(8):384-396.
134. Portela A, Esteller M. Epigenetic modifications and human disease. *Nat Biotechnol*. 2010;28(10):1057-1068.
135. Keverne EB. Significance of epigenetics for understanding brain development, brain evolution and behaviour. *Neuroscience*. 2014;264:207-217.

136. Seo MS, Scarr E, Lai CY, Dean B. Potential molecular and cellular mechanism of psychotropic drugs. *Clin Psychopharmacol Neurosci*. 2014;12(2):94-110.
137. Mitchell CP, Chen Y, Kundakovic M, Costa E, Grayson DR. Histone deacetylase inhibitors decrease reelin promoter methylation in vitro. *J Neurochem*. 2005;93(2):483-492.
138. Gavin DP, Kartan S, Chase K, Jayaraman S, Sharma RP. Histone deacetylase inhibitors and candidate gene expression: An in vivo and in vitro approach to studying chromatin remodeling in a clinical population. *J Psychiatr Res*. 2009;43(9):870-876.
139. Pisanu C, Katsila T, Patrinos GP, Squassina A. Recent trends on the role of epigenomics, metabolomics and noncoding RNAs in rationalizing mood stabilizing treatment. *Pharmacogenomics*. 2018;19(2):129-143.
140. Dwivedi T, Zhang H. Lithium-induced neuroprotection is associated with epigenetic modification of specific BDNF gene promoter and altered expression of apoptotic-regulatory proteins. *Front Neurosci*. 2014;8:457.
141. Moreau MP, Bruse SE, David-Rus R, Buyske S, Brzustowicz LM. Altered microRNA expression profiles in postmortem brain samples from individuals with schizophrenia and bipolar disorder. *Biol Psychiatry*. 2011;69(2):188-193.
142. Issler O, Chen A. Determining the role of microRNAs in psychiatric disorders. *Nat Rev Neurosci*. 2015;16(4):201-212.
143. Olena AF, Patton JG. Genomic organization of microRNAs. *J Cell Physiol*. 2010;222(3):540-545.
144. Lee Y, Kim M, Han J, et al. MicroRNA genes are transcribed by RNA polymerase II. *EMBO J*. 2004;23(20):4051-4060.
145. Bartel DP. MicroRNAs: genomics, biogenesis, mechanism, and function. *Cell*. 2004;116(2):281-297.
146. Esteller M. Non-coding RNAs in human disease. *Nat Rev Genet*. 2011;12(12):861-874.
147. Ko MH, Kim S, Hwang DW, Ko HY, Kim YH, Lee DS. Bioimaging of the unbalanced expression of microRNA9 and microRNA9* during the neuronal differentiation of P19 cells. *FEBS J*. 2008;275(10):2605-2616.
148. Cobb BS, Nesterova TB, Thompson E, et al. T cell lineage choice and differentiation in the absence of the RNase III enzyme Dicer. *J Exp Med*. 2005;201(9):1367-1373.
149. MANDEL P, METAIS P. [Not Available]. *C R Seances Soc Biol Fil*. 1948;142(3-4):241-243.
150. Chen X, Ba Y, Ma L, et al. Characterization of microRNAs in serum: a novel class of biomarkers for diagnosis of cancer and other diseases. *Cell Res*. 2008;18(10):997-1006.
151. Weiland M, Gao XH, Zhou L, Mi QS. Small RNAs have a large impact: circulating microRNAs as biomarkers for human diseases. *RNA Biol*. 2012;9(6):850-859.
152. Kocerha J, Dwivedi Y, Brennan KJ. Noncoding RNAs and neurobehavioral mechanisms in psychiatric disease. *Mol Psychiatry*. 2015;20(6):677-684.
153. Fries GR, Carvalho AF, Quevedo J. The miRNome of bipolar disorder. *J Affect Disord*. 2018;233:110-116.
154. Kandaswamy R, McQuillin A, Curtis D, Gurling H. Allelic association, DNA resequencing and copy number variation at the metabotropic glutamate receptor GRM7 gene locus in bipolar disorder. *Am J Med Genet B Neuropsychiatr Genet*. 2014;165B(4):365-372.
155. Forstner AJ, Hofmann A, Maaser A, et al. Genome-wide analysis implicates microRNAs and their target genes in the development of bipolar disorder. *Transl Psychiatry*. 2015;5:e678.
156. Consortium C-DGotPG. Identification of risk loci with shared effects on five major psychiatric disorders: a genome-wide analysis. *Lancet*. 2013;381(9875):1371-1379.
157. Guella I, Sequeira A, Rollins B, et al. Analysis of miR-137 expression and rs1625579 in dorsolateral prefrontal cortex. *J Psychiatr Res*. 2013;47(9):1215-1221.
158. Duan J, Shi J, Fiorentino A, et al. A rare functional noncoding variant at the GWAS-implicated MIR137/MIR2682 locus might confer risk to schizophrenia and bipolar disorder. *Am J Hum Genet*. 2014;95(6):744-753.
159. Fiorentino A, O'Brien NL, Sharp SI, Curtis D, Bass NJ, McQuillin A. Genetic variation in the miR-708 gene and its binding targets in bipolar disorder. *Bipolar Disord*. 2016;18(8):650-656.

160. Kohen R, Dobra A, Tracy JH, Haugen E. Transcriptome profiling of human hippocampus dentate gyrus granule cells in mental illness. *Transl Psychiatry*. 2014;4:e366.
161. Maffioletti E, Cattaneo A, Rosso G, et al. Peripheral whole blood microRNA alterations in major depression and bipolar disorder. *J Affect Disord*. 2016;200:250-258.
162. Kim AH, Reimers M, Maher B, et al. MicroRNA expression profiling in the prefrontal cortex of individuals affected with schizophrenia and bipolar disorders. *Schizophr Res*. 2010;124(1-3):183-191.
163. Banigan MG, Kao PF, Kozubek JA, et al. Differential expression of exosomal microRNAs in prefrontal cortices of schizophrenia and bipolar disorder patients. *PLoS One*. 2013;8(1):e48814.
164. Miller BH, Zeier Z, Xi L, et al. MicroRNA-132 dysregulation in schizophrenia has implications for both neurodevelopment and adult brain function. *Proc Natl Acad Sci U S A*. 2012;109(8):3125-3130.
165. Smalheiser NR, Lugli G, Zhang H, Rizavi H, Cook EH, Dwivedi Y. Expression of microRNAs and other small RNAs in prefrontal cortex in schizophrenia, bipolar disorder and depressed subjects. *PLoS One*. 2014;9(1):e86469.
166. Bavamian S, Mellios N, Lalonde J, et al. Dysregulation of miR-34a links neuronal development to genetic risk factors for bipolar disorder. *Mol Psychiatry*. 2015;20(5):573-584.
167. Azevedo JA, Carter BS, Meng F, et al. The microRNA network is altered in anterior cingulate cortex of patients with unipolar and bipolar depression. *J Psychiatr Res*. 2016;82:58-67.
168. Banach E, Dmitrzak-Weglarz M, Pawlak J, et al. Dysregulation of miR-499, miR-708 and miR-1908 during a depression episode in bipolar disorders. *Neurosci Lett*. 2017;654:117-119.
169. Choi JL, Kao PF, Itriago E, et al. miR-149 and miR-29c as candidates for bipolar disorder biomarkers. *Am J Med Genet B Neuropsychiatr Genet*. 2017;174(3):315-323.
170. Squassina. The Science and Practice of Lithium Therapy. In: Malhi, ed.
171. Gardiner E, Carroll A, Tooney PA, Cairns MJ. Antipsychotic drug-associated gene-miRNA interaction in T-lymphocytes. *Int J Neuropsychopharmacol*. 2014;17(6):929-943.
172. Santarelli DM, Liu B, Duncan CE, et al. Gene-microRNA interactions associated with antipsychotic mechanisms and the metabolic side effects of olanzapine. *Psychopharmacology (Berl)*. 2013;227(1):67-78.
173. Lopez JP, Lim R, Cruceanu C, et al. miR-1202 is a primate-specific and brain-enriched microRNA involved in major depression and antidepressant treatment. *Nat Med*. 2014;20(7):764-768.
174. He S, Liu X, Jiang K, et al. Alterations of microRNA-124 expression in peripheral blood mononuclear cells in pre- and post-treatment patients with major depressive disorder. *J Psychiatr Res*. 2016;78:65-71.
175. Li Y, Kowdley KV. MicroRNAs in common human diseases. *Genomics Proteomics Bioinformatics*. 2012;10(5):246-253.
176. Zhang W, Dolan ME. The emerging role of microRNAs in drug responses. *Curr Opin Mol Ther*. 2010;12(6):695-702.
177. Zhou R, Yuan P, Wang Y, et al. Evidence for selective microRNAs and their effectors as common long-term targets for the actions of mood stabilizers. *Neuropsychopharmacology*. 2009;34(6):1395-1405.
178. Rong H, Liu TB, Yang KJ, et al. MicroRNA-134 plasma levels before and after treatment for bipolar mania. *J Psychiatr Res*. 2011;45(1):92-95.
179. Chen H, Wang N, Burmeister M, McClinnis MG. MicroRNA expression changes in lymphoblastoid cell lines in response to lithium treatment. *Int J Neuropsychopharmacol*. 2009;12(7):975-981.
180. Hunsberger JG, Fessler EB, Chibane FL, et al. Mood stabilizer-regulated miRNAs in neuropsychiatric and neurodegenerative diseases: identifying associations and functions. *Am J Transl Res*. 2013;5(4):450-464.
181. Weng JC, Y. Wu, LC. Lee, C. and Cheng, AT. MicroRNA and gene expression profiling of response to lithium treatment for bipolar I disorder. 2015.
182. Kim Y, Zhang Y, Pang K, et al. Bipolar Disorder Associated microRNA, miR-1908-5p, Regulates the Expression of Genes Functioning in Neuronal Glutamatergic Synapses. *Exp Neurobiol*. 2016;25(6):296-306.

183. Reinbold CS, Forstner AJ, Hecker J, et al. Analysis of the Influence of microRNAs in Lithium Response in Bipolar Disorder. *Front Psychiatry*. 2018;9:207.
184. Ehret MJ, Baker W, O'Neill H. BDNF Val66Met polymorphism and lithium response: a meta-analysis. *Per Med*. 2013;10(8):777-784.
185. Spitzer RL, Endicott J, Robins E. Research diagnostic criteria: rationale and reliability. *Arch Gen Psychiatry*. 1978;35(6):773-782.
186. Endicott J, Spitzer RL. A diagnostic interview: the schedule for affective disorders and schizophrenia. *Arch Gen Psychiatry*. 1978;35(7):837-844.
187. Manchia M, Adli M, Akula N, et al. Assessment of Response to Lithium Maintenance Treatment in Bipolar Disorder: A Consortium on Lithium Genetics (ConLiGen) Report. *PLoS One*. 2013;8(6):e65636.
188. Neitzel H. A routine method for the establishment of permanent growing lymphoblastoid cell lines. *Hum Genet*. 1986;73(4):320-326.
189. Martin M. Cutadapt removes adapter sequences from high-throughput sequencing reads. In. Vol 17: EMBnet.journal; 2011:10-12.
190. Langmead B, Trapnell C, Pop M, Salzberg SL. Ultrafast and memory-efficient alignment of short DNA sequences to the human genome. *Genome Biol*. 2009;10(3):R25.
191. Robinson MD, McCarthy DJ, Smyth GK. edgeR: a Bioconductor package for differential expression analysis of digital gene expression data. *Bioinformatics*. 2010;26(1):139-140.
192. Core-Team R. R: a language and environment for statistical computing. 2000; <http://www.R-project.org/>.
193. Gentleman RC, Carey VJ, Bates DM, et al. Bioconductor: open software development for computational biology and bioinformatics. *Genome Biol*. 2004;5(10):R80.
194. Irizarry RA, Hobbs B, Collin F, et al. Exploration, normalization, and summaries of high density oligonucleotide array probe level data. *Biostatistics*. 2003;4(2):249-264.
195. JD S. A direct approach to false discovery rates. In. Vol Series B (Statistical Methodology) Journal of the Royal Statistical Society; 2002:479-498.
196. Smyth GK. Linear models and empirical bayes methods for assessing differential expression in microarray experiments. *Stat Appl Genet Mol Biol*. 2004;3:Article3.
197. Vila-Casadesús M, Gironella M, Lozano JJ. MiRComb: An R Package to Analyse miRNA-mRNA Interactions. Examples across Five Digestive Cancers. *PLoS One*. 2016;11(3):e0151127.
198. Dweep H, Sticht C, Pandey P, Gretz N. miRWalk--database: prediction of possible miRNA binding sites by "walking" the genes of three genomes. *J Biomed Inform*. 2011;44(5):839-847.
199. Heid CA, Stevens J, Livak KJ, Williams PM. Real time quantitative PCR. *Genome Res*. 1996;6(10):986-994.
200. Kramer MF. Stem-loop RT-qPCR for miRNAs. *Curr Protoc Mol Biol*. 2011;Chapter 15:Unit 15.10.
201. Mundalil Vasu M, Anitha A, Takahashi T, et al. Fluoxetine Increases the Expression of miR-572 and miR-663a in Human Neuroblastoma Cell Lines. *PLoS One*. 2016;11(10):e0164425.
202. Mundalil Vasu M, Anitha A, Thanseem I, et al. Serum microRNA profiles in children with autism. *Mol Autism*. 2014;5:40.
203. Camkurt MA, Acar Ş, Coşkun S, et al. Comparison of plasma MicroRNA levels in drug naive, first episode depressed patients and healthy controls. *J Psychiatr Res*. 2015;69:67-71.
204. Ghanbari M, Ikram MA, de Looper HW, et al. Genome-wide identification of microRNA-related variants associated with risk of Alzheimer's disease. *Sci Rep*. 2016;6:28387.
205. Kripke DF, Klimecki WT, Nievergelt CM, et al. Circadian polymorphisms in night owls, in bipolars, and in non-24-hour sleep cycles. *Psychiatry Investig*. 2014;11(4):345-362.
206. Pisanu C. Integrated analysis of converging genome-wide genotyping and transcriptomic data to identify genes associated with lithium response in bipolar disorder. CNR annual retreat; 2017; S. Margherita di Pula (CA), Italy.
207. Stankiewicz TR, Linseman DA. Rho family GTPases: key players in neuronal development, neuronal survival, and neurodegeneration. *Front Cell Neurosci*. 2014;8:314.

208. Lin GN, Corominas R, Lemmens I, et al. Spatiotemporal 16p11.2 protein network implicates cortical late mid-fetal brain development and KCTD13-Cul3-RhoA pathway in psychiatric diseases. *Neuron*. 2015;85(4):742-754.
209. Croall DE, Ersfeld K. The calpains: modular designs and functional diversity. *Genome Biol*. 2007;8(6):218.
210. Amini M, Ma CL, Farazifard R, et al. Conditional disruption of calpain in the CNS alters dendrite morphology, impairs LTP, and promotes neuronal survival following injury. *J Neurosci*. 2013;33(13):5773-5784.
211. Lee SA, Huang KC. Epigenetic profiling of human brain differential DNA methylation networks in schizophrenia. *BMC Med Genomics*. 2016;9(Suppl 3):68.
212. Doi M, Ishida A, Miyake A, et al. Circadian regulation of intracellular G-protein signalling mediates intercellular synchrony and rhythmicity in the suprachiasmatic nucleus. *Nat Commun*. 2011;2:327.
213. Kollarova J, Cenk E, Schmutz C, Marko D. The mycotoxin alternariol suppresses lipopolysaccharide-induced inflammation in THP-1 derived macrophages targeting the NF- κ B signalling pathway. *Arch Toxicol*. 2018.
214. Pinacho R, Villalmanzo N, Lalonde J, et al. The transcription factor SP4 is reduced in postmortem cerebellum of bipolar disorder subjects: control by depolarization and lithium. *Bipolar Disord*. 2011;13(5-6):474-485.
215. Zhou X, Qyang Y, Kelsoe JR, Masliah E, Geyer MA. Impaired postnatal development of hippocampal dentate gyrus in Sp4 null mutant mice. *Genes Brain Behav*. 2007;6(3):269-276.
216. Vila È, Huerta-Ramos E, Núñez C, Usall J, Ramos B. Specificity proteins 1 and 4 in peripheral blood mononuclear cells in postmenopausal women with schizophrenia: a 24-week double-blind, randomized, parallel, placebo-controlled trial. *Eur Arch Psychiatry Clin Neurosci*. 2018.
217. Chen J, He K, Wang Q, et al. Role played by the SP4 gene in schizophrenia and major depressive disorder in the Han Chinese population. *Br J Psychiatry*. 2016;208(5):441-445.
218. Gao Z, Lee P, Stafford JM, von Schimmelmann M, Schaefer A, Reinberg D. An AUTS2-Polycomb complex activates gene expression in the CNS. *Nature*. 2014;516(7531):349-354.
219. Oksenberg N, Ahituv N. The role of AUTS2 in neurodevelopment and human evolution. *Trends Genet*. 2013;29(10):600-608.
220. Jayawickrama GS, Sadig RR, Sun G, et al. Kynurenine Aminotransferases and the Prospects of Inhibitors for the Treatment of Schizophrenia. *Curr Med Chem*. 2015;22(24):2902-2918.
221. Schröder J, Ansaloni S, Schilling M, et al. MicroRNA-138 is a potential regulator of memory performance in humans. *Front Hum Neurosci*. 2014;8:501.
222. Castañeda P, Muñoz M, García-Rojo G, et al. Association of N-cadherin levels and downstream effectors of Rho GTPases with dendritic spine loss induced by chronic stress in rat hippocampal neurons. *J Neurosci Res*. 2015;93(10):1476-1491.
223. Chen RJ, Kelly G, Sengupta A, et al. MicroRNAs as biomarkers of resilience or vulnerability to stress. *Neuroscience*. 2015;305:36-48.
224. Lv X, Yan J, Jiang J, Zhou X, Lu Y, Jiang H. MicroRNA-27a-3p suppression of peroxisome proliferator-activated receptor- γ contributes to cognitive impairments resulting from sevoflurane treatment. *J Neurochem*. 2017;143(3):306-319.
225. Kim KH, Liu J, Sells Galvin RJ, et al. Transcriptomic Analysis of Induced Pluripotent Stem Cells Derived from Patients with Bipolar Disorder from an Old Order Amish Pedigree. *PLoS One*. 2015;10(11):e0142693.
226. Pisanu C. Convergent analysis of genome-wide genotyping and transcriptomic data suggests association of zinc finger genes with lithium response in bipolar disorder. CNR annual retreat; 2017; S. Margherita di Pula (CA), Italy.
227. Fabian MR, Sonenberg N. The mechanics of miRNA-mediated gene silencing: a look under the hood of miRISC. *Nat Struct Mol Biol*. 2012;19(6):586-593.
228. Elton TS, Sansom SE, Martin MM. Trisomy-21 gene dosage over-expression of miRNAs results in the haploinsufficiency of specific target proteins. *RNA Biol*. 2010;7(5):540-547.

229. Landgraf P, Rusu M, Sheridan R, et al. A mammalian microRNA expression atlas based on small RNA library sequencing. *Cell*. 2007;129(7):1401-1414.
230. Griffiths-Jones S, Grocock RJ, van Dongen S, Bateman A, Enright AJ. miRBase: microRNA sequences, targets and gene nomenclature. *Nucleic Acids Res*. 2006;34(Database issue):D140-144.
231. Faraoni I, Antonetti FR, Cardone J, Bonmassar E. miR-155 gene: a typical multifunctional microRNA. *Biochim Biophys Acta*. 2009;1792(6):497-505.
232. O'Connell RM, Kahn D, Gibson WS, et al. MicroRNA-155 promotes autoimmune inflammation by enhancing inflammatory T cell development. *Immunity*. 2010;33(4):607-619.
233. Kurowska-Stolarska M, Alivernini S, Ballantine LE, et al. MicroRNA-155 as a proinflammatory regulator in clinical and experimental arthritis. *Proc Natl Acad Sci U S A*. 2011;108(27):11193-11198.
234. Murugaiyan G, Beynon V, Mittal A, Joller N, Weiner HL. Silencing microRNA-155 ameliorates experimental autoimmune encephalomyelitis. *J Immunol*. 2011;187(5):2213-2221.
235. Ahmadvand M, Eskandari M, Pashaiefar H, et al. Over expression of circulating miR-155 predicts prognosis in diffuse large B-cell lymphoma. *Leuk Res*. 2018;70:45-48.
236. Thounaojam MC, Kundu K, Kaushik DK, et al. MicroRNA 155 regulates Japanese encephalitis virus-induced inflammatory response by targeting Src homology 2-containing inositol phosphatase 1. *J Virol*. 2014;88(9):4798-4810.
237. Pareek S, Roy S, Kumari B, Jain P, Banerjee A, Vrati S. MiR-155 induction in microglial cells suppresses Japanese encephalitis virus replication and negatively modulates innate immune responses. *J Neuroinflammation*. 2014;11:97.
238. Wood CD, Carvell T, Gunnell A, Ojeniyi OO, Osborne C, West MJ. Enhancer control of miR-155 expression in Epstein-Barr virus infected B cells. *J Virol*. 2018.
239. Kim J, Inoue K, Ishii J, et al. A MicroRNA feedback circuit in midbrain dopamine neurons. *Science*. 2007;317(5842):1220-1224.
240. Gaudet AD, Mandrekar-Colucci S, Hall JC, et al. miR-155 Deletion in Mice Overcomes Neuron-Intrinsic and Neuron-Extrinsic Barriers to Spinal Cord Repair. *J Neurosci*. 2016;36(32):8516-8532.
241. Tili E, Michaille JJ, Cimino A, et al. Modulation of miR-155 and miR-125b levels following lipopolysaccharide/TNF-alpha stimulation and their possible roles in regulating the response to endotoxin shock. *J Immunol*. 2007;179(8):5082-5089.
242. Freilich RW, Woodbury ME, Ikezu T. Integrated expression profiles of mRNA and miRNA in polarized primary murine microglia. *PLoS One*. 2013;8(11):e79416.
243. Prajapati P, Sripada L, Singh K, Bhatelia K, Singh R. TNF- α regulates miRNA targeting mitochondrial complex-I and induces cell death in dopaminergic cells. *Biochim Biophys Acta*. 2015;1852(3):451-461.
244. Peshdary V, Atlas E. Dexamethasone induced miR-155 up-regulation in differentiating 3T3-L1 preadipocytes does not affect adipogenesis. *Sci Rep*. 2018;8(1):1264.
245. Liao TL, Hsieh SL, Chen YM, et al. Rituximab May Cause Increased Hepatitis C Virus Viremia in Rheumatoid Arthritis Patients Through Declining Exosomal MicroRNA-155. *Arthritis Rheumatol*. 2018;70(8):1209-1219.
246. Cardoso AL, Guedes JR, Pereira de Almeida L, Pedroso de Lima MC. miR-155 modulates microglia-mediated immune response by down-regulating SOCS-1 and promoting cytokine and nitric oxide production. *Immunology*. 2012;135(1):73-88.
247. Pena-Philippides JC, Caballero-Garrido E, Lordkipanidze T, Roitbak T. In vivo inhibition of miR-155 significantly alters post-stroke inflammatory response. *J Neuroinflammation*. 2016;13(1):287.
248. Ksiazek-Winiarek D, Szpakowski P, Turniak M, Szemraj J, Glabinski A. IL-17 Exerts Anti-Apoptotic Effect via miR-155-5p Downregulation in Experimental Autoimmune Encephalomyelitis. *J Mol Neurosci*. 2017;63(3-4):320-332.
249. Harrison EB, Emanuel K, Lamberty BG, et al. Induction of miR-155 after Brain Injury Promotes Type 1 Interferon and has a Neuroprotective Effect. *Front Mol Neurosci*. 2017;10:228.
250. Liu S, Zhu B, Sun Y, Xie X. MiR-155 modulates the progression of neuropathic pain through targeting SGK3. *Int J Clin Exp Pathol*. 2015;8(11):14374-14382.

251. Guedes JR, Custódia CM, Silva RJ, de Almeida LP, Pedroso de Lima MC, Cardoso AL. Early miR-155 upregulation contributes to neuroinflammation in Alzheimer's disease triple transgenic mouse model. *Hum Mol Genet.* 2014;23(23):6286-6301.
252. Butovsky O, Jedrychowski MP, Cialic R, et al. Targeting miR-155 restores abnormal microglia and attenuates disease in SOD1 mice. *Ann Neurol.* 2015;77(1):75-99.
253. Song J, Lee JE. miR-155 is involved in Alzheimer's disease by regulating T lymphocyte function. *Front Aging Neurosci.* 2015;7:61.
254. Varendi K, Kumar A, Härma MA, Andressoo JO. miR-1, miR-10b, miR-155, and miR-191 are novel regulators of BDNF. *Cell Mol Life Sci.* 2014;71(22):4443-4456.
255. Cai Z, Li S, Song F, et al. Antagonist Targeting microRNA-155 Protects against Lithium-Pilocarpine-Induced Status Epilepticus in C57BL/6 Mice by Activating Brain-Derived Neurotrophic Factor. *Front Pharmacol.* 2016;7:129.
256. Panwar B, Omenn GS, Guan Y. miRmine: a database of human miRNA expression profiles. *Bioinformatics.* 2017;33(10):1554-1560.
257. Tarassishin L, Loudig O, Bauman A, Shafit-Zagardo B, Suh HS, Lee SC. Interferon regulatory factor 3 inhibits astrocyte inflammatory gene expression through suppression of the proinflammatory miR-155 and miR-155*. *Glia.* 2011;59(12):1911-1922.
258. Zhou H, Huang X, Cui H, et al. miR-155 and its star-form partner miR-155* cooperatively regulate type I interferon production by human plasmacytoid dendritic cells. *Blood.* 2010;116(26):5885-5894.
259. Tang B, Lei B, Qi G, et al. MicroRNA-155-3p promotes hepatocellular carcinoma formation by suppressing FBXW7 expression. *J Exp Clin Cancer Res.* 2016;35(1):93.
260. Mycko MP, Cichalewska M, Cwiklinska H, Selmaj KW. miR-155-3p Drives the Development of Autoimmune Demyelination by Regulation of Heat Shock Protein 40. *J Neurosci.* 2015;35(50):16504-16515.
261. Xie M, Li M, Vilborg A, et al. Mammalian 5'-capped microRNA precursors that generate a single microRNA. *Cell.* 2013;155(7):1568-1580.
262. Sepramaniam S, Armugam A, Lim KY, et al. MicroRNA 320a functions as a novel endogenous modulator of aquaporins 1 and 4 as well as a potential therapeutic target in cerebral ischemia. *J Biol Chem.* 2010;285(38):29223-29230.
263. Li WA, Efendizade A, Ding Y. The role of microRNA in neuronal inflammation and survival in the post ischemic brain: a review. *Neurol Res.* 2017:1-9.
264. White RE, Giffard RG. MicroRNA-320 induces neurite outgrowth by targeting ARPP-19. *Neuroreport.* 2012;23(10):590-595.
265. Li H, Yu L, Liu J, et al. miR-320a functions as a suppressor for gliomas by targeting SND1 and β -catenin, and predicts the prognosis of patients. *Oncotarget.* 2017;8(12):19723-19737.
266. Lu C, Liao Z, Cai M, Zhang G. MicroRNA-320a downregulation mediates human liver cancer cell proliferation through the Wnt/ β -catenin signaling pathway. *Oncol Lett.* 2017;13(2):573-578.
267. Sommariva E, D'Alessandra Y, Farina FM, et al. MiR-320a as a Potential Novel Circulating Biomarker of Arrhythmogenic CardioMyopathy. *Sci Rep.* 2017;7(1):4802.
268. Regev K, Healy BC, Paul A, et al. Identification of MS-specific serum miRNAs in an international multicenter study. *Neurol Neuroimmunol Neuroinflamm.* 2018;5(5):e491.
269. Aung LL, Mouradian MM, Dhib-Jalbut S, Balashov KE. MMP-9 expression is increased in B lymphocytes during multiple sclerosis exacerbation and is regulated by microRNA-320a. *J Neuroimmunol.* 2015;278:185-189.
270. Talebizadeh Z, Butler MG, Theodoro MF. Feasibility and relevance of examining lymphoblastoid cell lines to study role of microRNAs in autism. *Autism Res.* 2008;1(4):240-250.
271. Liu X, Zhang L, Cheng K, Wang X, Ren G, Xie P. Identification of suitable plasma-based reference genes for miRNAome analysis of major depressive disorder. *J Affect Disord.* 2014;163:133-139.
272. Vachev T. Alterations of miR-320 Family Members as a Novel Diagnostic Biomarkers in Peripheral Blood of Schizophrenia Patients. 2016;5:865-875.

273. Rybakowski JK, Skibinska M, Leszczynska-Rodziewicz A, Kaczmarek L, Hauser J. Matrix metalloproteinase-9 gene and bipolar mood disorder. *Neuromolecular Med.* 2009;11(2):128-132.
274. Rybakowski JK, Skibinska M, Suwalska A, Leszczynska-Rodziewicz A, Kaczmarek L, Hauser J. Functional polymorphism of matrix metalloproteinase-9 (MMP-9) gene and response to lithium prophylaxis in bipolar patients. *Hum Psychopharmacol.* 2011;26(2):168-171.
275. Hervouet E, Vallette FM, Cartron PF. Dnmt3/transcription factor interactions as crucial players in targeted DNA methylation. *Epigenetics.* 2009;4(7):487-499.
276. Le François B, Soo J, Millar AM, et al. Chronic mild stress and antidepressant treatment alter 5-HT1A receptor expression by modifying DNA methylation of a conserved Sp4 site. *Neurobiol Dis.* 2015;82:332-341.
277. Pinacho R, Valdizán EM, Pilar-Cuellar F, et al. Increased SP4 and SP1 transcription factor expression in the postmortem hippocampus of chronic schizophrenia. *J Psychiatr Res.* 2014;58:189-196.
278. Ramos B, Gaudillière B, Bonni A, Gill G. Transcription factor Sp4 regulates dendritic patterning during cerebellar maturation. *Proc Natl Acad Sci U S A.* 2007;104(23):9882-9887.
279. Uhlén M, Fagerberg L, Hallström BM, et al. Proteomics. Tissue-based map of the human proteome. *Science.* 2015;347(6220):1260419.
280. Ramos B, Valín A, Sun X, Gill G. Sp4-dependent repression of neurotrophin-3 limits dendritic branching. *Mol Cell Neurosci.* 2009;42(2):152-159.
281. Fountoulakis KN. The possible involvement of NMDA glutamate receptor in the etiopathogenesis of bipolar disorder. *Curr Pharm Des.* 2012;18(12):1605-1608.
282. Lakhan SE, Caro M, Hadzimichalis N. NMDA Receptor Activity in Neuropsychiatric Disorders. *Front Psychiatry.* 2013;4:52.
283. Priya A, Johar K, Wong-Riley MTT. Specificity protein 4 functionally regulates the transcription of NMDA receptor subunits GluN1, GluN2A, and GluN2B. *Biochim Biophys Acta.* 2013;1833(12):2745-2756.
284. Basselin M, Chang L, Bell JM, Rapoport SI. Chronic lithium chloride administration attenuates brain NMDA receptor-initiated signaling via arachidonic acid in unanesthetized rats. *Neuropsychopharmacology.* 2006;31(8):1659-1674.
285. Shyn SI, Shi J, Kraft JB, et al. Novel loci for major depression identified by genome-wide association study of Sequenced Treatment Alternatives to Relieve Depression and meta-analysis of three studies. *Mol Psychiatry.* 2011;16(2):202-215.
286. Shi J, Potash JB, Knowles JA, et al. Genome-wide association study of recurrent early-onset major depressive disorder. *Mol Psychiatry.* 2011;16(2):193-201.
287. Tam GW, van de Lagemaat LN, Redon R, et al. Confirmed rare copy number variants implicate novel genes in schizophrenia. *Biochem Soc Trans.* 2010;38(2):445-451.
288. Zhou X, Tang W, Greenwood TA, et al. Transcription factor SP4 is a susceptibility gene for bipolar disorder. *PLoS One.* 2009;4(4):e5196.
289. Pinacho R, Saia G, Fusté M, et al. Phosphorylation of transcription factor specificity protein 4 is increased in peripheral blood mononuclear cells of first-episode psychosis. *PLoS One.* 2015;10(4):e0125115.
290. Fusté M, Pinacho R, Meléndez-Pérez I, et al. Reduced expression of SP1 and SP4 transcription factors in peripheral blood mononuclear cells in first-episode psychosis. *J Psychiatr Res.* 2013;47(11):1608-1614.
291. Young LT, Li PP, Kish SJ, et al. Cerebral cortex Gs alpha protein levels and forskolin-stimulated cyclic AMP formation are increased in bipolar affective disorder. *J Neurochem.* 1993;61(3):890-898.
292. Friedman E, Wang HY. Receptor-mediated activation of G proteins is increased in postmortem brains of bipolar affective disorder subjects. *J Neurochem.* 1996;67(3):1145-1152.
293. Dowlatshahi D, MacQueen GM, Wang JF, Reisch JS, Young LT. G Protein-coupled cyclic AMP signaling in postmortem brain of subjects with mood disorders: effects of diagnosis, suicide, and treatment at the time of death. *J Neurochem.* 1999;73(3):1121-1126.
294. Vivot K, Moullé VS, Zarrouki B, et al. The regulator of G-protein signaling RGS16 promotes insulin secretion and β -cell proliferation in rodent and human islets. *Mol Metab.* 2016;5(10):988-996.

295. Carper MB, Denvir J, Boskovic G, Primerano DA, Claudio PP. RGS16, a novel p53 and pRb cross-talk candidate inhibits migration and invasion of pancreatic cancer cells. *Genes Cancer*. 2014;5(11-12):420-435.
296. Gerstner JR, Vander Heyden WM, Lavaute TM, Landry CF. Profiles of novel diurnally regulated genes in mouse hypothalamus: expression analysis of the cysteine and histidine-rich domain-containing, zinc-binding protein 1, the fatty acid-binding protein 7 and the GTPase, ras-like family member 11b. *Neuroscience*. 2006;139(4):1435-1448.
297. Mansour HA, Monk TH, Nimgaonkar VL. Circadian genes and bipolar disorder. *Ann Med*. 2005;37(3):196-205.
298. Budde M, Degner D, Brockmöller J, Schulze TG. Pharmacogenomic aspects of bipolar disorder: An update. *Eur Neuropsychopharmacol*. 2017;27(6):599-609.
299. Lee JK, Bou Dagher J. Regulator of G-protein Signaling (RGS)1 and RGS10 Proteins as Potential Drug Targets for Neuroinflammatory and Neurodegenerative Diseases. *AAPS J*. 2016;18(3):545-549.
300. Grafstein-Dunn E, Young KH, Cockett MI, Khawaja XZ. Regional distribution of regulators of G-protein signaling (RGS) 1, 2, 13, 14, 16, and GAIIP messenger ribonucleic acids by in situ hybridization in rat brain. *Brain Res Mol Brain Res*. 2001;88(1-2):113-123.
301. Moserova I, Kralova J. Role of ER stress response in photodynamic therapy: ROS generated in different subcellular compartments trigger diverse cell death pathways. *PLoS One*. 2012;7(3):e32972.
302. Gross J, Olze H, Mazurek B. Differential expression of transcription factors and inflammation-, ROS-, and cell death-related genes in organotypic cultures in the modiolus, the organ of Corti and the stria vascularis of newborn rats. *Cell Mol Neurobiol*. 2014;34(4):523-538.
303. Lu S, Kanekura K, Hara T, et al. A calcium-dependent protease as a potential therapeutic target for Wolfram syndrome. *Proc Natl Acad Sci U S A*. 2014;111(49):E5292-5301.
304. Li S, Zhang L, Ni R, et al. Disruption of calpain reduces lipotoxicity-induced cardiac injury by preventing endoplasmic reticulum stress. *Biochim Biophys Acta*. 2016;1862(11):2023-2033.
305. Demarchi F, Schneider C. The calpain system as a modulator of stress/damage response. *Cell Cycle*. 2007;6(2):136-138.
306. Marcassa E, Raimondi M, Anwar T, et al. Calpain mobilizes Atg9/Bif-1 vesicles from Golgi stacks upon autophagy induction by thapsigargin. *Biol Open*. 2017;6(5):551-562.
307. Wasserman MJ, Corson TW, Sibony D, et al. Chronic lithium treatment attenuates intracellular calcium mobilization. *Neuropsychopharmacology*. 2004;29(4):759-769.
308. Fairfax BP, Vannberg FO, Radhakrishnan J, et al. An integrated expression phenotype mapping approach defines common variants in LEP, ALOX15 and CAPNS1 associated with induction of IL-6. *Hum Mol Genet*. 2010;19(4):720-730.
309. Brietzke E, Scheinberg M, Lafer B. Therapeutic potential of interleukin-6 antagonism in bipolar disorder. *Med Hypotheses*. 2011;76(1):21-23.
310. Wang E, Wang D, Li B, et al. Capn4 promotes epithelial-mesenchymal transition in human melanoma cells through activation of the Wnt/ β -catenin pathway. *Oncol Rep*. 2017;37(1):379-387.
311. Zhang Y, Xu W, Ni P, Li A, Zhou J, Xu S. MiR-99a and MiR-491 Regulate Cisplatin Resistance in Human Gastric Cancer Cells by Targeting CAPNS1. *Int J Biol Sci*. 2016;12(12):1437-1447.
312. Zheng XB, Chen XB, Xu LL, et al. miR-203 inhibits augmented proliferation and metastasis of hepatocellular carcinoma residual in the promoted regenerating liver. *Cancer Sci*. 2017;108(3):338-346.
313. Cai JJ, Qi ZX, Chen LC, Yao Y, Gong Y, Mao Y. miR-124 suppresses the migration and invasion of glioma cells in vitro via Capn4. *Oncol Rep*. 2016;35(1):284-290.
314. Godshalk SE, Bhaduri-McIntosh S, Slack FJ. Epstein-Barr virus-mediated dysregulation of human microRNA expression. *Cell Cycle*. 2008;7(22):3595-3600.
315. Rollins B, Martin MV, Morgan L, Vawter MP. Analysis of whole genome biomarker expression in blood and brain. *Am J Med Genet B Neuropsychiatr Genet*. 2010;153B(4):919-936.
316. Viswanath B, Jose SP, Squassina A, et al. Cellular models to study bipolar disorder: A systematic review. *J Affect Disord*. 2015;184:36-50.

317. Gurwitz D. Human iPSC-derived neurons and lymphoblastoid cells for personalized medicine research in neuropsychiatric disorders. *Dialogues Clin Neurosci*. 2016;18(3):267-276.
318. Thomas SM, Kagan C, Pavlovic BJ, et al. Reprogramming LCLs to iPSCs Results in Recovery of Donor-Specific Gene Expression Signature. *PLoS Genet*. 2015;11(5):e1005216.
319. Takahashi K, Yamanaka S. Induction of pluripotent stem cells from mouse embryonic and adult fibroblast cultures by defined factors. *Cell*. 2006;126(4):663-676.
320. Brennand KJ, Simone A, Tran N, Gage FH. Modeling psychiatric disorders at the cellular and network levels. *Mol Psychiatry*. 2012;17(12):1239-1253.
321. Tafreshi AP, Sylvain A, Sun G, Herszfeld D, Schulze K, Bernard CC. Lithium chloride improves the efficiency of induced pluripotent stem cell-derived neurospheres. *Biol Chem*. 2015;396(8):923-928.
322. Mertens J, Wang QW, Kim Y, et al. Differential responses to lithium in hyperexcitable neurons from patients with bipolar disorder. *Nature*. 2015;527(7576):95-99.
323. Tobe BTD, Crain AM, Winkquist AM, et al. Probing the lithium-response pathway in hiPSCs implicates the phosphoregulatory set-point for a cytoskeletal modulator in bipolar pathogenesis. *Proc Natl Acad Sci U S A*. 2017;114(22):E4462-E4471.
324. Vierbuchen T, Ostermeier A, Pang ZP, Kokubu Y, Südhof TC, Wernig M. Direct conversion of fibroblasts to functional neurons by defined factors. *Nature*. 2010;463(7284):1035-1041.
325. Pang ZP, Yang N, Vierbuchen T, et al. Induction of human neuronal cells by defined transcription factors. *Nature*. 2011;476(7359):220-223.
326. Krützfeldt J, Poy MN, Stoffel M. Strategies to determine the biological function of microRNAs. *Nat Genet*. 2006;38 Suppl:S14-19.
327. Jin Y, Chen Z, Liu X, Zhou X. Evaluating the microRNA targeting sites by luciferase reporter gene assay. *Methods Mol Biol*. 2013;936:117-127.
328. Afonina I, Zivarts M, Kutyavin I, Lukhtanov E, Gamper H, Meyer RB. Efficient priming of PCR with short oligonucleotides conjugated to a minor groove binder. *Nucleic Acids Res*. 1997;25(13):2657-2660.
329. Kutyavin IV, Lukhtanov EA, Gamper HB, Meyer RB. Oligonucleotides with conjugated dihydropyrroloindole tripeptides: base composition and backbone effects on hybridization. *Nucleic Acids Res*. 1997;25(18):3718-3723.
330. Livak KJ, Schmittgen TD. Analysis of relative gene expression data using real-time quantitative PCR and the 2(-Delta Delta C(T)) Method. *Methods*. 2001;25(4):402-408.
331. Chen C, Ridzon DA, Broomer AJ, et al. Real-time quantification of microRNAs by stem-loop RT-PCR. *Nucleic Acids Res*. 2005;33(20):e179.

Appendices

Appendix A: Sequencing of total miRNome using sequencing by synthesis (MiSeq®, Illumina, CA, US)

Basic Principle

The MiSeq® sequencing is based in Illumina Sequencing by Synthesis, this means that microRNA libraries with their adaptors and indexes are amplified clonally with bridge amplification, bound to the oligos of the flow cell. Each base is carrying a different fluorophore and is added and called by the instrument in a different cycle. The samples are multiplexed and separated based on their indexes.

The workflow of Sequencing by Synthesis includes three basic stages:

1. Library preparation
2. Loading and starting the instrument
3. Cluster Generation and Sequencing
4. Data analysis

Library preparation

The TruSeq® Small RNA Library Prep protocol is used to prepare libraries for sequencing of various RNA species, including microRNAs. Most mature miRNAs have a 5'-phosphate and a 3'-hydroxyl group as a result of their biosynthesis. The adapters contained in the kit ligate to the naturally created 5'-phosphate and 3'-hydroxyl ends of the microRNAs. There is possibility to produce libraries from total RNA as well as purified small RNAs. We used 1µg of total RNA as starting material.

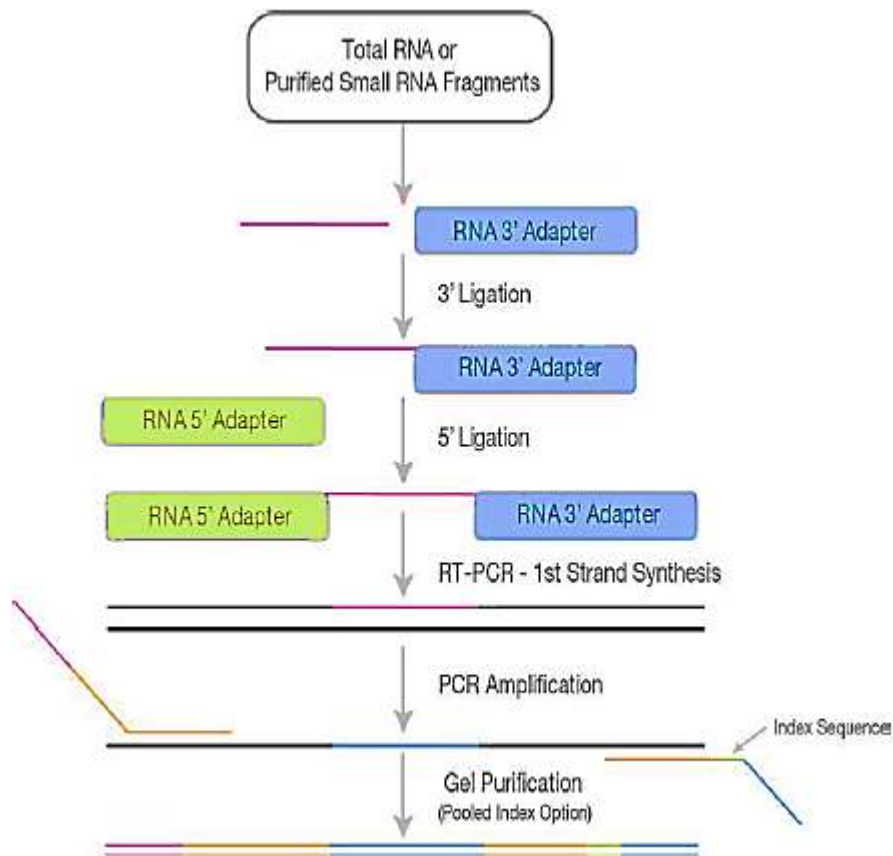


Figure 1: Library Preparation Workflow

The library preparation protocol is summarized in 4 basic steps (Figure 1):

7. Adapter ligation
8. Reverse Transcription (RT)
9. PCR amplification
10. Pooling and Gel purification
11. Library Validation

1. Adapter Ligation

The RNA 3' adapter is modified to target microRNAs and other small RNAs that have a 3' hydroxyl group resulting from enzymatic cleavage by Dicer or other RNA processing enzymes. The adapters are ligated to each end of the RNA molecule, first to the 3'-hydroxyl end and subsequently to the 5'-phosphate group.

2. Retro transcription reaction

Primers complementary to the adapters added at the 1st step are used for the synthesis of the 1st complementary DNA strand by the Reverse Transcriptase.

3. PCR amplification and indexing

The initial strand then functions as template for the creation of cDNA. The cDNA is then amplified. At this step there is the possibility of single or double indexing. The cDNA is amplified using a common primer and a primer containing 1 of 48 index sequences. The separation of index introduction from the ligation step allows the indexes to be read using a second read and significantly reduces bias compared to designs that include the index within the first read. The kits are configured for 24 reactions with 12 different indexes per kit. The total 48 indexes are found in 4 different kits.

4. Pooling and Gel purification

Before pooling, the samples should be indexed, as mentioned during the PCR amplification step. Each index sequence is composed from 6 bases and aims to distinguish different samples that run in a single lane of a flow cell. Indexing is necessary to perform pooled sequencing when using TruSeq Small RNA Library Prep Kit. In this kit the indexes are referred to as RNA PCR Primer Index tubes. Each tube contains a unique single 6 base index adapter. Libraries prepared with these adapters can be sequenced on the MiSeq® (Illumina, San Diego, CA, US) using a 6 cycle Single Index Read Adapter. Pooling can be performed based on equimolar amounts or equal volumes, and can be performed before or after cDNA construct gel purification and library validation. The index read will make sure that the pooled samples will be separated during bioinformatics analysis of raw reads.

5. Library Validation

The Library is further purified or concentrated with ethanol precipitation if needed before loaded on the MiSeq® System, Next Generation Sequencer (Illumina, San Diego, CA, US).

Loading and starting the instrument

The produced libraries were denatured and diluted and finally loaded onto the cartridge (Figure 2). The sample sheet and all the information about the run were prepared at excel and or Illumina Experiment Manager Software and loaded as a .csv file (comma delimited file) during run set up. This file contains also all the user options for the run such as name of the experiment, date, workflow, type of output generated, numbers of reads, type of libraries, chemistry, the adapter sequences and a

list of all samples and their corresponding indexes. The full MiSeq[®] sequencer workflow is demonstrated in Figure 3.



Figure 2: MiSeq Instrument. The figure shows the different compartments of the instrument

MiSeq Workflow

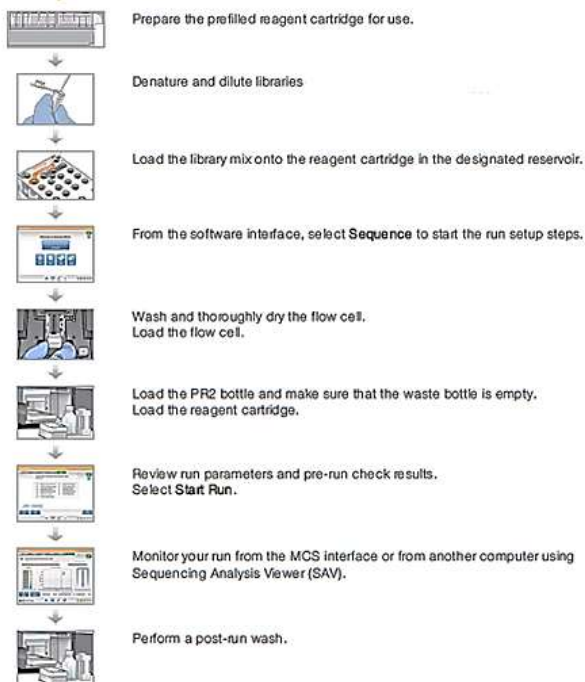


Figure 3: MiSeq[®] Workflow

Cluster Generation

When the library preparation is complete small RNA strands having Dicer-cleaved ends acquired one index (or two) and an adapter. Through reduced cycle amplification the adapter helps integrate other

useful oligonucleotide sequences, such as the sequencing-primer binding site, the index, the index sequencing primer and a region complementary to the flow cell oligos (Figure 4).

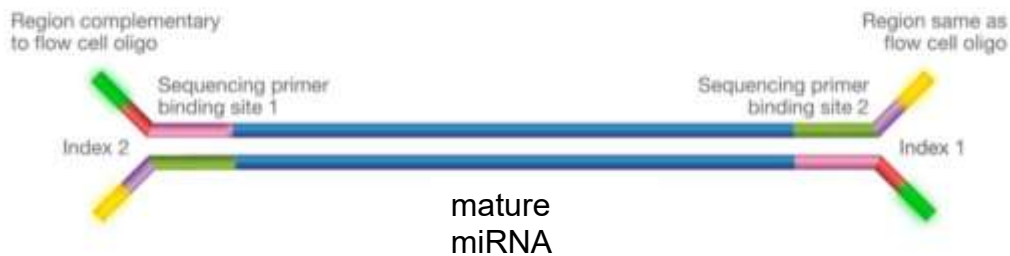


Figure 4: mature miRNAs ready for sequencing after undergoing the library preparation procedure

Clustering is the process during which, generated during library preparation is amplified. This procedure takes place on (Figure 5). The flow cell is a glass slide coated with two types of oligonucleotide



Figure 5: Flow cell

every template isothermally the flow cell with lanes sequences,

each one being complementary to one end of the generated templates. Initially, the template is hybridized on one of the oligos of the flow cell and a polymerase creates a complement of the template. The original template is then denatured and washed off. The newly produced fragment bends and binds to the other kind of flow cell oligo (Figure 6a) and bridge amplification with the help of a polymerase initiates (Figure 6b). The two strands denature (Figure 6c and 6d) and bridge amplification (Figure 6) is repeated many times resulting in clonal amplification of the original template and the creation of clusters. In preparation for the sequencing the reverse strands are cleaved and washed off. The forward strands remain attached on the flow cell and their 3' end get blocked to prevent unwanted priming.

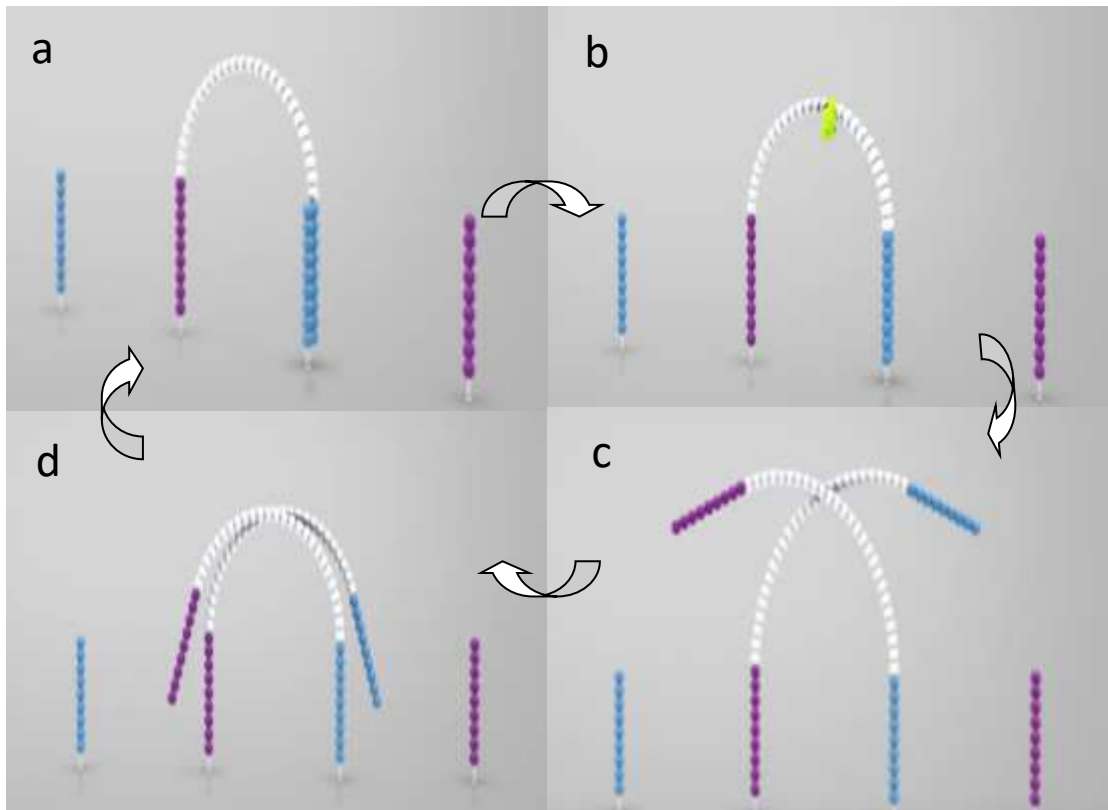


Figure 6: Bridge amplification during cluster generation on the flow cell

Sequencing

Sequencing takes place on the clusters generated on the flow cell. The flow cell is divided in tiles. After 1st read, index read and 2nd read of a tile is complete, the flow cell is moved into place to expose the next tile (Figure 7). The process is repeated for each cycle of sequencing.

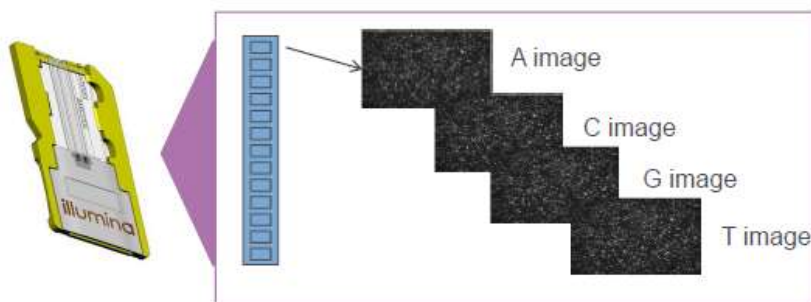


Figure 7: representation of tile imaging on flow cell

1st read

Sequencing begins with the hybridization of the 1st sequencing primer to the anchored forward strand. The primer extends with the help of a polymerase to produce the 1st read. Each cycle is completed with the addition of a fluorescent dideoxynucleotide. Each dideoxynucleotide is attached to a different fluorophore. All four dideoxynucleotides compete for being added at the 3' end of the extending strand. Finally only one dideoxynucleotide binds based on the complementarity for the template. At the end of each cycle the clusters are excited by a light source and fluorescence is emitted according to the dideoxynucleotide incorporated. After each cycle the unbound dideoxynucleotides are washed away. According to this procedure it is obvious that the number of cycles determines the length of the read.

Emission wave length (color) and signal intensity determine the base call for a given clonal cluster. Millions of clusters are sequenced simultaneously.

Index read

After the 1st read, the read product is denatured and washed away. The index primer is introduced and hybridized to the template, in order to synthesize the index sequence. The index sequence is detected in the same way as described for the 1st read. The product is denatured and washed away.

2nd read

The 3' end of the forward template is unprotected and the bridge is created again so that the 2nd index is sequenced by synthesis. A polymerase extends the second oligo forming again the double stranded bridge. The bridge strands denature and the 3' ends are blocked. This time the forward strand is cleaved and washed away, leaving the reverse strand to be read with the introduction of the read 2 sequencing primer. Then the software takes over, again by exciting the fluorophores and reading the emission wave length (color) and signal intensity to call the base. From each cluster we read one base. At the end of each cycle, each cluster emits in one wave length which is interpreted by the instrument resulting in one base call. Each cluster at the end of the programmed cycles has produced one read. Millions of clusters are sequenced simultaneously resulting in millions of reads. The result is similar to Figure 8.

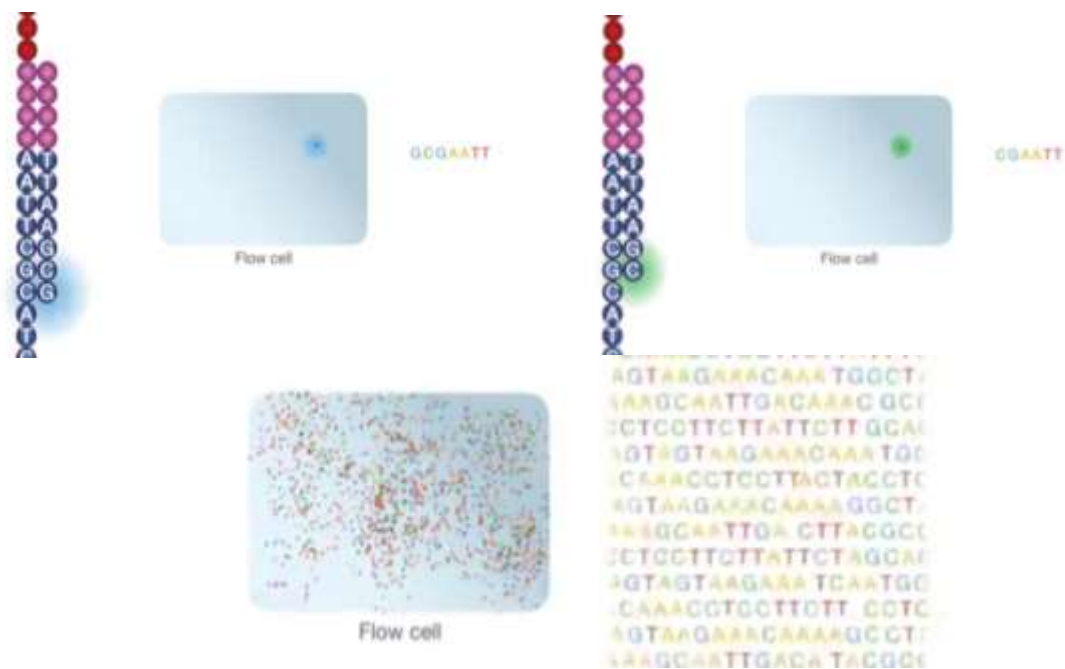


Figure 8: Cluster visualization and base calling

Data analysis

Following image analysis, the software performs base calling, filtering, and quality scoring. The reads are separated based on the indices (de-multiplexing). Reads with similar stretches of base calls are clustered together. Forward and reverse reads are paired forming a contiguous sequence. This way it is easier to clarify ambiguous alignments. The sequence that we assembled is aligned back to a reference sequence.

During the sequencing run, Real-time Analysis (RTA) generates data files that include analysis metrics used by MiSeq Reporter for secondary analysis. The following metrics appear in reports from MiSeq Reporter software:

1) Clusters passing filter

2} Base call quality scores

3} Phasing and prephasing values

MiSeq Reporter performs secondary analysis according to the workflow using a series of analysis procedures, which include demultiplexing, FASTQ file generation, alignment (if required).

Analysis Procedure Description

Demultiplexing: Performed for all workflows if the run has index reads and the sample sheet lists multiple samples. Read sequences are matched to the index sequences specified in the sample sheet. No quality values are considered in this step. Demultiplexing separates data from pooled samples based on short index sequences that tag samples from different libraries. Index reads are identified using the following steps:

- Samples are numbered starting from 1 based on the order they are listed in the sample sheet.
- Sample number 0 is reserved for clusters that were not successfully assigned to a sample.
- Clusters are assigned to a sample when the index sequence matches exactly or there is up to a single mismatch per Index Read.

FASTQ File Generation: FASTQ files are the primary input for the alignment step and are produced for all workflows. FASTQ files contain non-indexed reads for each sample and their quality scores, excluding reads identified as inline controls and reads that did not pass filter.

Alignment: Performed for workflows when alignment against a reference is required. Alignment compares sequences against the reference specified in the sample sheet and assigns a score based on regions of similarity. MiSeq Reporter uses an alignment method best-suited for the workflow. Aligned reads are written to files in BAM file format.

Phasing and Prephasing (Figure 9): During the sequencing reaction, each DNA strand in a cluster extends by 1 base per cycle. A small portion of strands can become out of phase with the current incorporation cycle.

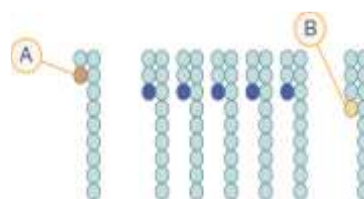


*Figure 9: Phasing and Prephasing.
A Read with a base that is phasing.
B Read with a base that is prephasing.*

A small portion of strands can become out of phase with the current incorporation cycle.

Phasing occurs when a base falls behind. Prephasing occurs when a base jumps ahead. Phasing and prephasing rates indicate an estimate of the fraction of molecules that became phased or prephased in each cycle. The number of cycles performed in a read is 1 more cycle than the number of cycles analyzed. For example, a paired-end 150-cycle run performs 2 151-cycle reads (2×151) for a total of 302 cycles. At the end of the run, 2×150 cycles are analyzed. The 1 extra cycle for Read 1 and Read 2 is required for prephasing calculations. Phasing and prephasing calculations use statistical averaging over many clusters and sequences to estimate the correlation of signal between different cycles.

Appendix B: Full Protocol for TruSeq Small RNA Library Preparation

Ligate Adapters

This process describes the sequential ligation of the RNA 3' and RNA 5' RNA adapters to the 3' hydroxyl end and subsequently to the 5'-phosphate group of the mature miRNAs and other Dicer produced species in the sample.

Materials

- 1µg of total RNA in 5µl of nuclease free water
- 10 mM ATP 1 tube -25°C to -15°C Illumina
- Ligation Buffer (HML) 1 tube -25°C to -15°C Illumina
- RNA 3' Adapter (RA3) 1 tube -25°C to -15°C Illumina
- RNA 5' Adapter (RA5) 1 tube -25°C to -15°C Illumina
- RNase Inhibitor 1 tube -25°C to -15°C Illumina
- Stop Solution (STP) 1 tube -25°C to -15°C Illumina
- T4 RNA Ligase 1 tube -25°C to -15°C Illumina
- Ultra-Pure Water 1 tube -25°C to -15°C Illumina
- Nuclease-free 200 µl PCR tubes 15°C to 30°C User supplied
- T4 RNA Ligase 2, Deletion Mutant (200 U/µl) 1 µl per sample -25°C to -15°C User supplied
- 96-well working rack User supplied
- Ice User supplied

Method

Preparation

- Remove the Illumina-supplied consumables and T4 RNA Ligase 2, Deletion Mutant from -25°C to -15°C storage and thaw on ice.
- Briefly centrifuge the thawed consumables at 600 × g for 5 seconds, and then place them on ice.
- Preheat the thermal cycler to 70°C.

- Choose the thermal cycler preheat lid option and set to 100°C.

Ligation of 3' Adapter

1 Set up the ligation reaction in a sterile, nuclease-free 200 µl PCR tube on ice using the following:

Reagent Volume	(µl)
RNA 3' Adapter (RA3)	1
1 µg Total RNA in nuclease-free water	5
Total Volume	6

Multiply each reagent volume by the number of samples being prepared. Make 10% extra reagent if you are preparing multiple samples.

2 Gently pipette the entire volume up and down 6–8 times to mix thoroughly, and then centrifuge briefly.

3 Place the tube on the preheated thermal cycler. Close the lid and incubate the tube at 70°C for 2 minutes and then immediately place the tube on ice.

4 Preheat the thermal cycler to 28°C.

5 Prepare the following mix in a separate, sterile, nuclease-free 200 µl PCR tube on ice.

Reagent Volume	(µl)
Ligation Buffer (HML)	2
RNase Inhibitor	1
T4 RNA Ligase 2, Deletion Mutant	1
Total Volume	4

Multiply each reagent volume by the number of samples being prepared. Make 10% extra reagent if you are preparing multiple samples.

6 Gently pipette the entire volume up and down 6–8 times to mix thoroughly, and then centrifuge briefly.

7 Add 4 µl of the mix to the reaction tube from step 1 and gently pipette the entire volume up and down 6–8 times to mix thoroughly. The total volume of the reaction is 10 µl.

8 Place the tube on the preheated thermal cycler. Close the lid and incubate the tube at 28°C for 1 hour.

9 With the reaction tube on the thermal cycler, add 1 µl Stop Solution (STP) and gently pipette the entire volume up and down 6–8 times to mix thoroughly. Continue to incubate the reaction tube on the thermal cycler at 28°C for 15 minutes and then place the tube on ice.

Ligation of 5' Adapter

1 Preheat the thermal cycler to 70°C.

2 Add $1.1 \times N$ µl RNA 5' Adapter (RA5) into a separate, nuclease-free 200 µl PCR tube, with N equal to the number of samples being prepared. Work on ice

3 Place the tube on the preheated thermal cycler. Close the lid and incubate the tube at 70°C for 2 minutes and then immediately place the tube on ice.

4 Preheat the thermal cycler to 28°C.

5 Add $1.1 \times N$ µl 10mM ATP to the RNA 5' Adapter aliquot tube, with N equal to the number of samples being prepared. Gently pipette the entire volume up and down

6–8 times to mix thoroughly.

6 Add $1.1 \times N$ µl T4 RNA Ligase to the RNA 5' Adapter aliquot tube, with N equal to the number of samples being prepared. Gently pipette the entire volume up and down 6–8 times to mix thoroughly.

7 Add 3 µl of the mix from the RNA 5' Adapter aliquot tube to the reaction from step 9 of *Ligate 3' Adapter*. Gently pipette the entire volume up and down 6–8 times to mix thoroughly.

The total volume of the reaction is 14 µl.

8 Place the tube on the preheated thermal cycler. Close the lid and incubate the reaction tube at 28°C for 1 hour and then place the tube on ice.

Production of cDNA construct

Reverse transcription followed by PCR is used to create cDNA constructs based on the small RNA ligated with 3' and 5' adapters. This process selectively enriches those fragments that have adapter molecules on both ends. PCR is performed with 2 primers that anneal to the ends of the adapters.

Materials

- 25 mM dNTP Mix 1 tube -25°C to -15°C Illumina
- PCR Mix (PML) 1 tube -25°C to -15°C Illumina
- RNA PCR Primer (RP1) 1 tube -25°C to -15°C Illumina
- RNA PCR Primer Index (1–12) (RPI1–RPI12) -25°C to -15°C Illumina
- RNA RT Primer (RTP) 1 tube -25°C to -15°C Illumina
- RNase Inhibitor 1 tube -25°C to -15°C Illumina
- Ultra-Pure Water 1 tube -25°C to -15°C Illumina
- 5X First Strand Buffer 2 µl per sample -25°C to -15°C User
- 100 mM DTT 1 µl per sample -25°C to -15°C User
- High Sensitivity DNA chip 1 per sample 15°C to 30°C User
- Nuclease-free 200 µl PCR tubes 3 + 1 per index used 15°C to 30°C User supplied
- SuperScript II Reverse Transcriptase 1 µl per sample -25°C to -15°C User supplied

Preparation

- Remove the Illumina-supplied consumables, 5X First Strand Buffer, 100 mM DTT, and SuperScript II Reverse Transcriptase from -25°C to -15°C storage and thaw on ice.
- Briefly centrifuge the thawed consumables at 600 × g for 5 seconds, and then place them on ice.
- Preheat the thermal cycler to 70°C.
- Choose the thermal cycler preheat lid option and set to 100°C.
- Label a sterile, nuclease-free, 200 µl PCR tube 12.5 mM dNTP Mix with a smudge resistant pen.

Dilution of 25 mM dNTP Mix

1 Dilute the 25 mM dNTPs by premixing the following reagents in a sterile, nuclease-free, 200 µl PCR tube, labeled 12.5 mM dNTP Mix. Multiply each reagent volume by the number of samples being prepared. Make 10% extra reagent if you are preparing multiple samples.

Reagent Volume	(μ l)
25 mM dNTP Mix	0.5
Ultra Pure Water	0.5
Total Volume	1

2 Gently pipette the entire volume up and down 6–8 times to mix thoroughly, centrifuge briefly and then place it on ice.

Reverse Transcription

1 Transfer 6 μ l of each 5' and 3' adapter-ligated RNA to a separate, sterile, nuclease-free, 200 μ l PCR tube.

2 Add 1 μ l RNA RT Primer to each tube containing adapter-ligated RNA and gently pipette the entire volume up and down 6–8 times to mix thoroughly, and then centrifuge briefly.

4 Place the tube on the preheated thermal cycler. Close the lid and incubate the tube at 70°C for 2 minutes and then immediately place the tube on ice.

5 Preheat the thermal cycler to 50°C.

6 Prepare the following mix in a separate, sterile, nuclease-free, 200 μ l PCR tube placed on ice.

Reagent Volume	(μ l)
5X First Strand Buffer	2
12.5 mM dNTP mix	0.5
100 mM DTT	1
RNase Inhibitor	1
SuperScript II Reverse Transcriptase	1
Total Volume	5.5

Multiply each reagent volume by the number of samples being prepared. Make 10% extra reagent if you are preparing multiple samples.

7 Gently pipette the entire volume up and down 6–8 times to mix thoroughly, and then centrifuge briefly.

8 Add 5.5 µl of the mix to the reaction tube from step 4. Gently pipette the entire volume up and down 6–8 times to mix thoroughly, and then centrifuge briefly.

The total volume is 12.5 µl.

9 Place the tube on the preheated thermal cycler. Close the lid and incubate the tube at 50°C for 1 hour and then place the tube on ice.

PCR Amplification

1 Prepare a separate PCR tube for each index used. Combine the following reagents in a separate, sterile, nuclease-free, 200 µl PCR tube placed on ice.

Reagent Volume	(µl)
Ultra-Pure Water	8.5
PCR Mix (PML)	25
RNA PCR Primer (RP1)	2
RNA PCR Primer Index (RPI1-12)	2
Total Volume	37.5

Multiply each reagent volume by the number of samples being prepared. Make 10% extra reagent if you are preparing multiple samples with the same index.

For each reaction, only 1 of the 48 RNA PCR Primer indexes is used during the PCR step. We used 12 different index sequences.

2 Gently pipette the entire volume up and down 6–8 times to mix thoroughly, centrifuge briefly, and then place the tube on ice.

3 Add 37.5 µl of PCR master mix to the reaction tube from step 9 of *Perform Reverse*

Transcription.

4 Gently pipette the entire volume up and down 6–8 times to mix thoroughly, centrifuge briefly, and then place the tube on ice.

The total volume is 50 µl.

5 Place the tube on the preheated thermal cycler. Close the lid and incubate the tube using the following PCR cycling conditions:

Preheat lid option and set to 100°C.

Temperature (°C)	Time (seconds)	
98	30	Hold
98	10	11 cycles
60	30	
72	15	
72	600	Hold
4	∞	Hold

SAFE STOPPING POINT

Store at -25°C to -15°C for up to 7 days. When proceeding, thaw the samples on ice.

Purification of cDNA

This process gel purifies the amplified cDNA construct in preparation for subsequent cluster generation. After gel purification, the cDNA is eluted and we purified further and concentrated the elution using the ampure xp beads.

Material

Custom RNA Ladder (CRL) 1 tube -25°C to -15°C Illumina

High Resolution Ladder (HRL) 1 tube -25°C to -15°C Illumina

Ultra-Pure Water 1 tube -25°C to -15°C Illumina

5 µm filter tubes 2 15°C to 30°C User supplied

Amplified cDNA Construct 50 µl -25°C to -15°C User supplied

DNA loading dye 13 μ l 15°C to 30°C User supplied

Gel breaker tubes 2 15°C to 30°C User supplied

Novex TBE gels, 6%, 10 well 1 15°C to 30°C User supplied

Novex TBE running buffer (5X) as needed -25°C to -15°C User supplied

Nuclease-free 200 μ l PCR tube 1 15°C to 30°C User supplied

Nuclease-free 1.5 ml microcentrifuge tubes 3 15°C to 30°C User supplied

Razor blade 1 15°C to 30°C User supplied

Ultra-pure ethidium bromide 10mg/ml and 0.5 μ g/ml in water User supplied

Run Gel Electrophoresis

1 Determine the volume of 1X TBE Buffer needed. Dilute the Novex TBE running buffer (5X) to 1X for use in electrophoresis.

2 Place a Novex TBE gel, 6% into a gel electrophoresis unit according to manufacturer instructions.

3 Add 2 μ l Custom RNA Ladder (CRL) and 2 μ l DNA loading dye to a sterile, nuclease-free, 1.5 ml microcentrifuge tube. Gently pipette the entire volume up and down 6–8 times to mix thoroughly.

4 Add 1 μ l High Resolution Ladder (HRL) and 1 μ l DNA loading dye to a sterile, nuclease-free, 1.5 ml microcentrifuge tube. Gently pipette the entire volume up and down 6–8 times to mix thoroughly.

5 Add all of the amplified cDNA construct (typically 48–50 μ l) and 10 μ l DNA Loading Dye to a sterile, nuclease-free, 1.5 ml microcentrifuge tube. Gently pipette the entire volume up and down 6–8 times to mix thoroughly.

6 Load 2 μ l of the Custom RNA Ladder and loading dye mixture, from step 3, into 2 lanes of the gel.

7 Load 2 μ l of the High Resolution Ladder and loading dye mixture, from step 4, into a different lane of the gel.

8 Load 25 μ l each of the Amplified cDNA Construct and loading dye mixture, from step 5, into 2 lanes of the gel. Load a total volume of 50 μ l on the gel.

9 Run the gel for 60 minutes at 145 V or until the blue front dye exits the gel.

10 Immediately remove the gel from the electrophoresis unit.

Recovery of Purified Construct

1 Open the cassette according to manufacturer instructions and stain the gel with ethidium bromide (0.5 μ g/ml in water) in a clean container for 2–3 minutes.

2 Place the gel breaker tube into a sterile, round-bottom, nuclease-free, 2 ml microcentrifuge tube.

3 View the gel on a Dark Reader transilluminator or a UV transilluminator.

The Custom RNA Ladder consists of 3 dsDNA fragments 145 bp, 160 bp, and 500 bp. Sequencing can be conducted on individual bands or from pooled bands. The 147 nucleotide band primarily contains mature microRNA generated from approximately 22 nucleotide small RNA fragments. A second, 157 nucleotide band containing piwi-interacting RNAs, as well as some microRNAs and other regulatory small RNA molecules, is generated from approximately 30 nucleotide RNA fragments (Figure 10).

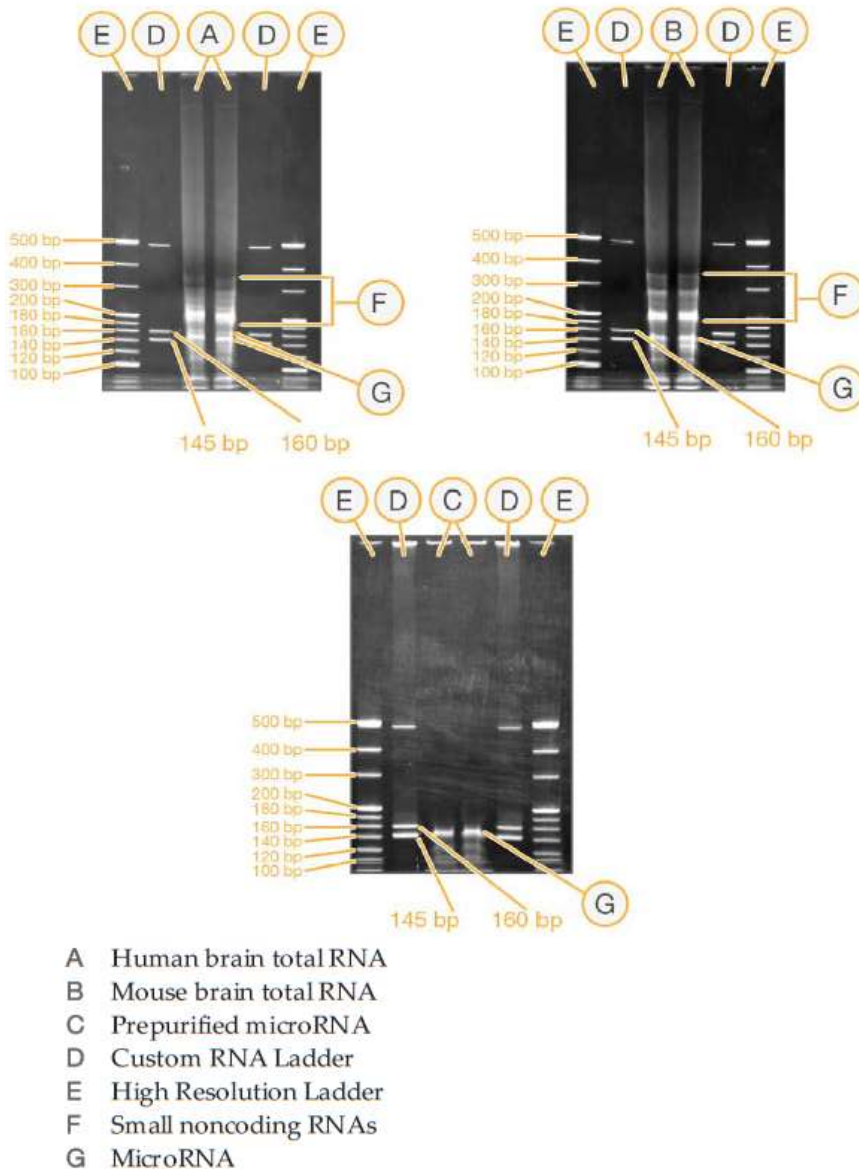


Figure 10: Example of Gels as seen under the UV transilluminator

4 Using a razor blade, cut out the bands from both lanes that correspond approximately to the adapter-ligated constructs derived from the 22 nt and 30 nt small RNA fragments. MicroRNAs often vary in length, often called isomiRs. The tighter the band selection, the tighter size distribution of the final microRNA representation. Align the razor blade with the top of the 160 bp band of the Custom RNA Ladder, then with the bottom of the 145 bp band of the Custom RNA Ladder. Excise the gel fragment by connecting these cuts on the sides. Both lanes can be combined into 1 slice. The band containing the 22 nucleotide RNA fragment with both adapters are a total of 147 nucleotides in length. The band containing the 30 nucleotide RNA fragment with both adapters are 157 nucleotides in length.

- 5 Place the band of interest into the 0.5 ml Gel Breaker tube from step 2.
- 6 Centrifuge the stacked tubes at $20,000 \times g$ for 2 minutes at room temperature to move the gel through the holes into the 2 ml tube. Make sure that all the gel has moved through the holes into the bottom tube.
- 7 If not performing the optional step of Ethanol precipitation, add 200 μ l Ultra-Pure Water to the gel debris in the 2 ml tube.
- 8 Elute the DNA by rotating or shaking the tube at room temperature for at least 2 hours. The tube can be rotated or shaken overnight.
- 9 Transfer the eluate and the gel debris to the top of a 5 μ m filter.
- 10 Centrifuge the filter for 10 seconds at $600 \times g$.
- 11 Proceed to *Validate Library*.

Concentration of the pooled samples

Concentrate the each library with size selecting beads,

Materials

- AMPure XP beads
- 80% ethanol
- Magnetic rack
- Vortex
- Benchtop centrifuge
- Microcentrifuge 1.5ml tubes
- PCR tubes

Method

- Transfer 100 μ l sample to a 1.5 ml tube. Add 130 μ l (1.3X) of resuspended AMPure XP beads and mix well on a vortex mixer or by pipetting up and down at least 10 times.
- Incubate for 5 minutes at room temperature.

- Place the tube on an appropriate magnetic stand to separate the beads from the supernatant. After the solution is clear (about 5 minutes), carefully transfer the supernatant (230 μ l) to a new tube. Discard the beads that contain the large DNA fragments.
- Add 370 μ l (3.7X) of resuspended AMPure XP beads to the supernatant (230 μ l), mix well and incubate for 5 minutes at room temperature.
- Place the tube on an appropriate magnetic stand to separate the beads from the supernatant. After the solution is clear (about 5 minutes), carefully remove and discard the supernatant. Be careful not to disturb the beads that contain DNA targets
- Add 1ml of freshly prepared 80% ethanol to the tube while in the magnetic stand. Incubate at room temperature for 30 seconds, and then carefully remove and discard the supernatant.
- Repeat Step 6 once.
- Briefly spin the tube, and put the tube back in the magnetic stand.
- Completely remove the residual ethanol, and air dry beads for 10 minutes while the tube is on the magnetic stand with lid open.
- Elute the DNA target from the beads with 15 μ l of nuclease-free water. Mix well on a vortex mixer or by pipetting up and down, and put the tube in the magnetic stand until the solution is clear.
- Transfer the supernatant to a clean PCR tube.

Library Validation

For quality control analysis of the produced libraries.

1 Load 1 μ l of the resuspended construct on Fragment Analyzer™ Automated CE System (Advanced Analytical, Technologies, IA,US).

2 Check the size, purity, and concentration of the sample with Qubit® 2.0 Fluorometer (Thermo Fisher Scientific, Waltham, MA, US).

Library Normalization and Denaturation

1 Normalize the concentration of the library to 2 nM using Tris-HCl 10 mM, pH 8.5.

2 Denature with NaOH 0.1M for 5 minutes

Appendix C: Fragment Analyzer

The Fragment Analyzer™ system is a multiplexed capillary electrophoresis (CE) instrument for performing automated, high throughput separation and quantification of double stranded nucleic acids (DNA and/or RNA). Separation is achieved by applying an electric field through a narrow bore (50 µm i.d.) fused silica capillary array filled with various conductive gel matrices designed to sieve DNA/RNA molecules of a specific size range. When a high voltage is applied to the capillary array, injected DNA/RNA migrates differentially through the gel matrix as a function of length or size, with smaller sized fragments eluting faster than larger sized fragments.

At a point toward the far end of the capillary array, detection of the separated DNA/RNA is achieved by fluorescence of a sensitive intercalating dye present in separation gel matrix, which fluoresces when bound to double stranded DNA or RNA molecules. The Fragment Analyzer™ system utilizes a high intensity light emitting diode (LED) excitation light source that is focused across the capillary array detection window and imaged onto a sensitive, two-dimensional charge-coupled device (CCD) detector. By monitoring the relative fluorescence unit (RFU) intensity as a function of time during the CE separation, digital electropherogram traces representative of the DNA/RNA content of an entire row of 12 samples, or plate of 96 samples can be collected in a single experimental run. For small RNAs and miRNAs there is the Small RNA Analysis Kit. The Small RNA Analysis Kit (DNF-470) is able to measure the size and concentration of small RNAs, including functional microRNAs, due to the Small RNA Ladder (DNF-361)

Materials

- Small RNA Separation Gel, *part # DNF-262*
- Intercalating Dye, *part # DNF-600-U030*
- 5X 930 dsDNA Inlet Buffer, *part # DNF-355 (Dilute to 1X)*
- 5X Capillary Conditioning Solution, *part # DNF-475 (Dilute to 1X)*
- 0.25X TE Rinse Buffer, *part # DNF-497*
- Small RNA Diluent Marker, *part # DNF-368*

- Small RNA Ladder, *part # DNF-361*
- BF-25 Blank Solution, *part # DNF-300*
- *Capillary Storage Solution, part # GP-440-0100 (sold separately)*

Gel Guide:
For 12-capillary Fragment Analyzer™ systems:

# of Samples to be Analyzed ¹	Volume of Intercalating Dye	Volume of Gel
12	1.0 µL	10 mL
24	1.5 µL	15 mL
36	2.0 µL	20 mL
48	2.5 µL	25 mL
96	4.5 µL	45 mL

Typically one sample well per separation is dedicated to the ladder

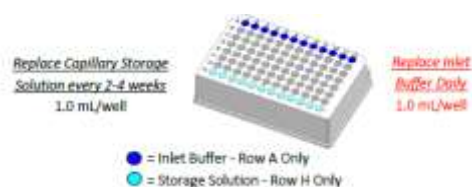
Specifications	Description
Sample Volume Required	2 µL
Diluent Marker Volume Required	18 µL
RNA Sizing Range	15 - 200 nt
Qualitative Range	25 pg/µL - 2500 pg/µL (microRNA region)
Quantitative Range	50 pg/µL - 2000 pg/µL (microRNA region)
Quantification Precision	25% CV (Small RNA Ladder)
Total Electrophoresis Run Time	17 minutes (Ultra-Short Array, 22-47); 22 minutes (Short Array, 33-55)

Preparation

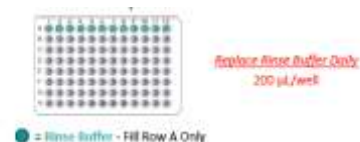
1. Mix fresh Gel and Refill 1X as needed.



2. Place a fresh **1X Inlet Buffer** Tray on Fragment Analyzer.

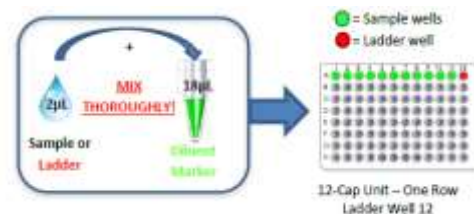


3. Place **Rinse Buffer** plate in Marker Drawer location.



4. Heat denature **Samples** and **Ladder** at 70°C for 10 minutes, immediately cool to 4°C and keep on ice before use.

5. Mix **Samples** or **Ladder** with **Diluent Marker** in Sample Plate. Add 20 µL of **Blank Solution** to unused wells of the row to be analyzed.

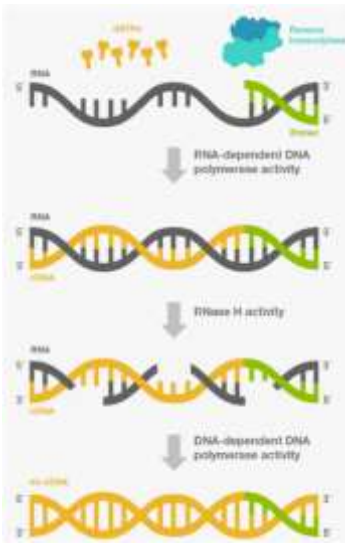


Software:

1. Select Tray and Row to run for 12-Cap.
2. Enter Sample ID and Tray ID (optional).
3. Select “Add to Queue”, select the **DNF-470-(22 or 33) Small RNA** method from the Dropdown menu.
4. Enter Tray Name, Folder Prefix, and Notes (optional), Select **OK** to add Method to the Queue.
5. Select to Start the Separation.

Appendix D: Introduction to qRT-PCR

Reverse Transcription



RNA needs to be converted in cDNA in order to be used in qRT-PCR. Reverse transcriptases are converting single strand RNA into cDNA (single or double stranded). Moreover, they are enzymes composed of distinct domains that exhibit different biochemical activities as demonstrated in Figure 11, but also, different optimal functioning temperature, thermostability, length of elongation and cDNA yields. MultiScribe™ Reverse Transcriptase is a recombinant moloney murine leukemia virus (rMoMuLV) reverse transcriptase with reduced RNase H activity and capacity to produce up to 7kb of first strand cDNA being optimum for first strand generation with Random Hexamer Primers.

Figure 11: Properties of a Reverse Transcriptase

Reverse transcriptase is attached to a messenger RNA with the help of a six base pair random primer and elongates the primer with DNA bases, producing single strand DNA the cDNA, as demonstrated in Figure 12.

The retrotranscription is composed from two step the primer annealing and DNA polymerization. Random primer hexamers due to their short length have a lower T_m (10-15°C) which makes them perfect to be combined with less thermostable enzymes like rMoMuLV reverse transcriptase. Other options are the poly-dT primers which anneal to all the polyadenylated mRNAs or specific primers.

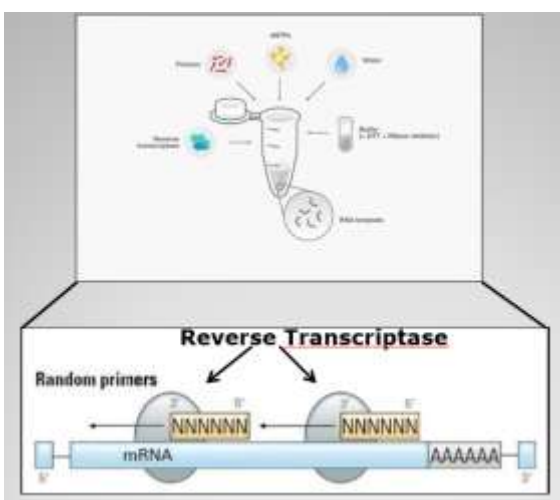


Figure 12: Reverse Transcriptase required reagents (up) and representation of binding on the mRNA (down)

qRT-PCR for gene expression

TaqMan Gene Expression Assays are based on 5' nuclease chemistry, and each assay contains the primer and probe set for your target of interest. TaqMan probes are dual labeled, hydrolysis probes that increase the specificity of Real-Time PCR (RT-PCR) assays. TaqMan probes contain:

- A reporter dye (for example, FAM™ dye) linked to the 5' end of the probe
- A non-fluorescent quencher (NFQ) at the 3' end of the probe
- MGB moiety attached to the NFQ

TaqMan MGB probes also contain a minor groove binder (MGB) at the 3' end of the probe. MGBs increase the melting temperature (T_m) without increasing probe length; allowing for the design of shorter probes^{328,329}. Here's how an assay works (Figure 13):

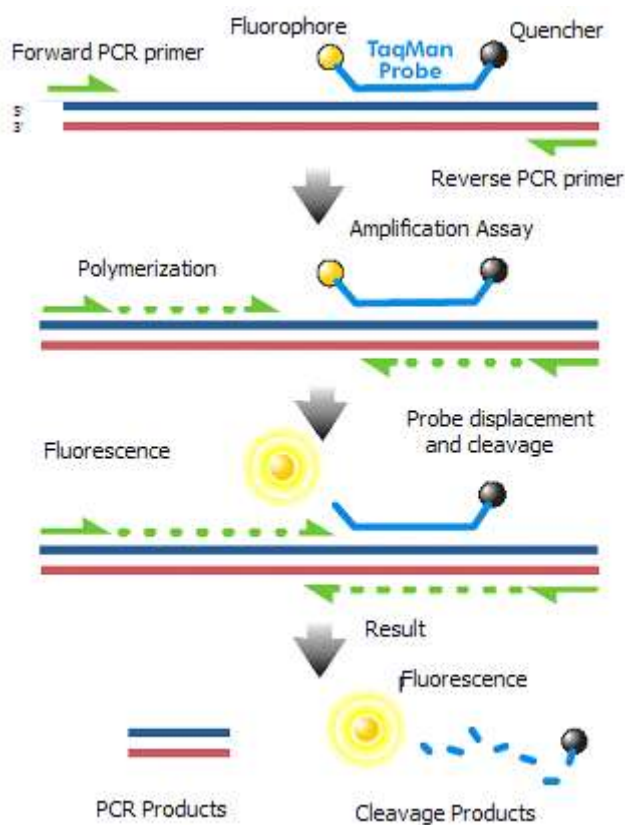


Figure 13: Taqman Chemistry

1. At the start of the RT-PCR reaction, the temperature is raised to denature the double-stranded cDNA. During this step, the signal from the fluorescent dye on the 5' end of the Applied Biosystems™ TaqMan™ probe is quenched by the MGB–NFQ on the 3' end of the probe.

2. In the next step, the reaction temperature is lowered to allow the primers and probe to anneal to their specific target sequences.

3. Taq polymerase synthesizes a complementary DNA strand using the unlabeled primers and template. When the polymerase reaches the TaqMan probe, its endogenous 5' nuclease activity cleaves the probe, separating the dye from the quencher. With each cycle of PCR, more dye molecules are released, resulting in an increase in fluorescence intensity proportional to the amount of amplicons synthesized.

The results of the reaction can be visualized via Sequence Detector Software (SDS) and are presented to the user in the form of an amplification plot (Figure 14).

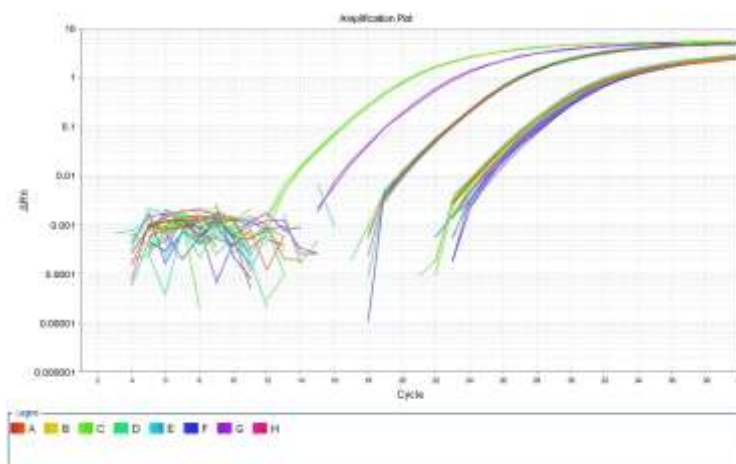


Figure 14: Example of Amplification plot. With the same color are represented the technical replicates.

The amplification plot contains all the information needed to estimate the relative quantity and consists in the following characteristics (Figure 15)¹⁹⁹:

- Baseline: is defined as PCR cycles in which a reporter fluorescent signal is accumulating but is beneath the limits of detection of the instrument.
- ΔR_n : is an increment of fluorescent signal at each time point. The ΔR_n values are plotted versus the cycle number.
- Threshold: is an arbitrary level of fluorescence chosen on the basis of the baseline variability. A signal that is detected above the threshold is considered a real signal that can be used to define the threshold cycle (Ct) for a sample. Threshold can be adjusted for each experiment so that it is in the region of exponential amplification across all plots.

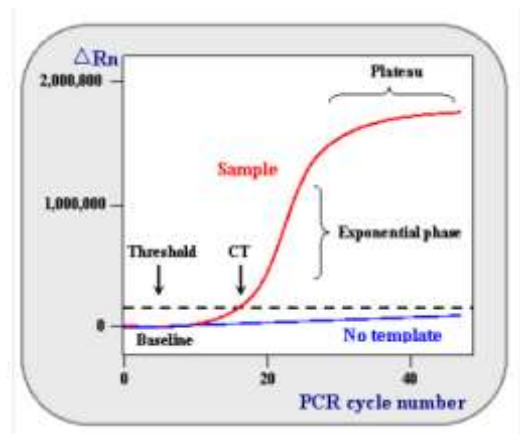


Figure 15: Amplification plot characteristics

- Ct: is defined as the fractional PCR cycle number at which the reporter fluorescence is greater than the threshold. The Ct is a basic principle of real time PCR and is an essential component in producing accurate and reproducible data.
- Exponential phase: Exact doubling of product occurs at every cycle (assuming 100% reaction efficiency). Exponential amplification occurs because all of the reagents are fresh and available, the kinetics of the reaction push the reaction to favor doubling of amplicon.
- Plateau: The reaction has stopped, no more products are made, and if left long enough, the PCR products begin to degrade. Each tube or reaction plateaus at a different point, due to the different reaction kinetics for each sample. These differences can be seen in the plateau phase. The plateau phase is the end point, where traditional PCR takes its measurement.

The calculation of $\Delta\Delta Ct$ is automatically done by the instrument according to the following equations ³³⁰.

$\Delta Ct \text{ gene} = \text{mean Ct target} - \text{mean Ct of endogenous control}$

$\Delta\Delta Ct = \Delta Ct \text{ sample (n)} - \Delta Ct \text{ calibrator}$

$2^{-\Delta\Delta Ct} = \text{Relative Quantity (RQ)}$

Introduction to Retrotranscription and qRT-PCR of miRNA

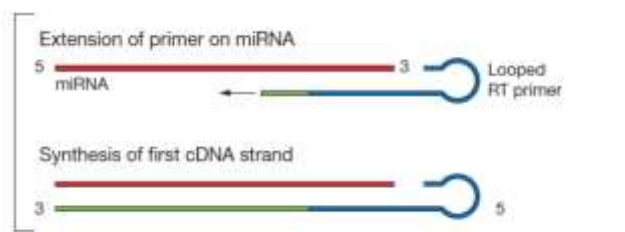


Figure 16: Retrotranscription with Taqman® Small RNA Assay's specific miRNA primers.

MiRNA levels are quantified with a two-step RT-PCR. The first step for the RT-PCR is the retrotranscription. MiRNAs do not have a poly-A chain and are not fully covered with random primers, therefore, specific primers are necessary. Moreover, miRNA sequence is too short for implementing Taqman chemistry and therefore has to be extended specifically during the reverse transcription step ²⁰⁰. Such as mRNA retrotranscription, a reverse transcriptase needs a single primer to produce a cDNA strand using as template RNA. Taking into account the special requirements of a

miRNA quantification using RT-PCR the primer used for the reverse transcription of miRNA has a stem-loop structure (Figure 16). The bonds that are spontaneously formed at the stem-loop enhance the thermal stability of the RNA–DNA heteroduplex, while the spatial constraint of the stem-loop improves the specificity in comparison to conventional linear primers³³¹. The RT-PCR chemistry for miRNAs is similar with the normal RT-PCR for mRNA targets (Figure 17). During every cycle the primers and the probe specifically anneal to the cDNA of the target miRNA. The 5' nuclease properties of the polymerase that elongates the primers allow the separation of the non-fluorescent quencher from the fluorescent reporter during PCR amplification and thus, increase the emitted fluorescence of the sample.

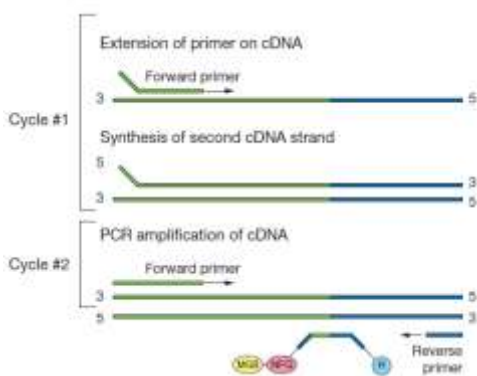


Figure 17: qRT-PCR with Taqman® Small RNA Assay specific probe, specific forward primer and loop-specific reverse primer. NFQ = Non-fluorescent quencher, MGB = Minor groove binder, R = Fluorescent FAM Reporter